X-ray Polarimetry and the IXPE Mission

Enrico Costa

Senior CoI of the Imaging X-Ray Polarimetry Explorer

Istituto di Astrofisica e Planetologia Spaziali – Roma
INAF



Scientific Landscape around CTAO-LSTs
La Palma 2026 10 16

X-Ray Polarimetry in the Landscape Of CTAO-LSTs?

X-Ray is the band of higher energy where we can perform observations with arcsecond imaging, high spectral resolution, large fluxes for timing analysis. Therefore X-Ray data are the first ingredient for any scenario of High Energy source.

IXPE data show that polarimetry can select different models all compatible with spectroscopic and timing data, can fix relevant parameters in particular by disentangling geometric terms from physics terms, and in some case can falsify models.

Morover Polarimetry is a tool to spot in the images and in spectra, non thermal components of the sources.

As a conclusion X-Ray Polarimetry should be a very effective support to VHE science, but I am not sure that this is actually the case

This may derive from the story: Polarimetry has recently moved out of niche.

IXPE
Imaging X-Ray Polarimetry Explorer

WHY X-RAY ASTROPHYSICAL POLARIMETRY ?

Polarization from celestial sources may derive from:

- **Emission processes themselves: cyclotron, synchrotron, non-thermal bremsstrahlung, inverse compton**

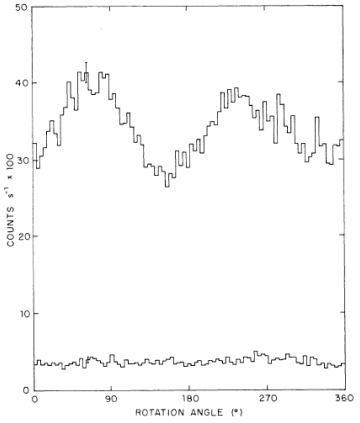
(Westfold, 1959; Gnedin & Sunyaev, 1974; Rees, 1975)

- **Scattering on aspherical accreting plasmas: disks, blobs, columns.**

(1975; Sunyaev & Titarchuk, 1985; Mészáros, P. et al. 1988)

- **Vacuum polarization and birefringence through extreme magnetic fields**

(Gnedin et al., 1978; Ventura, 1979; Mészáros & Ventura, 1979)



Only one source was detected by OSO-8 back in the ’70 until IXPE: The Crab Nebula (Weisskopf et al. 1978).

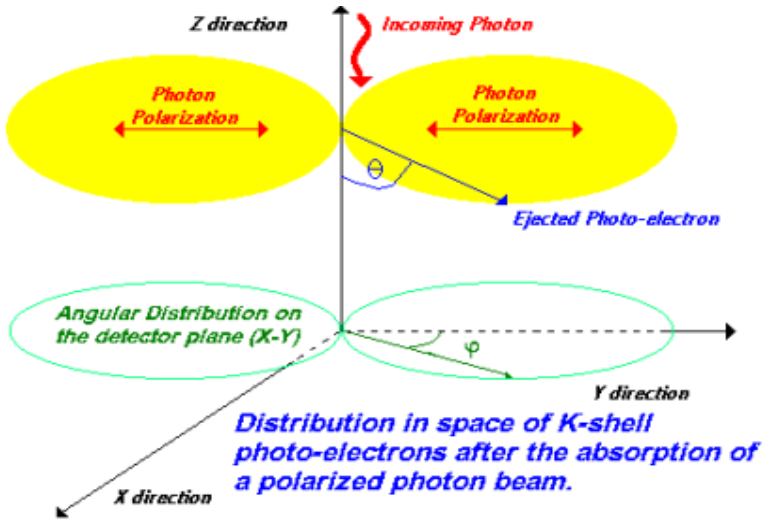
P = (19.2 ± 1.0) %; θ = 156°.4 ± 1°.4 (2.6 keV)

The technique was the limit!

Conventiomnal polarimeters are not suited to be combined with Optics and thence do not benefit of the corresponding increase of sensitivity

IXPE Imaging X-Ray Polarimetry Explorer

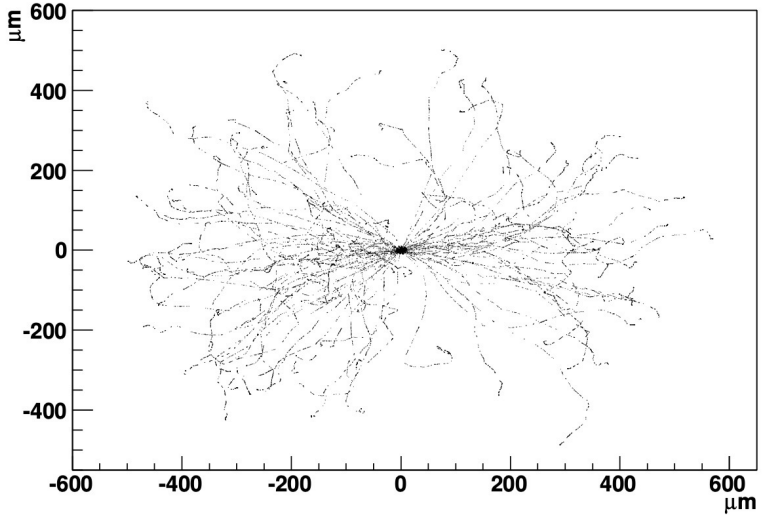
THE CHANGE: PHOTOELECTRIC TECHNIQUE AT 2-10 KEV



Costa, Nature, 2001

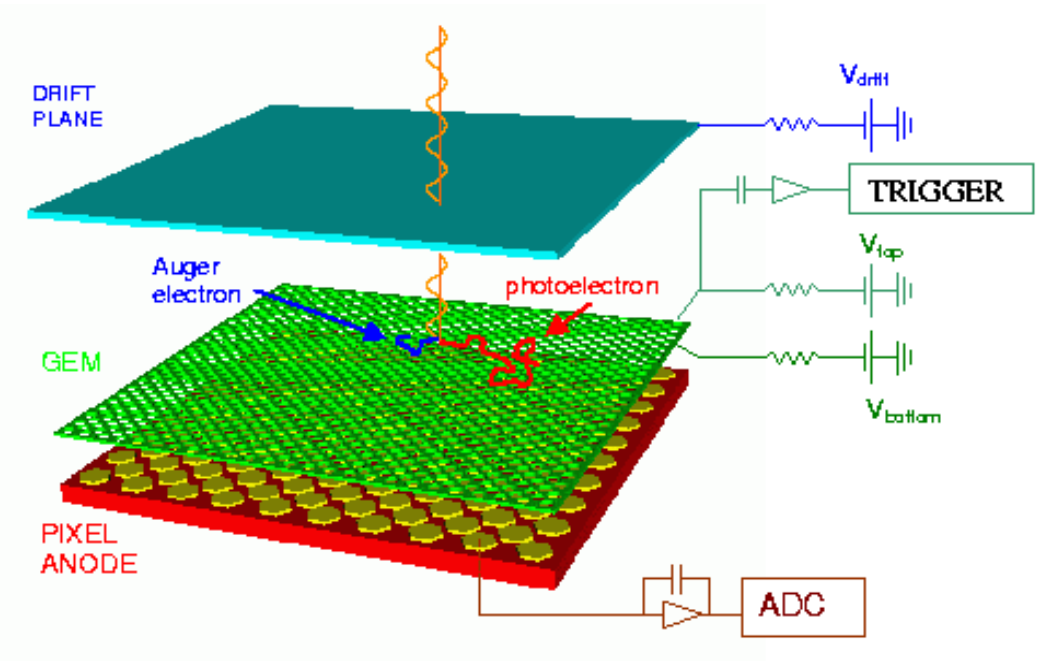
Heitler W.,The Quantum Theory of Radiation $\beta = v/c$

$$\frac{\partial\sigma}{\partial\Omega} = r_o^2 \frac{Z^5}{137^4}\left(\frac{mc^2}{h\nu}\right)^{7/2} \frac{4\sqrt{2}\sin^2(\theta)\cos^2(\varphi)}{(1-\beta\cos(\theta))^4}$$



IXPE
Imaging X-Ray Polarimetry Explorer

X-RAY POLARIMETRY WITH A GAS PIXEL DETECTOR



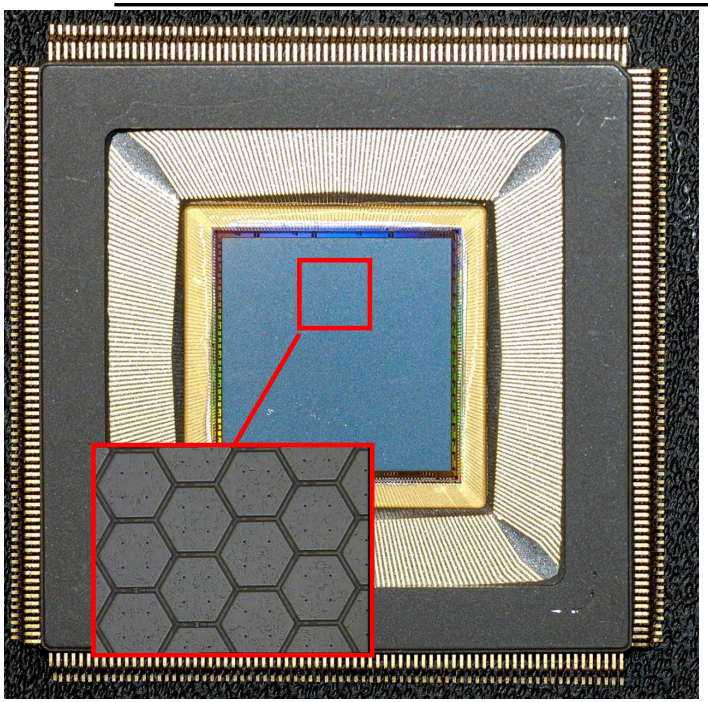
Costa et al., 2001, Bellazzini et al. 2006, 2007

- A Beryllium window
- A gas cell for photon conversion
- An electric field to drift the track
- A multiplication plane to get more charge
- An ASIC CMOS chip to make the image of the track

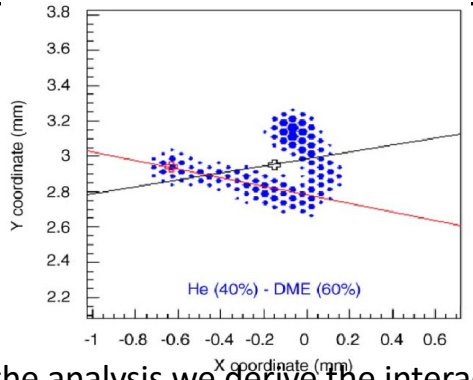
The Gas Pixel Detector makes the charge image of the photoelectron track. .

IXPE
Imaging X-Ray Polarimetry Explorer

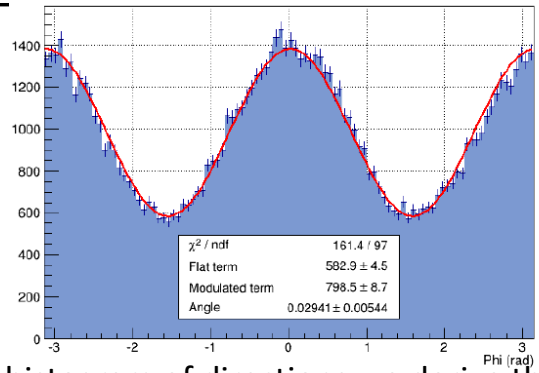
PHOTOELECTRIC EFFECT TO MEASURE POLARIZATION OF X-RAYS



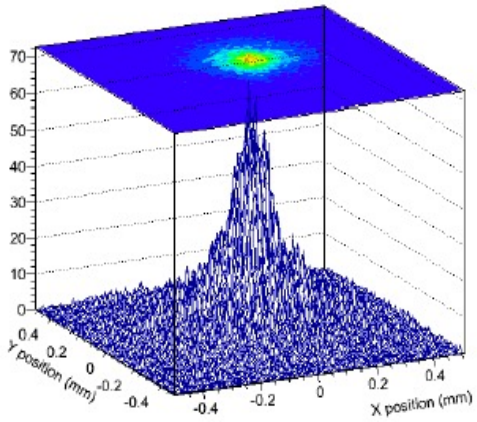
An ASIC VLSI Chip is the core of this detector. The charges of the ionization tracks amplified by the Gas Electron Multiplier are detected by pixels of 50µm pitch, on a honeycomb pattern, each read by a linear electronics. The charges of about 1000 pixels (1% of the total number of 100000) around those that triggered are A/D



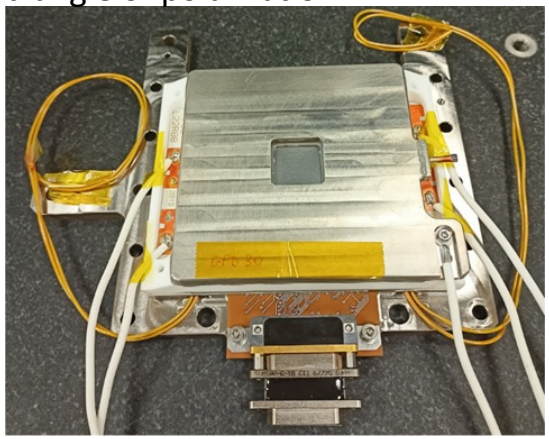
From the analysis we derive the interaction point and the direction of the photoelectron



From the histogram of directions we derive the degree and angle of polarization



With the interaction point we build the psf in the focal plane (IXPE 1mm = 1')



The gas, the GEM and the ASIC are hosted in a sealed box with a 50µ Be window

IXPE
Imaging
X-Ray
Polarimetry
Explorer

Ready for a mission

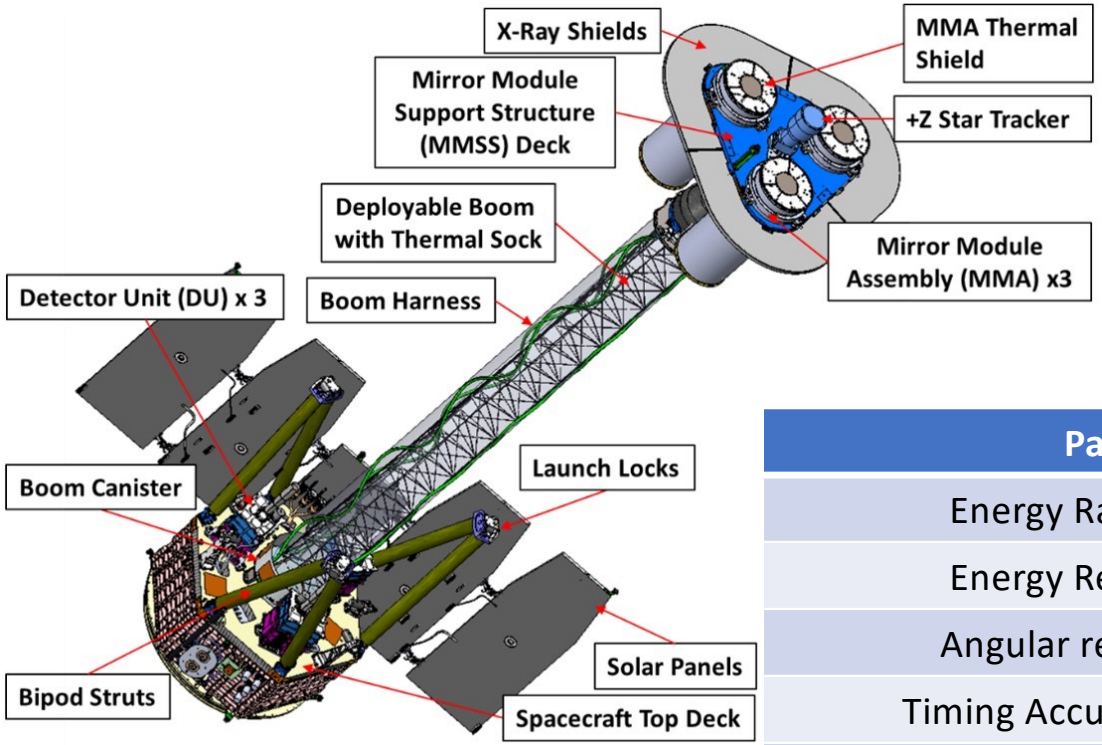
A detector with 0.08 mm resolution capable to measure degree and angle in the focus of a telescope would extend to polarimetry the revolution in sensitivity achieved with Einstein and Chandra.

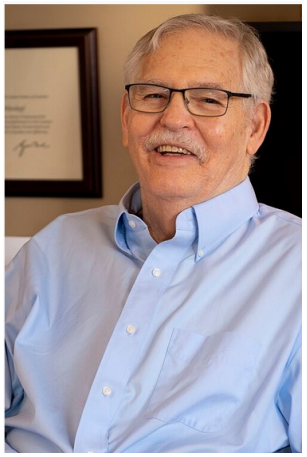
That is the X-ray equivalent of the revolution introduction of Cherenkov telescopes at Very High Energy.

We proposed 10 times (15 with the not hotoelectric). IXPE was proposed on 2014, approved on 2016, launched on 2021.

IXPE
Imaging X-Ray Polarimetry Explorer

THE IXPE OBSERVATORY



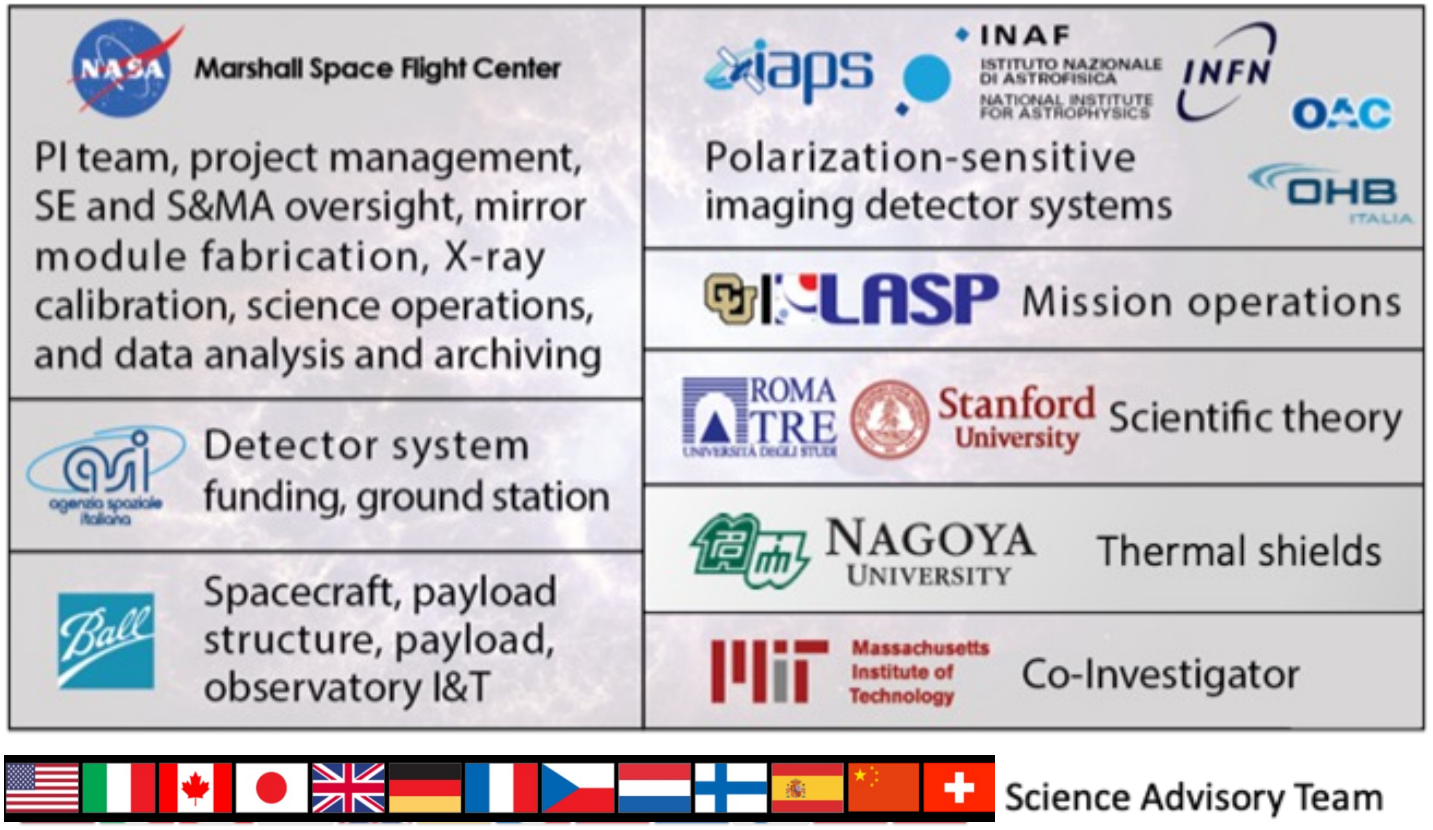


Martin Wisskopf

Parameter	Value
Energy Range	2-8keV (1-12 keV)
Energy Resolution	1.0 keV @ 6.4 keV (scaling as sqrt(E))
Angular resolution (HEW)	30'' (DU-2 and DU-3) and 25'' (DU-1
Timing Accuracy (resolution)	1-2 μs (1 μs)
Minimum Detectable Polarization	5.5% ($F_{2-8} < 10^{-11}$ erg s-1 cm^{-2} (10 days)

IXPE
Imaging
X-Ray
Polarimetry
Explorer

IXPE INSTITUTIONS AND INDUSTRIES



PI Philip E. Kaaret

IXPE
Imaging X-Ray Polarimetry Explorer

WHY WE DO THIS: ASTROPHYSICS!

MORE THAN 110 DIFFERENT SOURCES SO FAR OBSERVED

Class	Objects
11 PWNe and isolated pulsars	Crab PWN, Vela PWN, MSH 15-52, PSR B0540-69, G21.5, 3C 58, PSR B1259-63, KES-75, PSR J1723-283.7, Lighthouse N, PSR J1023 +0038
6 SNRs (7 pointings)	Cas A, Tycho's, NE SN 1006, RCW 86, RX J1713.7-3946, Vela Jr, SN1006SW
17 Accreting stellar-BH	Cyg X-1, 4U 1630-472, Cyg X-3, LMC X-1, SS433, 4U 1957-115, SS 433 Lobes East, LMC X-3, SWIFT J1727.8-1613, 4U 1957+115, Swift J0243.6+6124, Swift J1727.8-1613, GX 339-4, SWIFT J151857.0-572, MAXI J1744-294, SS 433 Lobe West, GRS 1915+105
38 Accreting NS & WD	Cen X-3, Her X-1, GS1826-67, Vela X-1, Cyg X-2, GX 301-2, Xpersei, GX 9-9, 4U 1820, GRO J1008-57, XTE 1701-46, EXO 2030+375, LS V+44 17, GX 5-1, 4U 1624-49, Sco X-1, Cir X1, GX13+1, SMC X-1, SRGA J144459.2-604207, 4U 1538-52, V395 CAR, PSR J1023+00, GX 340+0, GX 3+1, 4U 1728-34, PSR J1723-2837, 4U 1735-44, GX 9+1, GX 349+2, 4U 1538-52, GX 17+2, 4U 1907+09, EX HYDRAE, 4U 1700-377, IGR J17091-3624,H 1417-624,UW CRB
6 Magnetars	4U 0142+61, 1RXS J170849, SGR 1806-20, 1E 2259+586, 1E 1841-045, 1E 1547.0–5408
10 Radio-quiet AGN & 1 Sgr A*	MCG 5-23-16, Circinus Galaxy, NGC 4151, IC 4329 A, Sgr A* Complex, NGC 1068, NGC 4945, NGC 2119, NGC 3227, 1ES 1927+654
21 Blazars & radio galaxies	Cen A, S5-0716-714, 1ES 19-59-650, Mrk 421, BL Lac, 3C 454, 3C 273, 3C 279, Mrk 501,1ES 1959-650, BL-Lac, 1ES 0229-200, PG 1553 -113, S4 0954+65, 1E 2259+586, RGB J0710+591, H 1426+428, 1ES 1101-232, PICTOR A WEST

Some sources have been revisited:

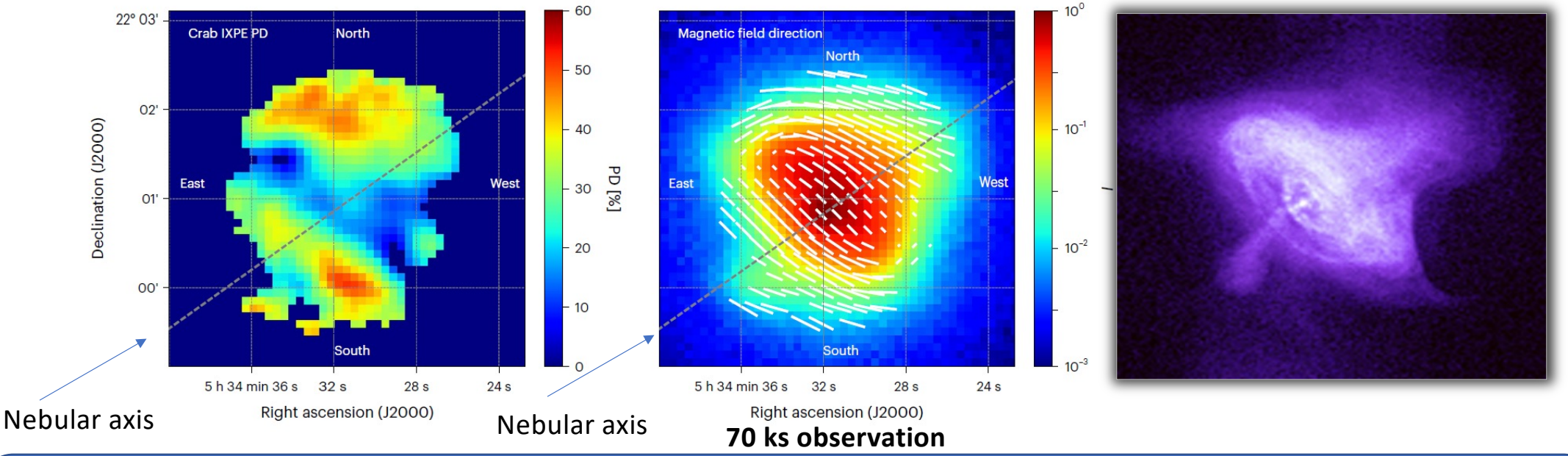
Mrk 421, Mrk 501, BL Lac, Vela X1, Her X-1, MCG 5-23-16, Crab, MSH 15-52, Cyg X-1, Sgr A (complex), NGC 4151 even Crab …

New source classes are being observed such as Galaxy Clusters, recurrent novae, extended black hole jets, and pulsars in binary systems.

About 50 % of the observed celestial sources displayed a polarization with at least 6 σ significance in the Quick Look Analysis (Integrating in time, energy and position). Resolved analysis showed significant polarization on > 80 % of sources.

IXPE
Imaging X-Ray Polarimetry Explorer

CRAB POLARIZATION MAP



Nebular axis

Nebular axis

70 ks observation

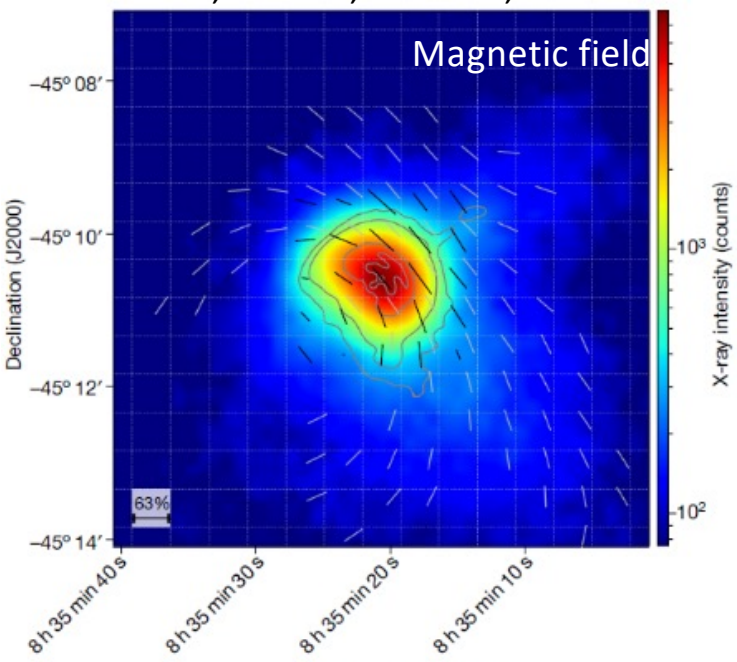
The map of the polarization degree (PD) shows two zones of high polarization and zones with low polarization due to the toroidal magnetic field and changing polarization angle (P.A.) .

The map of polarization degree is not symmetric with respect to the nebular axis. May be instabilities which randomizes the magnetic field are at work in the South-West region.

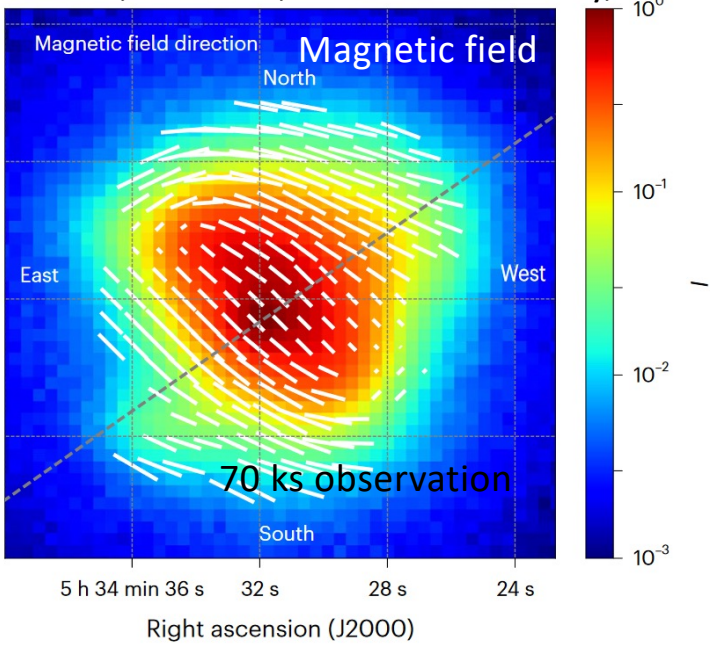
IXPE
Imaging X-Ray Polarimetry Explorer

PWNe: Vela, Crab and MSH 15-52

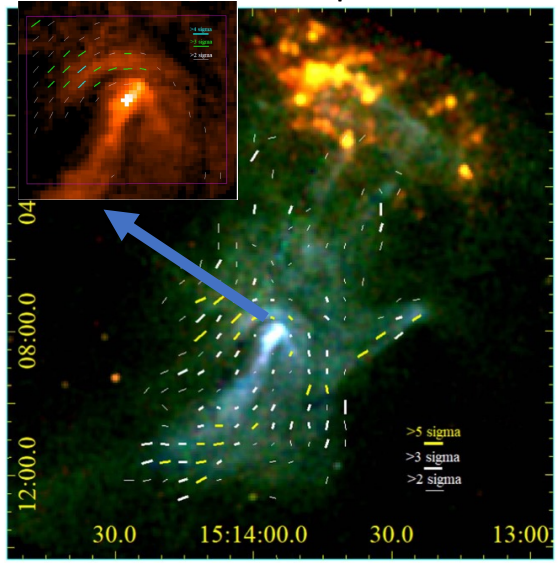
Xie, F. et al., Nature, 2022



Bucciantini, N. et al., Nature Astronomy, 2023



Romani, R. et al., ApJ, 2023

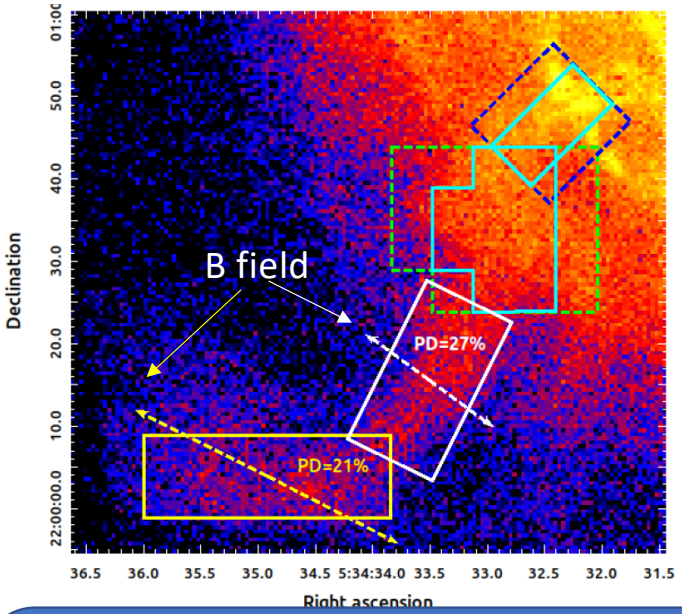


expected.

- **Vela polarization spatial structure symmetric with respect to the spin which is parallel to its proper motion.**
- **Crab IXPE polarization angle is rotated 12o counter-clockwise with respect to OSO-8.**
- **MSH 15-52 IXPE polarization reaches 70% at the base of the jet, in the arc and in the thumb. PSR B1509−58 high polarization at the phase of the maximum**

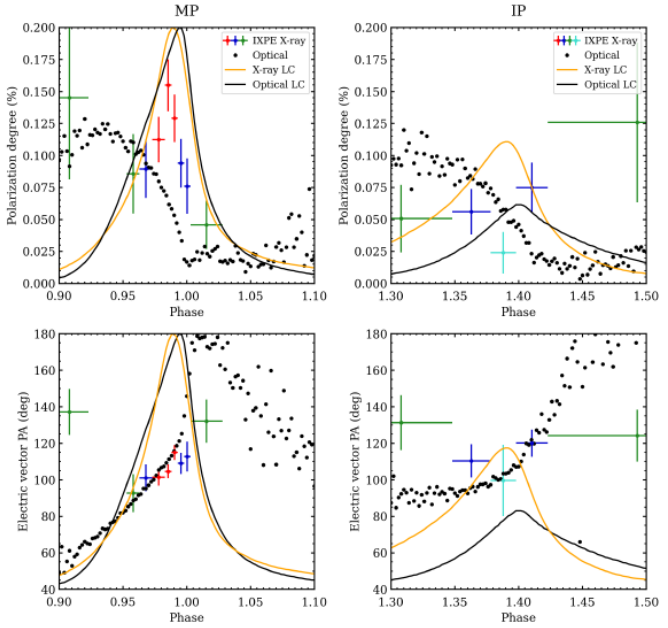
IXPE Imaging X-Ray Polarimetry Explorer

ADDING MORE OBSERVATIONS



300 ks

Wong, J. et al., ApJ 2024
confirming and extending
Bucciantini et al., NatAst2023
first 75 ks observation



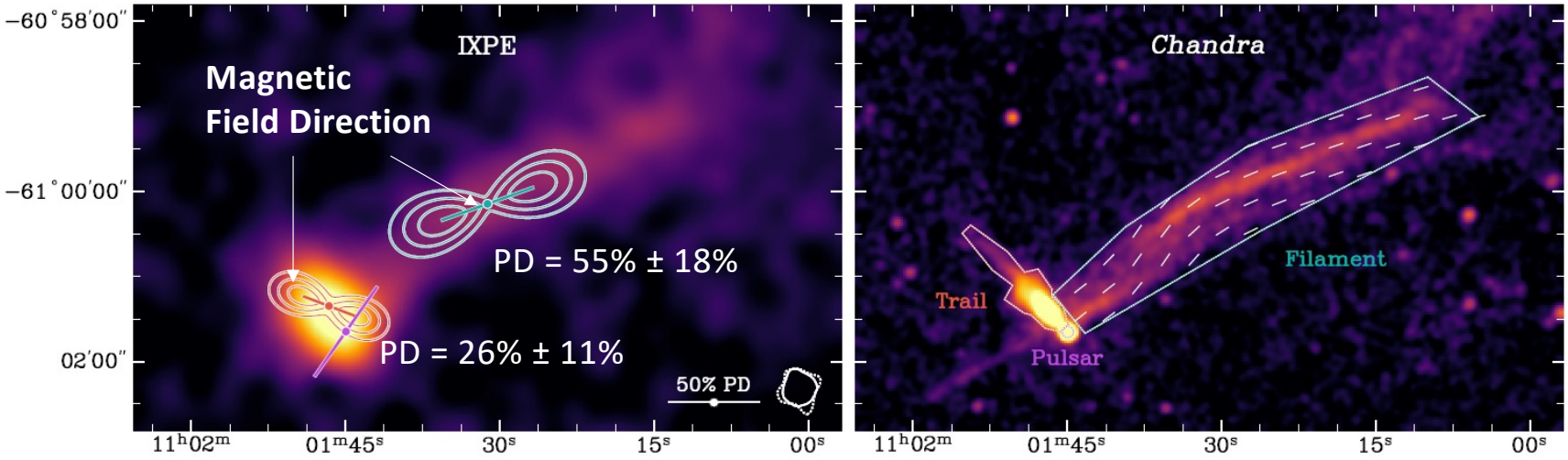
>5σ;
>3 σ
>1.9 σ

- The additional observation of Crab is confirming (Bucciantini et al) nebula while providing additional points especially for the jet with perpendicular and parallel magnetic field (kink instabilities, or collision with a dense medium).
- Pulsar polarization especially for the main pulse are compared with the OPTIMA optical data Slowikowska (2009).
- Deviation in X-rays from the optical polarization degree is evident by the data in the main pulse (but see González-Caniulef et al. A&A 2025).

IXPE
Imaging X-Ray Polarimetry Explorer

LIGHTHOUSE NEBULA

Trails occurr when supersonics pulsar shocks against the interstellar medium (bow-shock + trail)
Rare filaments are proposed to represent cosmic rays (CR) leptons escaping the bow shock onto the ISM

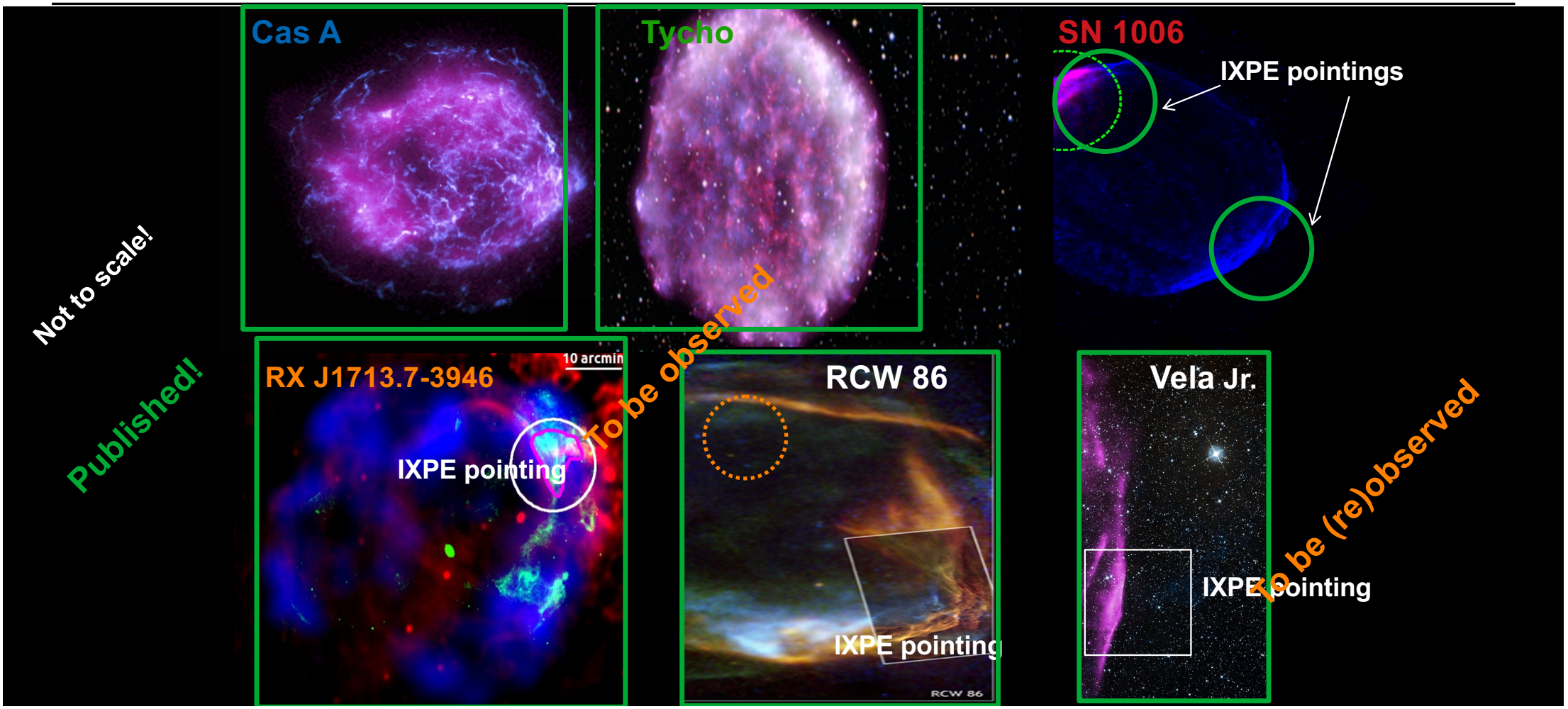


Polarimetry of the filament at 99 % confidence (radio undetected) echoes IXPE results on G0.13-0.11 (Churazov et al., 2024) showing low level of turbulence.
Polarimetry of the trail shows an EVPA almost orthogonal with respect to radio emission (different emitting regions) ?

IXPE
Imaging
X-Ray
Polarimetry
Explorer

(Courtesy of Riccardo Ferrazzoli) SNR with IXPE

THE SIX CURRENT TARGETS



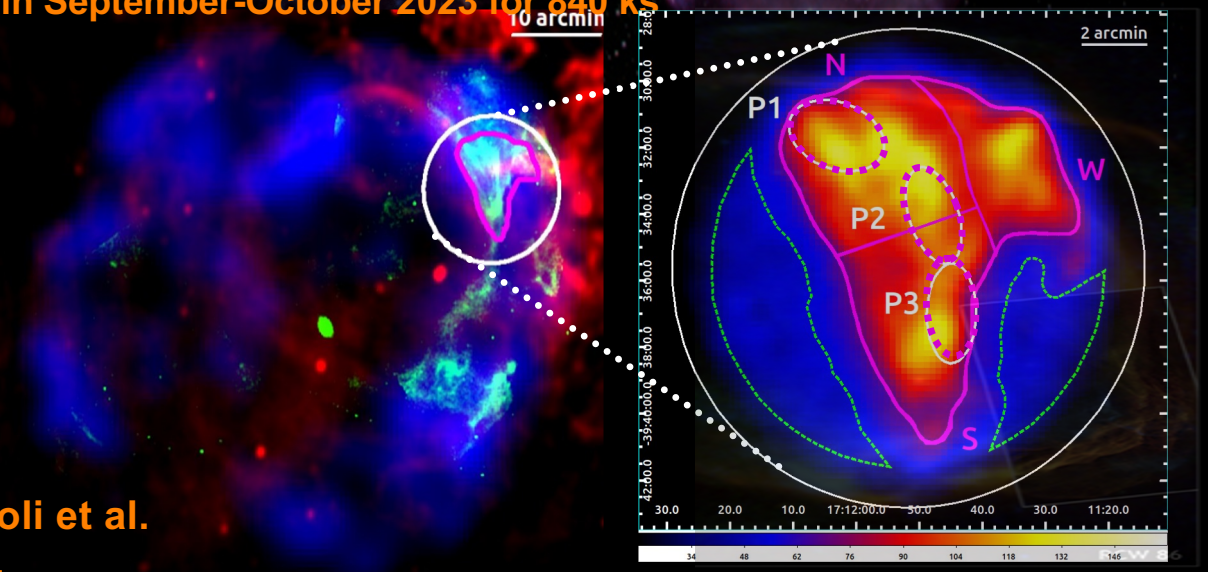
IXPE
Imaging X-Ray Polarimetry Explorer

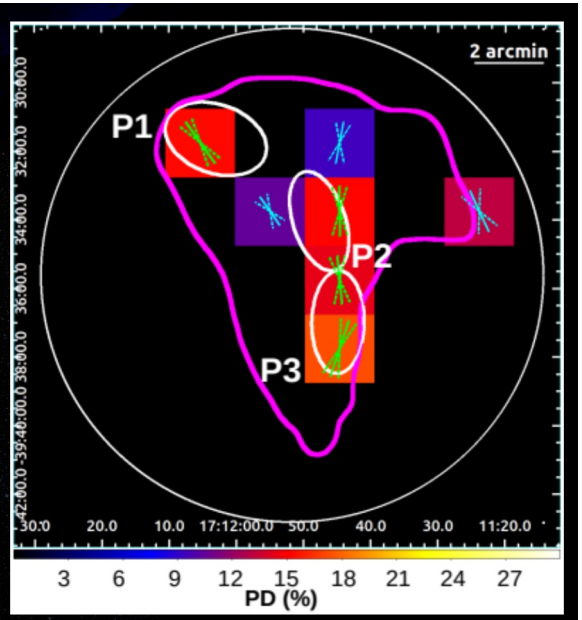
(Adapted from Riccardo Ferrazzoli) SNR with IXPE

RX J1713

- Shell type SNR discovered by ROSAT
- Result of peculiar Ib/c explosion (Core-stripped SN)
- Distance: 1 kpc; Diameter: 18 pc (1°); Age: 1600 yrs (SN 393?)
- Purely non-thermal spectrum (like SN 1006)
- NW region bright in radio, X-rays, Gamma-rays
- No clear polarization measurements from previous Radio observations
- Observed in September-October 2023 for 840 ks

	IXPE XSPEC				Radio
Shell region	PD (%)	PA (°)	Γ	χ/d.o.f.	PD_{radio} (%)
All	12.0 ± 3.1	93.7 ± 7.4	2.11 ± 0.04	1.10	4.5 ± 1.7
N+S	12.5 ± 3.3	96.7 ± 7.6	2.04 ± 0.04	1.02	4.8 ± 1.4
N	12.3 ± 3.8	114.0 ± 8.9	2.10 ± 0.04	0.99	4.8 ± 1.8
S	19.3 ± 4.7	79.0 ± 7.1	2.21 ± 0.05	0.91	4.8 ± 0.9
W	< 25.6	ND	2.04 ± 0.06	1.22	3.2 ± 1.6
P1	25.2 ± 6.7	135.3 ± 7.6	2.16 ± 0.08	0.93	5.6 ± 1.1
P2	35.6 ± 7.6	103.8 ± 6.1	2.21 ± 0.08	0.90	3.5 ± 1.4
P3	36.9 ± 9.1	76.0 ± 7.0	2.23 ± 0.10	1.03	5.2 ± 0.9





R. Ferrazzoli et al.
2024 ApJL

IXPE OBSERVATION OF RX J1713

RESULTS

IXPE detects polarization with **>5σ** confidence from NW limb regions.
PD =13%± 3.5%, similar to Tycho, but **the inferred magnetic field is tangential**
P1, P2, P3 regions: **PD = 20 - 40%**

Magnetic Field Geometry

.First time the magnetic field is mapped in this source: high Faraday rotation in previous radio measurements

.Tangential B-field ⇒ shock-compression of isotropic upstream turbulence

.Contrasts with radial fields in Cas A, Tycho, SN 1006

Gamma-Ray Implications

.X-ray/TeV morphology alignment and **low density** ⇒ **no trigger for radial instabilities** supports l

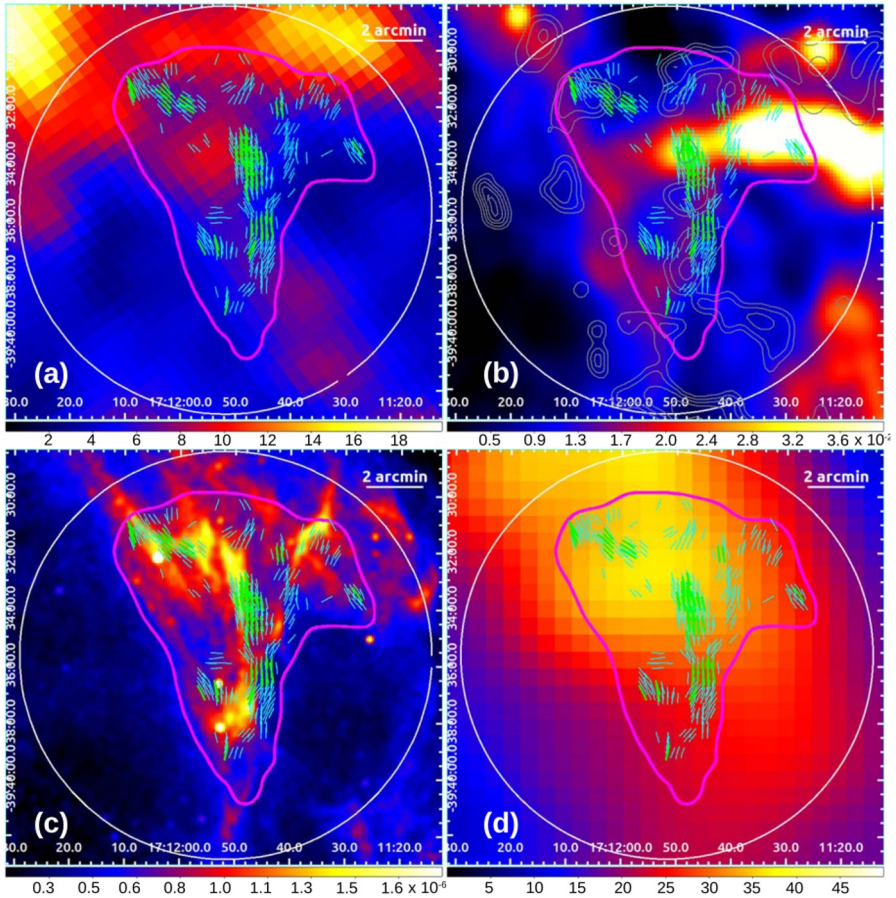
leptonic γ-ray origin (Inverse-Compton)

Environmental Factors

.Low ambient density (**0.01–0.1 cm^{-3}**) correlates with higher PD

.Slower shock speed: **~1800 – 3900 km/s**

.Possible age effect: **~1630 yr**



IXPE Imaging X-Ray Polarimetry Explorer

THE CURRENT PICTURE

X-RAY POLARIZATION MEASUREMENTS AND PROPERTIES

Source	Age (yrs)	B_{low} (μG)	V_s (km/s)	n_0 (cm^{-3})	η	PD (rim) (%)	PD (SNR) (%)	PD (Peak) (%)	B field orientation
Cas A	~350	25 - 40	~5800	~1	~1 - 6	4.5 ± 1.0	2.5 ± 0.5	~15	radial
Tycho	452	30 - 40	~4600	~0.1 – 0.2	~1 - 5	12 ± 2	9 ± 2	23 ± 4	radial
SN 1006 NE	1018	18 - 26	~5000	~0.05 – 0.085	~6 - 10	22.4 ± 3.5	...	31 ± 8	radial
SN 1006 SW			... ...	0.5 - 16	~8 - 16	21.6 ± 4.5		40 ± 8	radial
RX J1713 NW	~1600	~10	~1400 - 3900	~0.01 – 0.1	~1.4	13.0 ± 3.5	...	36 ± 10	tangential
Vela Jr. NW	~1700- 4300	~7	~3000	~ 0.01	~1	16.4 ± 5.2	...	≤70	tangential
RCW 86 SW	~1850	10 - 25	~1000–2000	~ 0.3	~2 - 4	<17	...	...	???

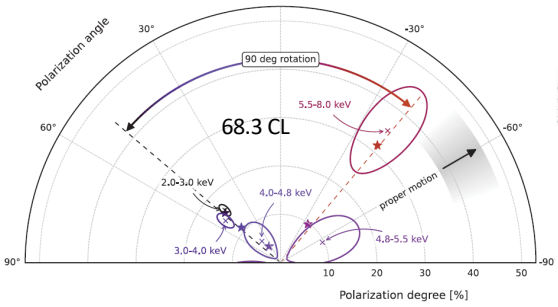
- **Cas A**, **Tycho**, and **SN 1006** all show **radial polarization** at scales dominated by thin rims.
- **PD increases with lower ambient density**: connection with higher levels of turbulence with dense, complex medium?
- Also higher PD for larger Bohm factors? Additional studies w/ higher sensitivity needed.
- **Radial field** associated with development of **Richtmyer–Meshkov instabilities**? Or following regions w/ high acceleration efficie
- **RX J1713 and Vela Jr. shows tangential field**: connected w/ lower shock velocity? Lower magnetic field and density?
- **RCW 86:** only upper limits for polarization, turbulence must be very high, B morphology undefined.

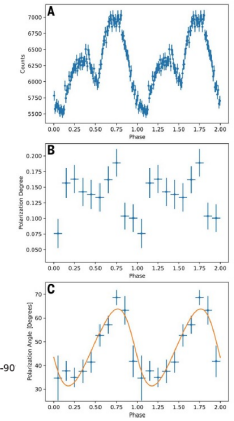
IXPE
Imaging X-Ray Polarimetry Explorer

MAGNETARS

Taverna et al. , Science 2022

4U 0162+61 B=1.5 10^{14} G





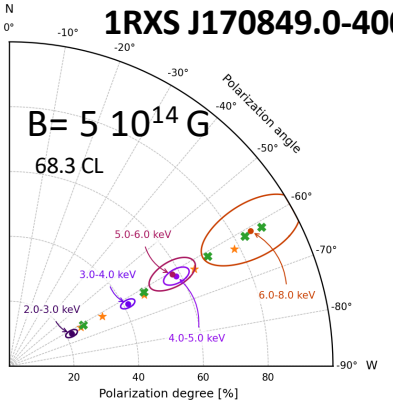
Equatorial belt condensed surface (low energy-O mode). Resonant Compton Scattering at high energy (X-mode)

Black-Body + Power-law

PD = 13.5±0.8%; PA = 48.5°±1.6°

Zane et al. ApJL 2023

1RXS J170849.0-400910



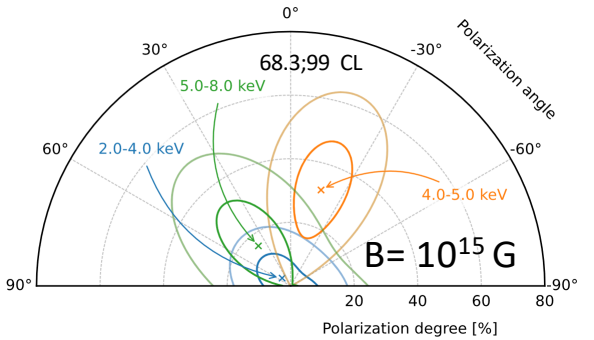
Condensed equatorial belt region (low-P) plus hot polar spot with on-top an atmosphere (high P).

2 Black-Body

PD = 35.1±1.6%; PA = 62.1°±1.3°

Turolla et al., ApJ 2023

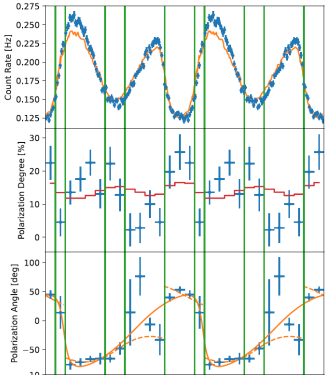
SGR 1806



Only upper limits (record low-flux). Hint of behavior similar to 4U 0162+61

Heyl et al., 2024

1E 2259+586



B= 6 10^{13} G

PD = 5.6±1.4%;

PA =-75.2°±7.4°

Hot condensed spot + plasma loop

The magnetars observed by IXPE have very different polarization dependence with energy may be due to the fact that their atmosphere have different pattern and different physical structure.

Additional magnetars observed by IXPE

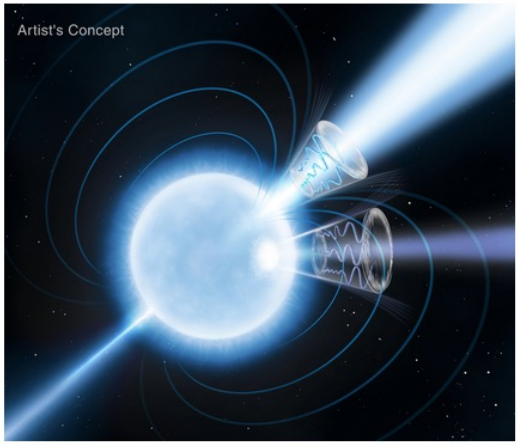
Source	Characteristics	Reference
1E 1841-045	Synchrotron emission of the hard tail component ?	Rigoselli et al. 2025, Stewart et al. 2025
1E 1547.0–5408	Vacuum birefringence	Taverna et al. 2026, Stewart et al. (2026 Nature)
1E 2259+586	Ri-observed after an anti-glitch	BA
EP J223759.5+531421	Recentrly discovered by EP	TBA

Press release just isssued by NASA on vacuum birefringence in a magnetar source

4 MIN READ

NASA's IXPE May Have Proven 90-Year-Old Theory

A first of its kind measurement of a magnetar may have captured empty space behaving in a way physicists have predicted for 90 years, but never directly observed. The results published Wednesday in Nature.



This artist's concept depicts magnetar 1E 1547.0-5408, a rapidly rotating neutron star with magnetic fields over a trillion times stronger than Earth's. Blue curves emanating from the star's two magnetic poles represent the magnetic field lines. The magnetar is a significant emitter of radio and X-ray radiation, with their peaks offset during its 2.1-second rotation period. This indicates the primary X-ray emitter is a secondary "hot spot" offset from the magnetic axis. These emitters are depicted as conical sections: the lighter blue radio emission peaks at the magnetic field's symmetry axis, while the darker blue X-ray emission peaks below. The upper and lower emission cones show X-ray polarization degrees of 40% and 80%, respectively. These high values, along with smooth, coherent variations in polarization across the rotation period, provide the most definitive signal to date of vacuum birefringence a long-sought prediction of quantum electrodynamics.
NASA/Pablo Garcia

nature

View all journals | Saved research | Search | Log in

Explore content | About the journal | Publish with us | Sign up for alerts | RSS feed

nature > articles > article

Article | Published: 05 August 2026

Vacuum birefringence and the polarized X-ray emission from a radio magnetar

Rachael E. Stewart, Hoa Dinh Thi, George Younes, Marcus E. Lower, Matthew G. Baring, Michela Negro, Fernando Camilo, Joel B. Coley, Teruaki Enoto, Alice K. Harding, Wynn C. G. Ho, Chin-Ping Hu, Philip Kaaret, Paul Scholz, Alex Van Kooten & Zorawar Wadiasingh

Nature (2026) | Cite this article

Save article

1E1547-54

You have full access to this article via **Consiglio Nazionale delle Ricerche Direzione Centrale Servizi**.

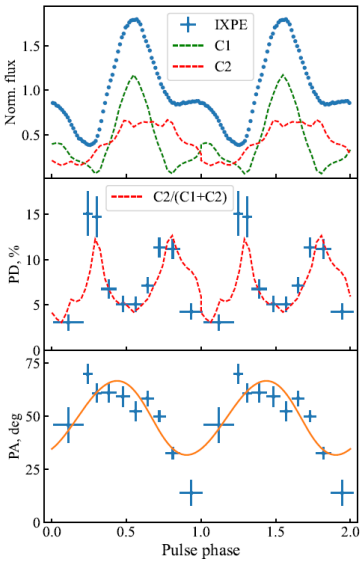
Download PDF

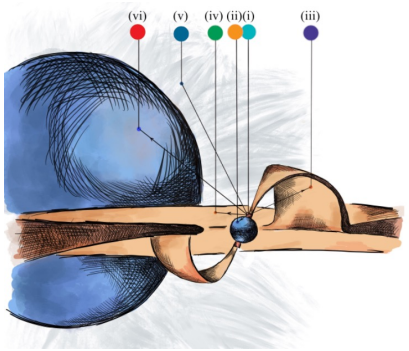
Associated content

Can empty space can interact with light – and even change its properties?

DISENTANGLING THE GEOMETRY OF X-RAY PULSATORS

Cen X-3





Intrinsic polarization from the hotspot

Reflection from the NS surface

Reflection from the accretion curtain

Reflection from the accretion disk

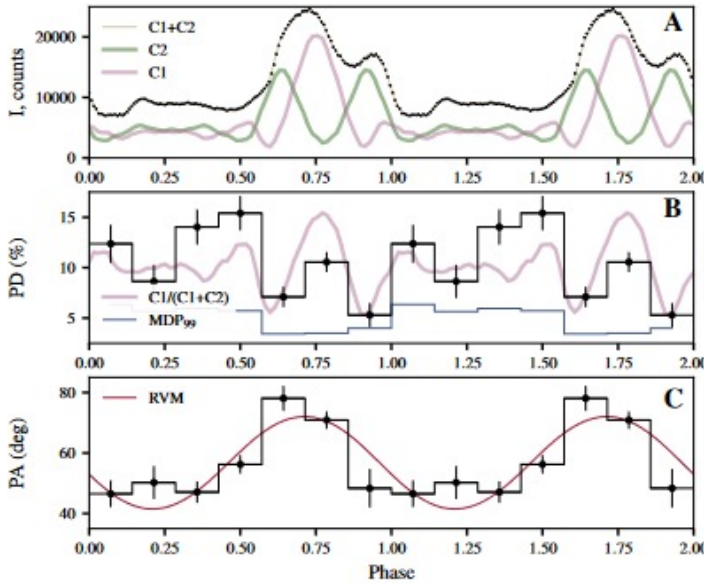
Scattering by the stellar wind

Reflection from the optical companion

$$\tan(\mathrm{PA} - \chi_p) = \frac{-\sin\theta\,\sin(\phi - \phi_0)}{\sin i_p\,\cos\theta - \cos i_p\,\sin\theta\,\cos(\phi - \phi_0)}$$

Rotating Vector model applies to the X-ray binary pulsar

Her X-1



Tsygankov et al 2022

Rotating Vector Model	
Magnetic obliquity	Θ = 16.4(±1.3)°
Inclination	I_p = 70°.2
Position angle	X_p = (49.2 ± 1.1)°

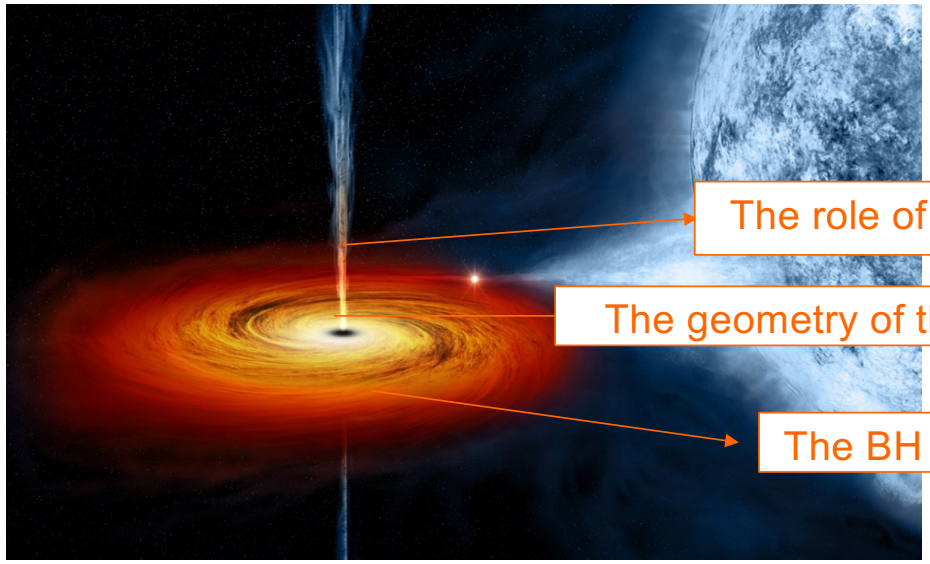
Doroshenko et al., 2022

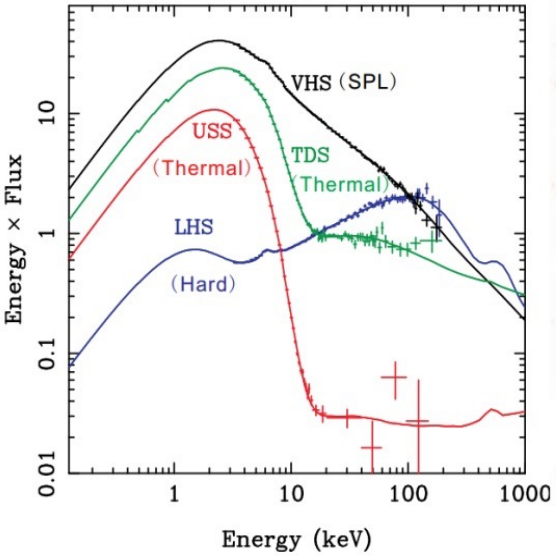
Table 1 | Orbital and pulsar geometrical parameters of Her X-1

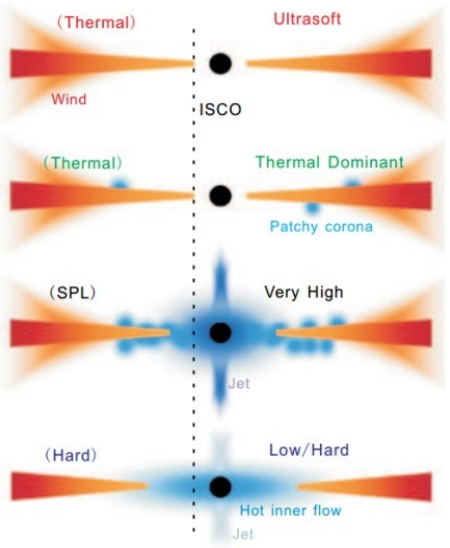
$\chi_{p,*}$	θ	i_p	$\chi_{orb,*}$	i_{orb}
deg	deg	deg	deg	deg
56.9±1.6	12.1±3.7	Eq. (2)	28.9±5.9	100.4±4.9

IXPE Imaging X-Ray Polarimetry Explorer

ACCRETING STELLAR-MASS BH







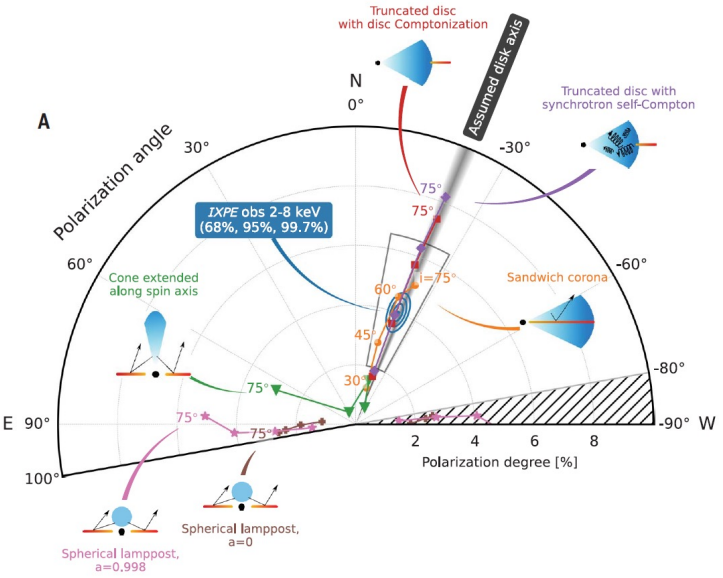
Polarimetry of Black Holes binaries in Hard State can probe the coronal geometry and the jet-Corona interplay.

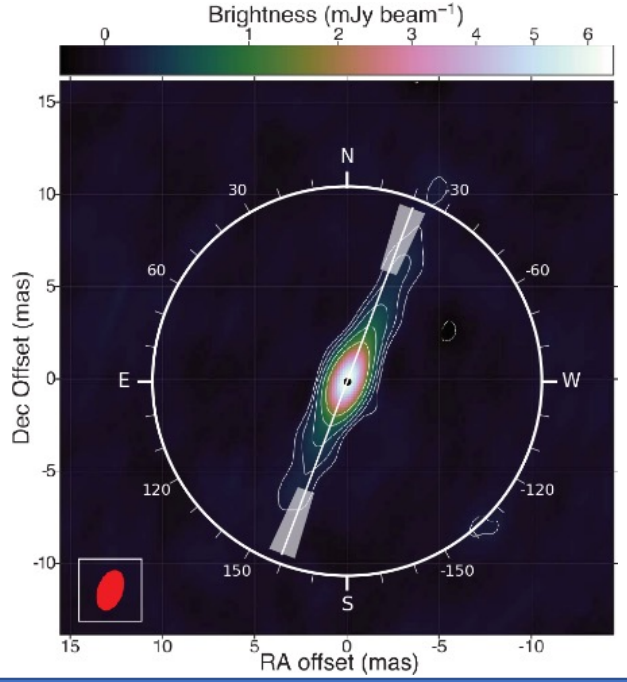
Polarimetry of Black Holes binaries in Soft state can probe the disk geometry and physical status.

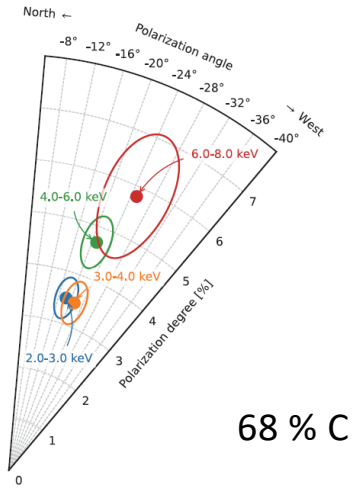
IXPE
Imaging
X-Ray
Polarimetry
Explorer

HIGH MASS BH XRB: CYG X-1

Krawczynski, H. at al, Science 2022







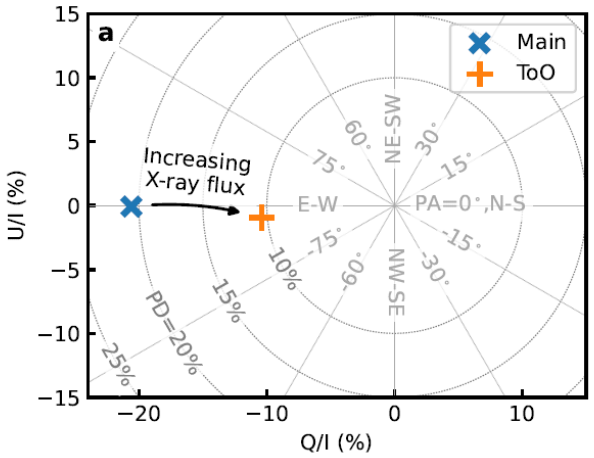
68 % CL

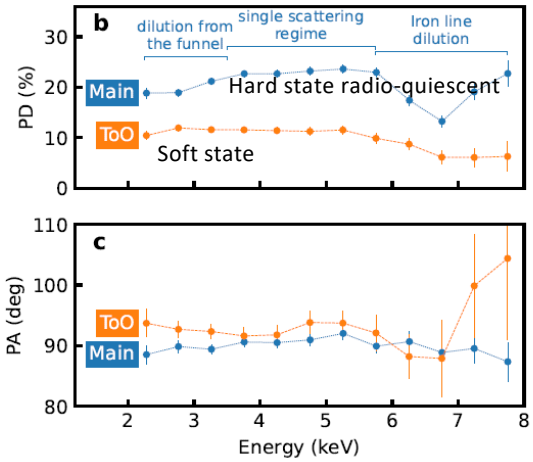
Low hard state.
PD = (4.01 +/-0.20) %
PA = (-20°.7+/-1.4°) i=28°

- **The polarization angle is parallel to the jet axis implying: (1a) the corona is sandwiched to the disk or (1b) an external cold truncated standard disk + an internal region optically thin geometrically thick. (2) the jet is launched perpendicularly to the inner flow.**
- **The polarization degree is larger than expected for the inclination angle I implying that the disk may be warped.**
- **Result consistent with low significance OSO-8 measurement.**

IXPE
Imaging X-Ray Polarimetry Explorer

High Mass BH XRB: Cyg X-3

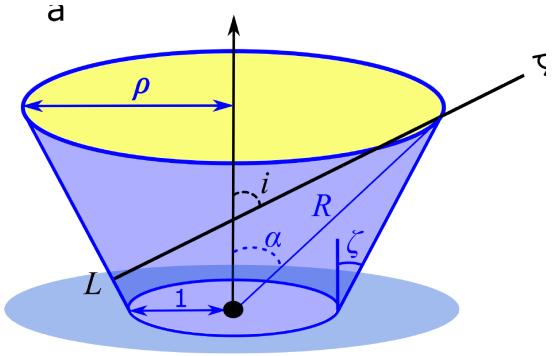




Veledina, A. et al., Nature Astronomy 2024
Veledina, A. A&A 2024.
Mikusincova R. et al., 2026

- Gamma emitter. Complicate behavior
- Companion heavily absorbed on the galactic plane
- Radio Ejection emitted in the north-sud plane
- One-side approaching jet

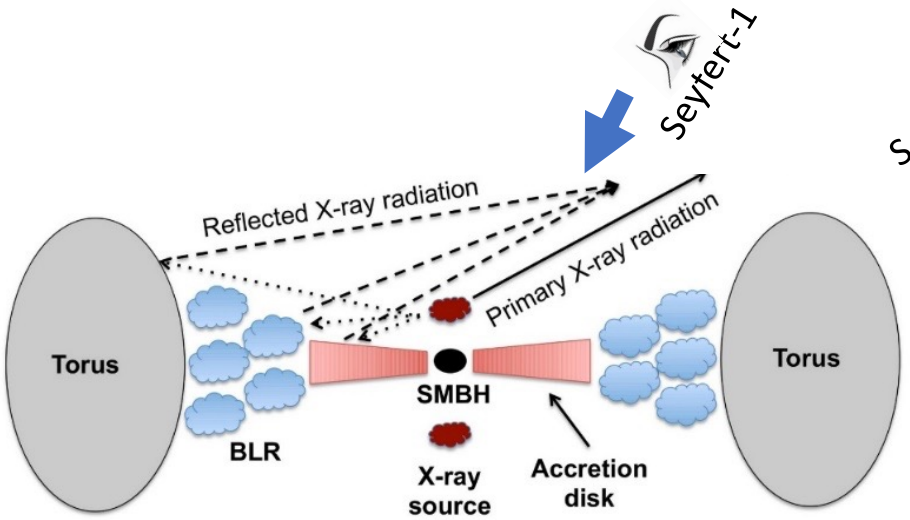
Main:
PD = (20.6+/-0.3)%
PA = (90º.1+/-0º.4)
ToO:
PD = (10.4+/-0.3)%
PA = (92.6+/-0.7)%

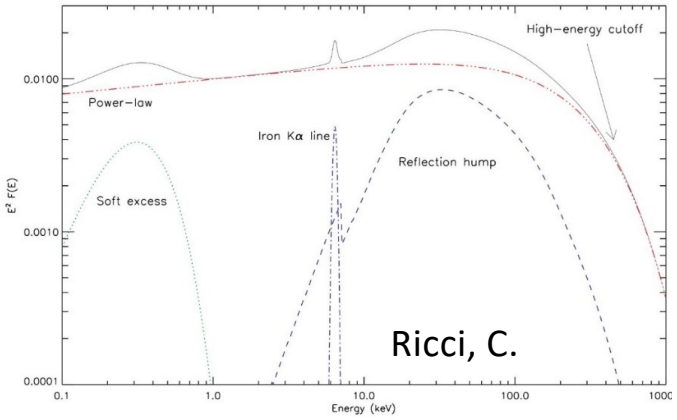


- **The large polarization degree and the angle perpendicular to the plasma emission is modeled as reflection from the inner part of an obscuring funnel (Observation main, low flux)**
- **The decrease of the PD at the same angle is modeled as a change in a funnel parameter when the accretion decreases but also the obscuration decrease providing a higher observed flux.**
- **Cyg X-3 is interpreted as a ULX seen by a side.**

IXPE Imaging X-Ray Polarimetry Explorer

THE RADIO QUIET AGNS

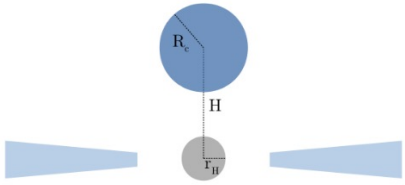




Ricci, C.

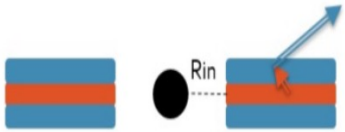
Physical parameters of the AGN's corona are degenerate with respect to geometry. Polarimetry can help to break this degeneration and determine the origin of the corona

Spherical lamppost



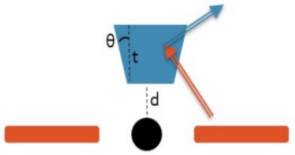
PD: 0-2%
PA: perpendicular to the disc axis;
Phenomenological model

Slab corona



PD: up to 14%;
PA: parallel to the disc axis;
Magnetic loops?

Conical outflow



PD: up to 6%;
PA: perpendicular to the disc axis;
Base of a jet?

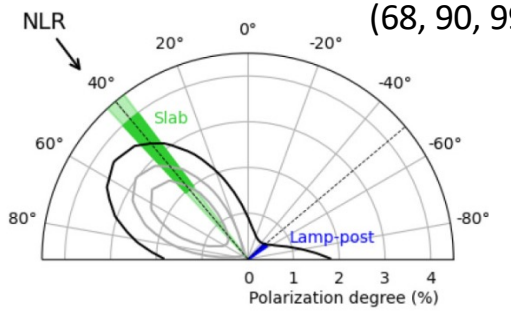
IXPE Imaging X-Ray Polarimetry Explorer

RADIO QUIET AGNS (SEYFERT-1)

Physical parameters of the AGN's corona are degenerate with respect to geometry.
Polarimetry can help to break this degeneration.

MCG-5-23-16 (Sefert-1)
Tagliacozzo, D. et al., MNRAS, 2023

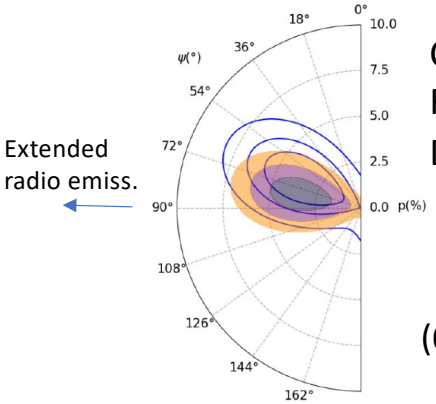
PD < 3.2 % (99 % C.L.)
(68, 90, 99) %



Relativistic ionized reflection + neutral reflection + cutoff power-law (95%)

IC4329A (Sefert-1)
Ingram, A. et al., MNRAS, 2023
3.3+/-1.1 %

Marginal hint of 90°jet

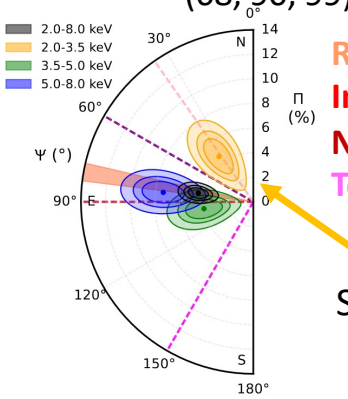


Coronal (66%);
Relat. Refl. (33%)
Distant Refl. (1%)

(68, 90, 99) %

NGC-4151
(Seyfert-1)

Gianolli V, et al MNRAS 2022,
A&A 2004 Submitted.
PD=4.5±0.9%,
(68, 90, 99) %



Radio emission
Inner few pc jet
Narrow Line Reg.
Torus axis

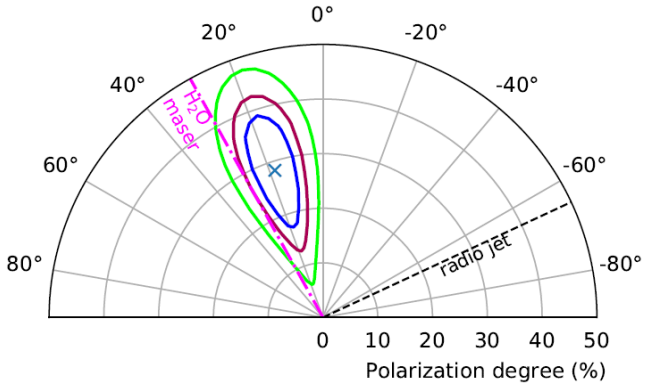
Scattering ?

Polarimetry of NGC 4151 showed the corona of the primary emission is not a lamp post but it is parallel to the disk.
MCG-5-23-16 and IC4329A suggest with low significance the same geometry.

IXPE
Imaging
X-Ray
Polarimetry
Explorer

RADIO QUIET AGNS (SEYFERT-2)

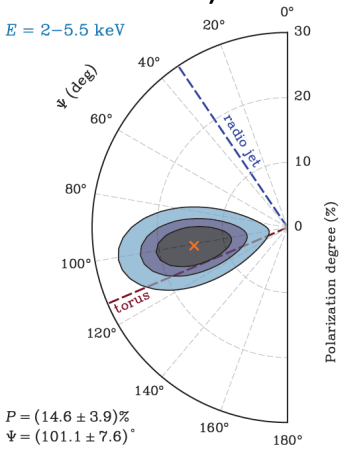
Circinus galaxy (Compton thick)
Ursini et al., MNRAS 2023



68 %, 90 % 99 %

The cold reflector (torus) IXPE measured a 2-6 keV polarization of:
P = 28 %+/- 7% and Theta = 18° +/-5°

NGC-1068 (Seyfer-2 archetypical)
(Marin et al. 2024)



68 %, 90 % 99 %

1.15 Ms observation!
P=12.4%±3.6%
Theta=100.7°±8.3°

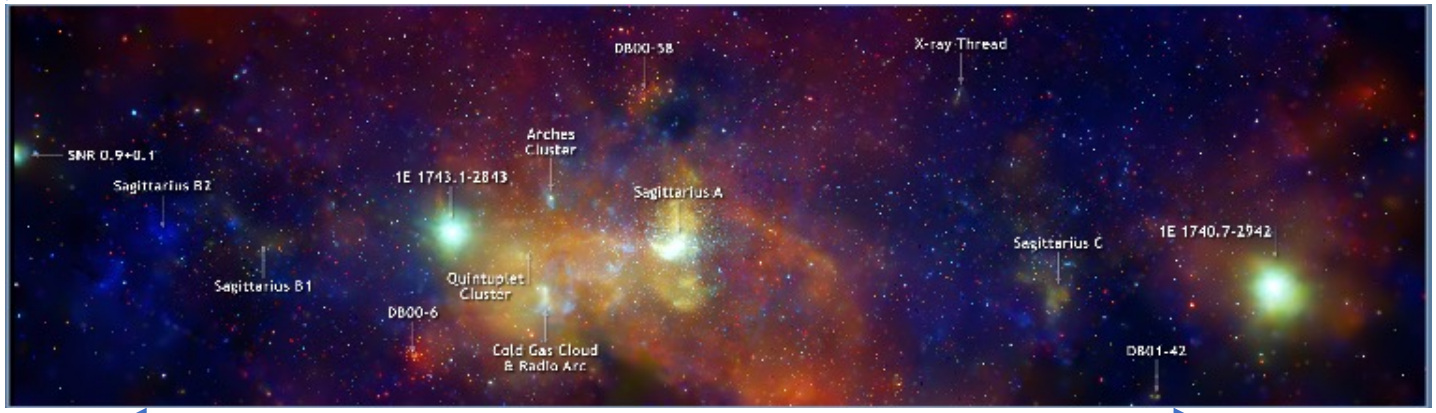
Assuming a polarization due to the warm reflector (conical winds) similar to UV.
The torus reflection is polarized P = 20%+/-10%
Theta=102°+/-15°

X-ray spectro-polarimetry in Circinus galaxy and NGC-1068 showed that the pc-scale torus axis and the radio jet are aligned. The torus is responsible for the reflected radiation

900 x 400 LY OF THE GALACTIC CENTER AS SEEN IN X-RAYS BY CHANDRA

117 arcmin; color code : **1-3 keV** ; **3-5 keV**; **5-8 keV**

36 arcmin



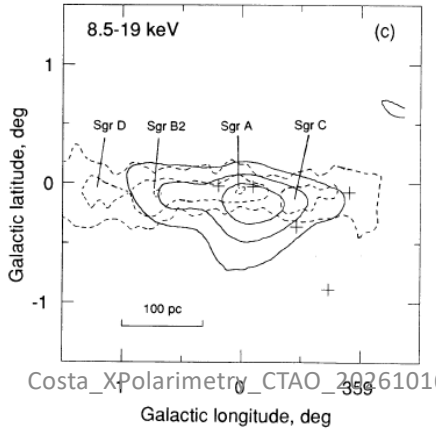
Center Nebular Zone

Sunyaev et al., 1993

Sgr B2

Sgr C

Sgr A Complex



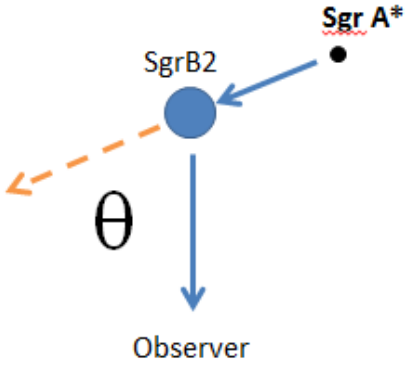
Art-P on GRANAT

Sunyaev et al., suggested that part of the emission in the galactic center region could be due to Thomson scattering by dense molecular clouds of the radiation coming from the galactic center.

CHURAZOV, SUNYAEV & SAZONOV PROPOSED TO USE X-RAY POLARIMETRY !

X-ray polarimetry can definitively proof or reject this hypothesis.

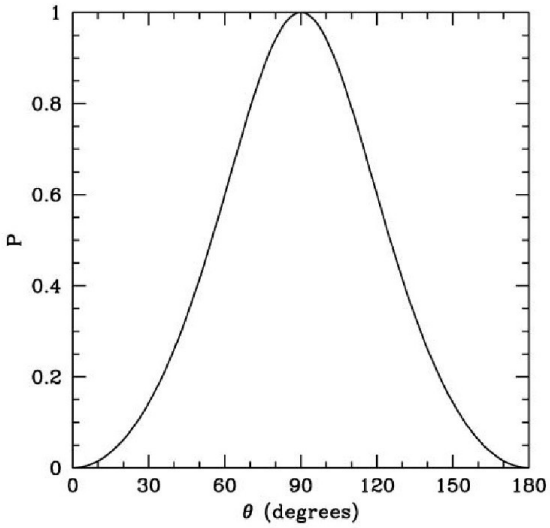
Molecular clouds should be highly polarized with the electric vector perpendicular to the line connecting the two sources.



$$P = \frac{1-\mu^2}{1+\mu^2}$$

$$\mu = \cos\theta$$

The polarization direction of the scattered radiation is **perpendicular** to the scattering plane.

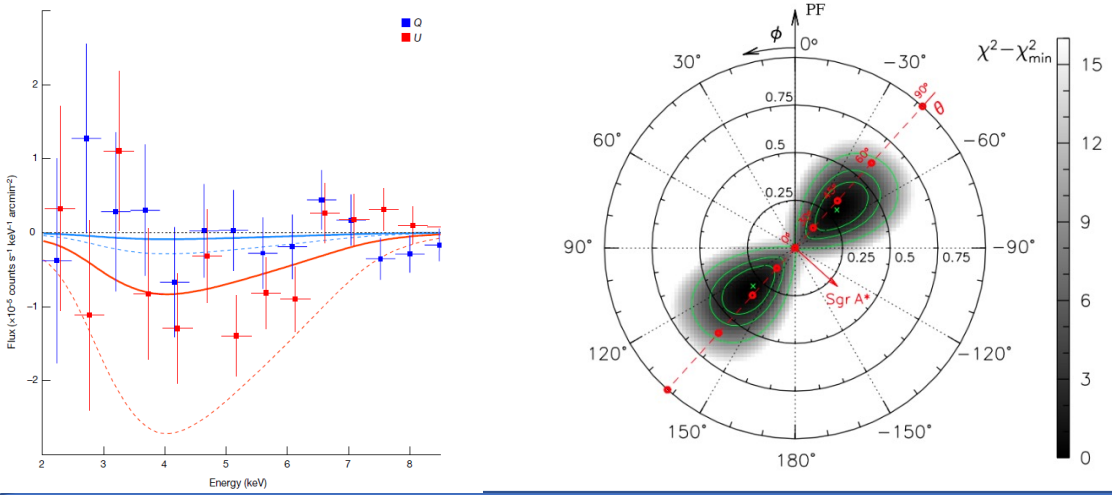


The degree of polarization would measure the angle and provide a full 3-d representation of the clouds (Churazov, Sunyaev & Sazonov, 2002)

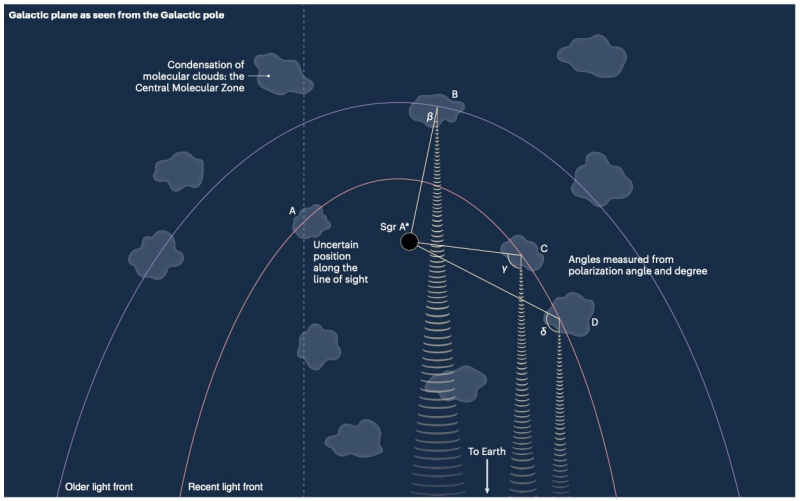
IXPE
Imaging X-Ray Polarimetry Explorer

THE GALACTIC CENTER WAS ACTIVE 200 YEARS AGO !

Marin, F., Churazov, E. et al., Nature 2023



Ponti et al., N&V 2023



Very difficult measurement!

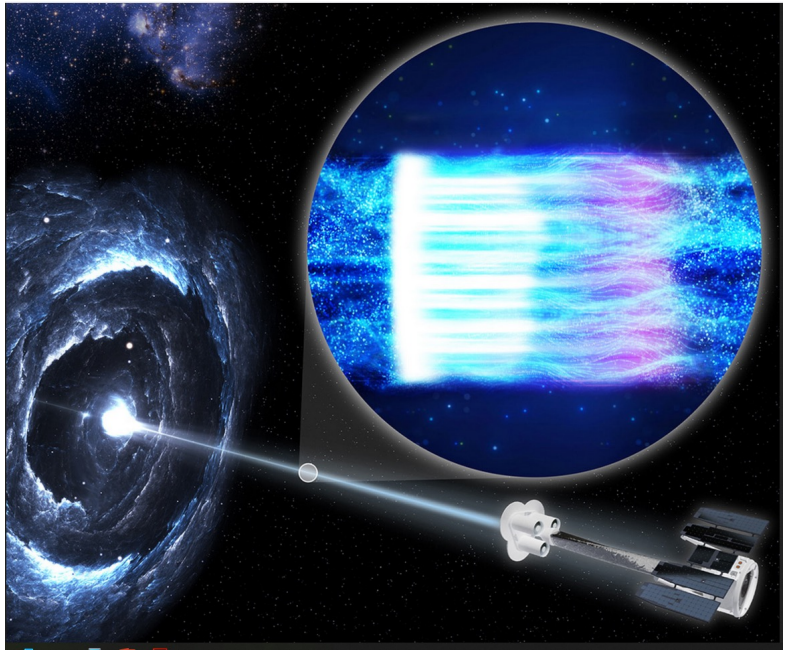
2.8σ result. P = (31 +/-11)% θ = -48°+/-11°

Polarization angle consistent with Sgr A* as the origin of the illuminating radiation.

From the polarization degree, two solutions for the age of the burst: ~30 or ~200 years ago. Second solution much more probable a flare 30 years old should have been visible by ASCA who detected bright molecular clouds but dim SgrA*. A second observation of SgrA Complex (Khabibullin et al., ApJ 2026) increased the significance to 4.1 σ.

IXPE Imaging X-Ray Polarimetry Explorer

BLAZARS



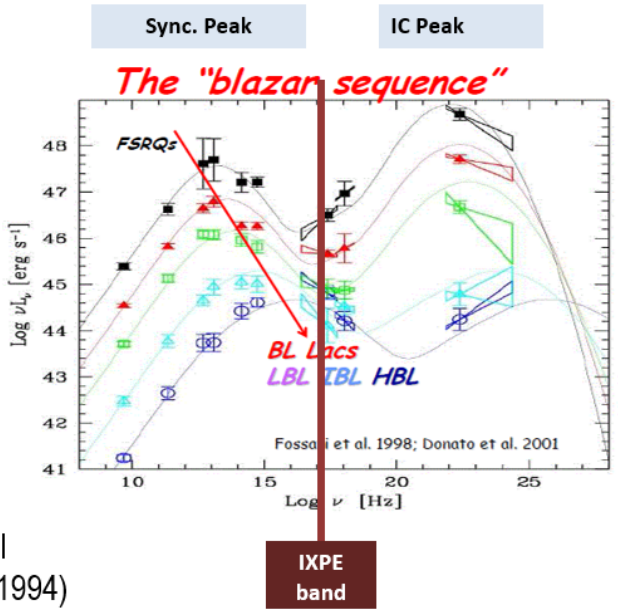
Synchrotron-dominated (with X-ray)

Blazars, multi-λ polarimetry probes **the structure** of the jet and of its **magnetic field**

Inverse Compton dominated (with X-ray)

Blazars, multi-λ polarimetry observations can determine:

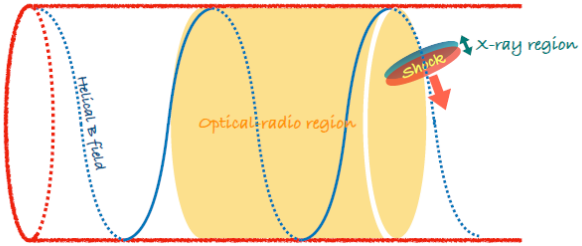
- **the composition of the jet** (hadronic vs. leptonic, Zhang & Bottcher, 2013)
- **the origin of the seed photons** Synchrotron-Self Compton (SSC) or External Compton (EC) (Celotti & Matt, 1994; Poutanen 1994)



A blazar is an active galactic nucleus (AGN) with a relativistic jet directed closely towards the observer. Relativistic beaming from the jet makes blazars appear much brighter than they would be if the jet were pointed in a direction away from Earth.

MRK 421: X-RAY POLARIZATION ANGLE ROTATION

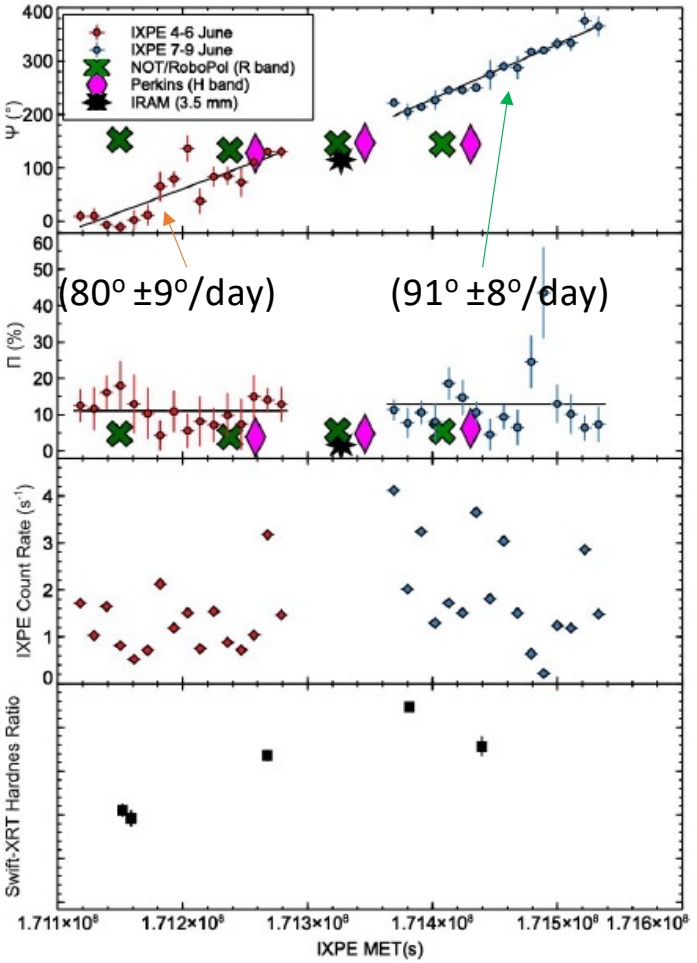
- During X-ray rotation millimiter-wave, infrared and optical polarization angle didn't vary substantially.
- Rotation in optical light is few-few tens of degree/day
- PD_X was roughly constant and higher wrt Optical, Infrared and Radio
- At GeV was in a quiescent state



A model may explain the observed rotation is a shock propagating along the helical magnetic field down the jet.

Note: PG1553+113 showed a rotation in optical and infrared but no in X-ray

Di Gesu L. et al., Nature Astronomy 2023



IXPE Imaging X-Ray Polarimetry Explorer

WHAT ABOUT INVERSE COMPTON DOMINATED BLAZARS ?

3C273, 3C 279, 3C 454.3, S6 0716+714 only upper limits 9-38 %

Table 1. Summary of IXPE Observations

Source	Instrument	Observation ID	MJD range	Exposure (ks)[a]	Π_X[b]
3C 273	IXPE	01005901	59732.37 - 59734.45	95.28	$< 9.0\%$
3C 279	IXPE	01005701	59743.02 - 59748.85	264.42	$< 12.7\%$
3C 454.3	IXPE	01005401	59730.19 - 59732.34	98.12	$< 28\%$
S5 0716+714	IXPE	01005301	59669.43 - 59674.80	358.68	$< 26\%$

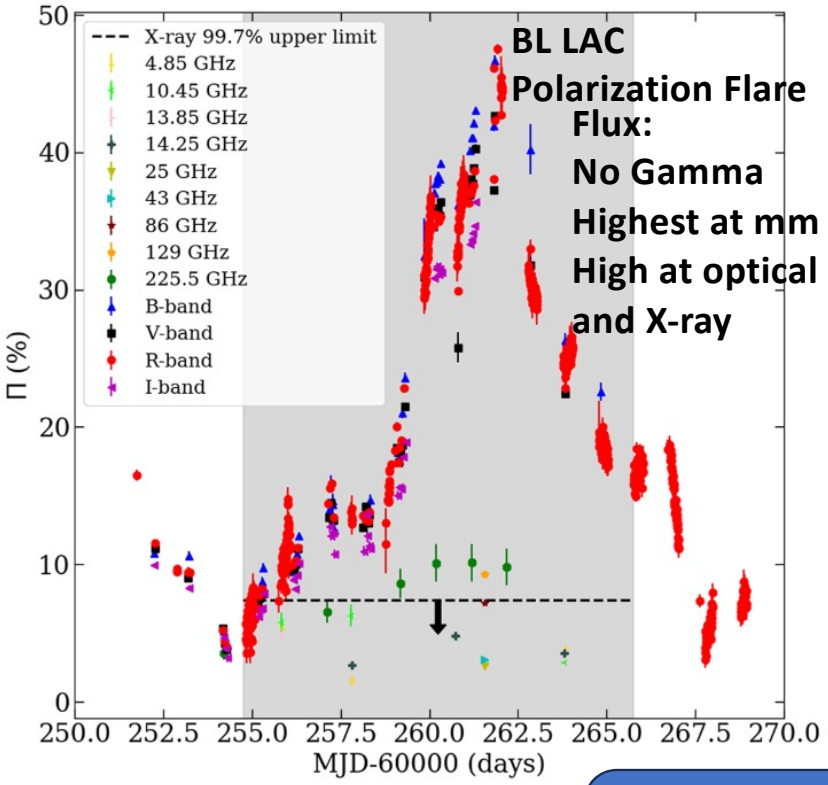
[a] Average of exposures for the three detector units.

[b] 99% confidence limits using the unbinned, event-based likelihood method (§ 2.1).

Marshall, H. et al. in Astro-ph, 2024

IXPE Imaging X-Ray Polarimetry Explorer

BL LAC POLARIZATION FLARE



Agudo et al., 2025

Table 1
Summary of the Multiwavelength Polarization Expectations for Different X-Ray Emission Scenarios Outlined in the Text

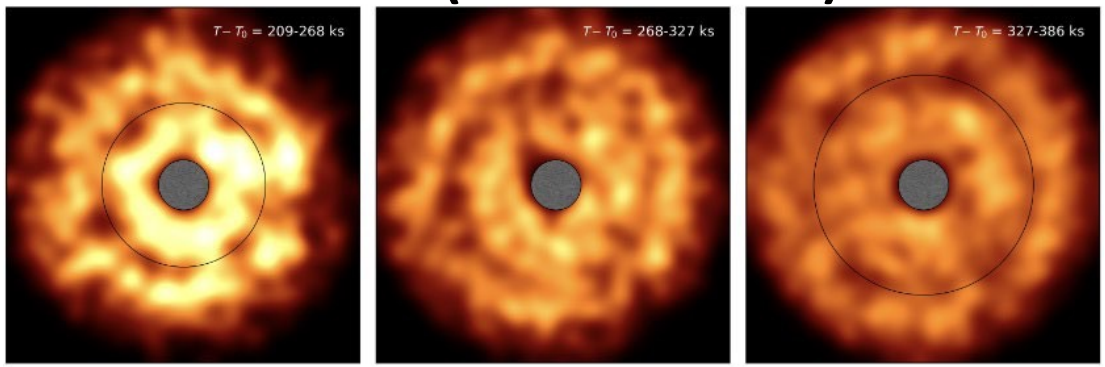
Model	X-Ray Polarization Degree	X-Ray Polarization Variability
Single-zone leptonic (EC)	Unpolarized	···
Single-zone leptonic (SSC)	$0.5 \times \Pi_O$	Similar to optical
Energy-stratified/multizone leptonic (SSC)	$\leqslant 0.3 \times \Pi_O$	Similar to millimeter
Single-zone hadronic	$\approx \Pi_O$	Less variable than optical
Energy-stratified/multizone hadronic (flare)	$\approx \Pi_O$	Less variable than optical
Energy-stratified/multizone hadronic (nonflare)	$\approx \Pi_{mm}$	Similar to millimeter

The observation of Bl Lac showed that the U.L. in X-ray polarization is smaller than a factor of 6 with respect to optical polarization. This rules out all the single zone hadronic model .

IXPE REPOINTING > 3 DAYS, USUALLY 1-2 WEEKS
IXPE ENERGY BAND (2-8 KEV) IS VERY NARROW

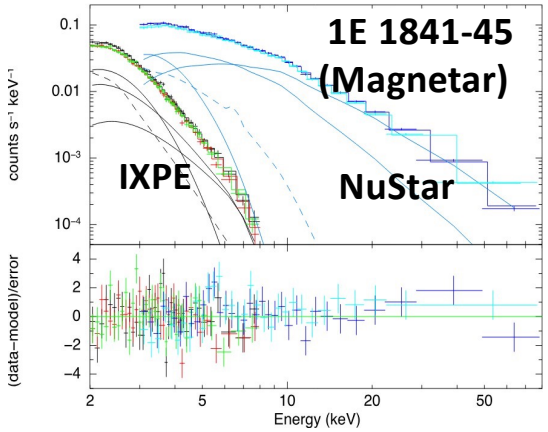
IXPE Imaging X-Ray Polarimetry Explorer

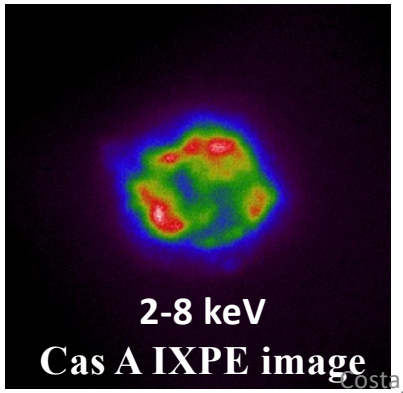
The BOAT (GRB 221009A)

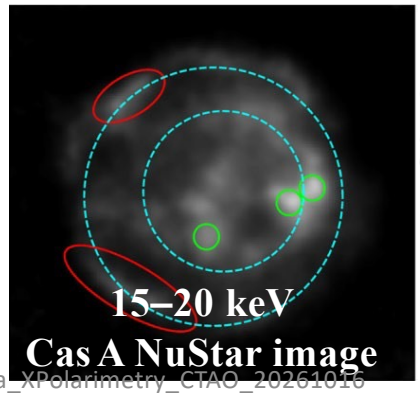


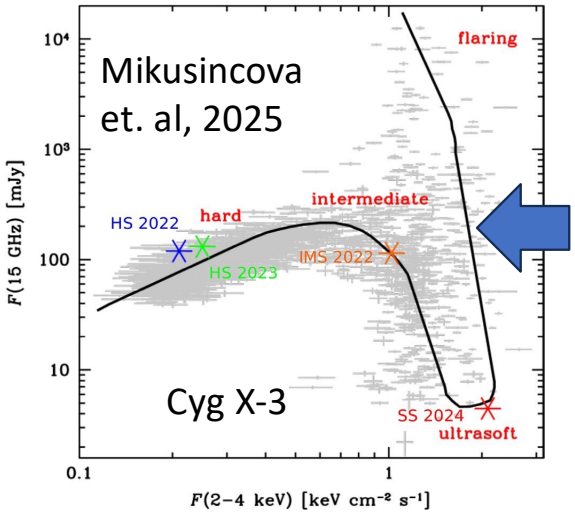
IXPE fastest reaction time ever (3-days) Negro, M. et al., 2023

Prompt emission < 53%; Afterglow < 13 % (very coarse!)





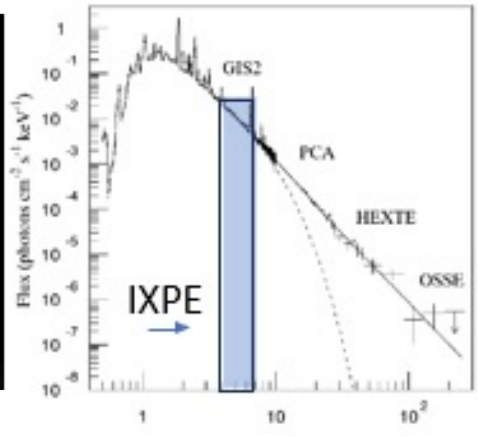




What is the interaction between the jet and the accretion disk ?'

The polarization during the flaring state will be unknown with IXPE.

Need a fast repointing about hours



IXPE uses a narrow energy band with no lines.

E> 6 keV only non thermal emission could be probed by polarimetry

IXPE
Imaging
X-Ray
Polarimetry
Explorer

The limits of IXPE (a SMEX!)

The last Senior Review approved IXPE until February 2018. The subsequent could be approved until 2021. Technically the instruments are expected to perform to that date.

Some of these limits derive from the fact that IXPE is a SMEX (Small Explorer Mission) namely with a tight boundary of mass, budget and time schedule and can be overcome with a more ambitious mission.

Some other can be solved with an adequate R&D

But what is arriving in a near future?

What in a more remote future?

enhanced X-ray Timing Polarimetry Explorer (eXTP): The main after IXPE.

A mission approved by the Chineese Academy of Science (CAS) and Chineese Space Agency (CNSA) to be launched in 2030.

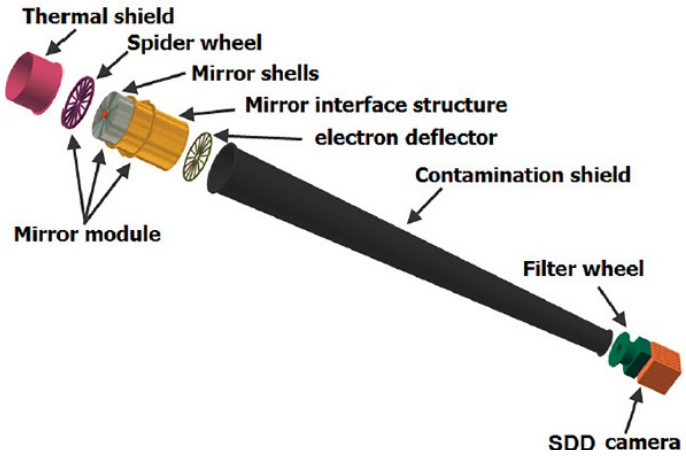
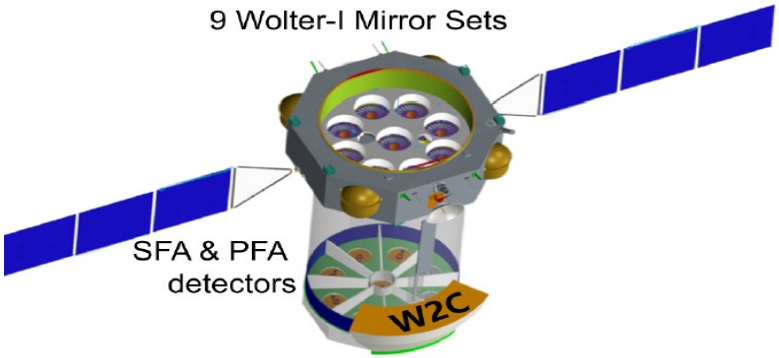
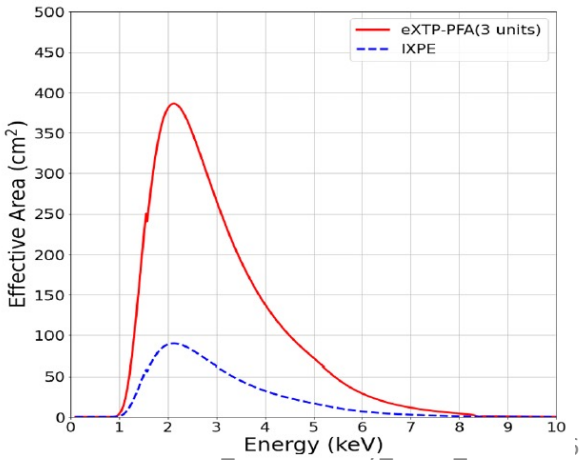


Table 5 PFA specifications (3 telescopes with GPD at focal plane)

Indicator	Requirement
Total effective area	$\geqslant$ 180 cm^2@3 keV
Energy range	2-8 keV
Energy resolution (FWHM)	$\leqslant$ 1.8 keV@6 keV
Field of view	$9.8' \times 9.8'$
Angular resolution	HPD $\leqslant 30''$@3 keV
Time resolution	$\leqslant$10 μs
Dead time	$\leqslant$ 10%@1 Crab
Polarization modulation factor	$\geqslant$ 50%@6 keV
Minimum detectable polarization	$\leqslant$ 3% (1 mCrab, 10^6 s)





- 3 Telescopes
- Same band than IXPE: (Ni coated optics, DME detector filling, similar ASIC with less dead time but a slightly lower modulation factor)
- Larger area
- Contemporary observation with more sensitive instruments: an effective help to disentangle spectral components but also to discourage long pointing of weak sources.
- More TOOs also triggered from the Wide Field Monitor. Much faster than IXPE. Could arrive to 20m.

But we are thinking to something more ambitious

- **An extension of the band** to include all the major physical situations not covered by IXPE (e.g. Cyclotron, Reflection bump, Hard Tails, shocked features above the thermal range)
- The capability to perform high Sensitivity **polarimetry of transients** with a re-pointing capability equivalent to Swift (or better).
- A significant **improvement of the angular resolution**

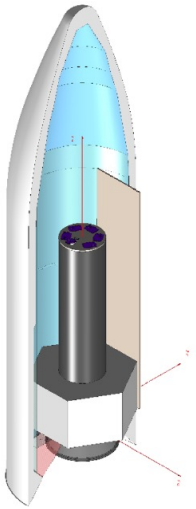
We proposd the **Enhanced X-ray Polarimetry Observatory (EXPO)**

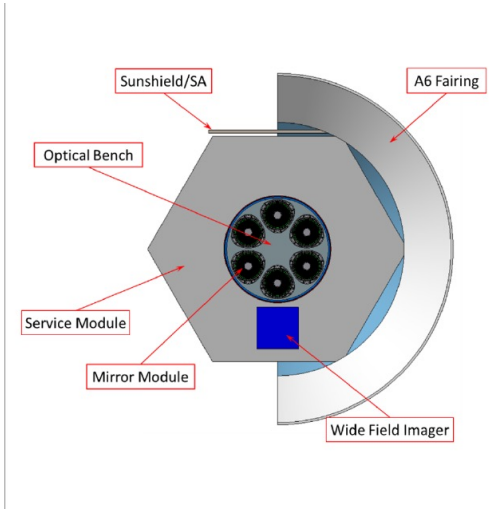
IXPE
Imaging X-Ray Polarimetry Explorer

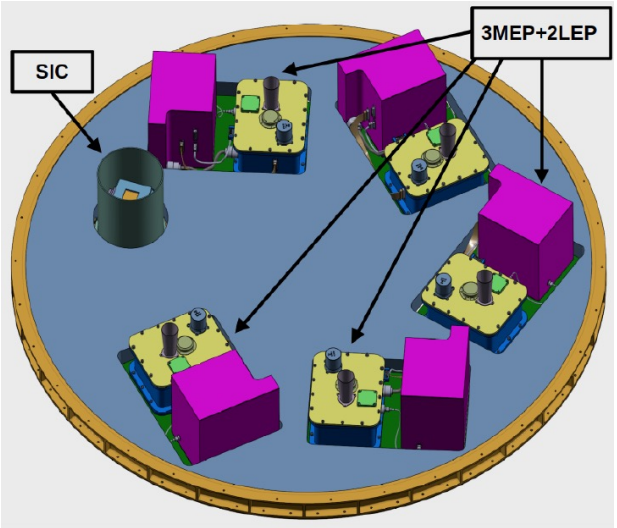
A MISSION PROPOSED TO M-8

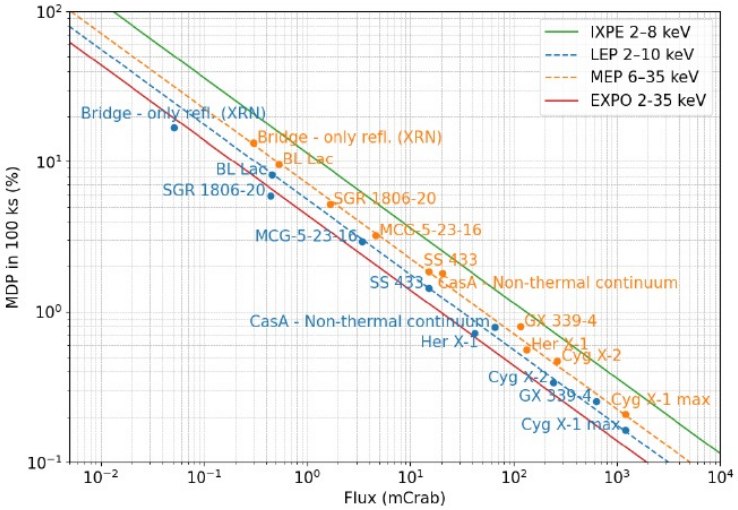
ESA M-8 proposed mission
EXPO Enhanced X-ray Polarimetry Mission

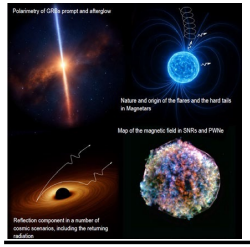
- **High Sensitive Imaging Polarimetry 2-35 keV** energy band.
- **Autonomous on-board detection (WFI) of Fast Transients** (GRBs, Magnetar Flares) **SWIFT like repointing** system.
- **Spectral-Imaging Camera (SIC)** to make **precise spectroscopy** (0.5-30 keV).













FEATURE OF EXPO

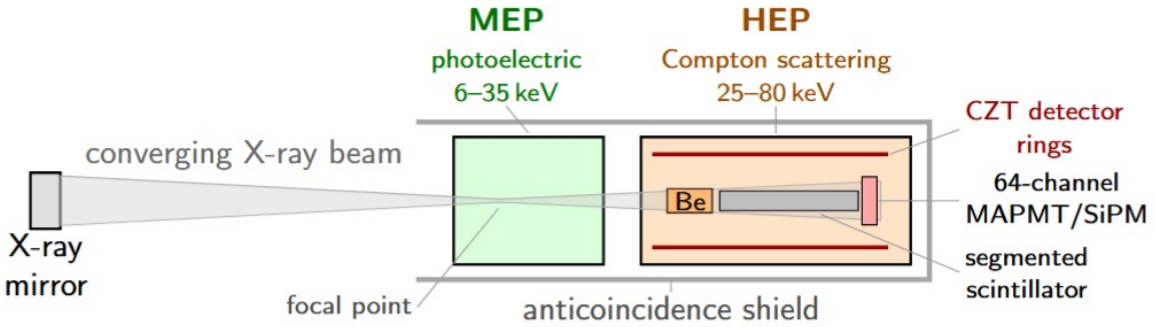
What more than IXPE

- An energy band 4 times larger than IXPE (2-35 against 2-8 keV)
- An area 3 times larger than IXPE (in the overlapping band)
- An angular resolution 1/3 of IXPE (HEW 10'' versus 30'')
- A background expected 20 times smaller than IXPE
- A fast (Swift-like, 1°/s) repointing capability 8000 times faster than IXPE
- An autonomous capability to detect and localize transients in 1/6 of the sky
- A telescope auxiliary to the polarimeters

IXPE Imaging X-Ray Polarimetry Explorer

A further increase of band. Ballon-borne scattering polarimetry

WUSTL, INAF-IAPS, KTH, OsakaU, KyiotoU, HiroshimaU



H. Krawczinsky PI

Goal 1. The design of different polarimeter stacks focusing on a LEP, MEP, and HEP stack (for a satellite) and a MEP, and HEP stack (Ballon).

Goal 2. The fabrication and testing of an flight ready MEP and HEP stack

Goal 3. the fabrication and testing of an flight ready MEP and HEP stack;

APRA funds request duration 3 years starting from feb. 2027 if funded.
Followed by a request of funds for a ballon-borne experiment.

The philosophy

If your detector cannot be local, as Compton of low energy photons, invent something else to suppress background.

IXPE Imaging X-Ray Polarimetry Explorer

EXPO Technologies

Optics 7.5 m focal . Gold +C coated.Band to 35 keV. FWHD 10 arcsec

New **detectors** with TIMEPIX ASIC Chips. High rate. 3-D imaging of the track.

Wide Field Mnitor: CdTe Coded Mask. A clone of SVOM. 4 – 150 KeV. 2 Ster.

SIC (Auxiliary Detector): 5 times Swift XRT. Band up to 30 keV.

No real technical challange in the payload

The most ambitios: Lynx

How long can Chandra survive and what after Chandra?

Lynx2020 was proposed to the Decadal Survey 2020 – 2030. Like Einstein or Chandra would be one telescope with various instrument on a revolver:

Focal 12 m

Band: 01 – 12 keV

Effective area $2m^2$ @ 1keV

Angular Resolution: <1 arcsec

With with different in the focal plane a calorimeter, an imager, and a spectrometer .

IXPE Imaging X-Ray Polarimetry Explorer

Lynx 2030

The new Lynx2030 currently under study for the Decadal Survey 2030 – 2040. Beside su arcsecond imaging in the center of the f.o.v. and an improvement of the calorimeter (>100000 pixels) Lynx2030 foresees a photoelectric polarimeter.

Our new technology can handle the high rates associated with 2 m^2.

We could do 3-4 arcseconds. The goal is 2".

To study non thermal features of X-Ray sources with>2m^2 area (30 IXPE) and 2" resolution (1/15 IXPE) is our long term goal would be of high interest for High Energy Astrophysics.

THANKS

IXPE Imaging X-Ray Polarimetry Explorer

THE FIRST LIMIT: IN POLARIMETRY THE SENSITIVITY IS A MATTER OF PHOTONS

$$MDP = \frac{4.29}{\mu R_S}\sqrt{\frac{R_S + R_B}{T}}$$

Minimum Detectable Polarization (MDP)

R_S is the Source rate, R_B is the Background rate, T is the observing time
μ is the modulation factor: the response of the polarimeter to a 100% polarized beam (spanning from 0 or no sensitivity, to 1 or maximum sensitivity)

If background is negligible: $$\mathrm{MDP} = \frac{4.29}{\mu\sqrt{N_{ph}}}$$

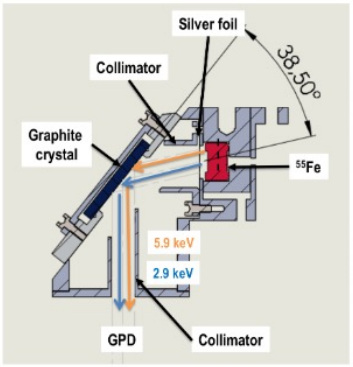
To reach MDP=1% with μ=0.5: $$N_{ph} = \left(\frac{4.29}{\mu\ \mathrm{MDP}}\right)^2 = 736\ 10^3\ \mathrm{ph}$$

Source detection > 10 counts
Source spectral slope > 100 counts
Source polarization > 100.000 counts

Caution: the MDP describes the capability of rejecting the null hypothesis (no polarization) at 99% confidence.

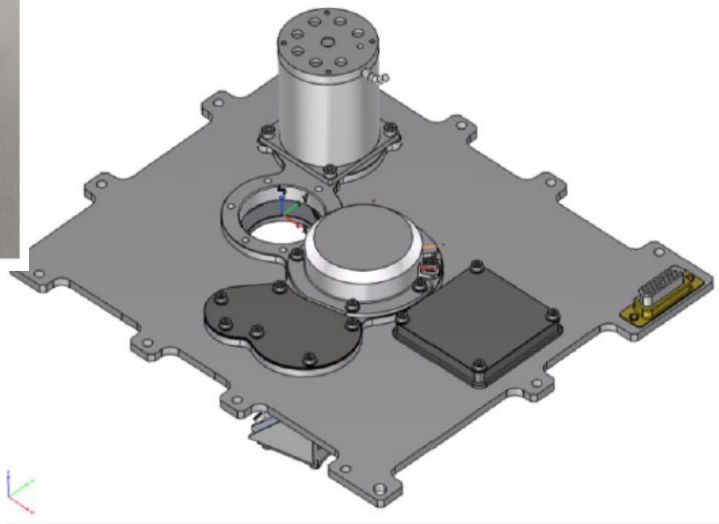
IXPE Imaging X-Ray Polarimetry Explorer

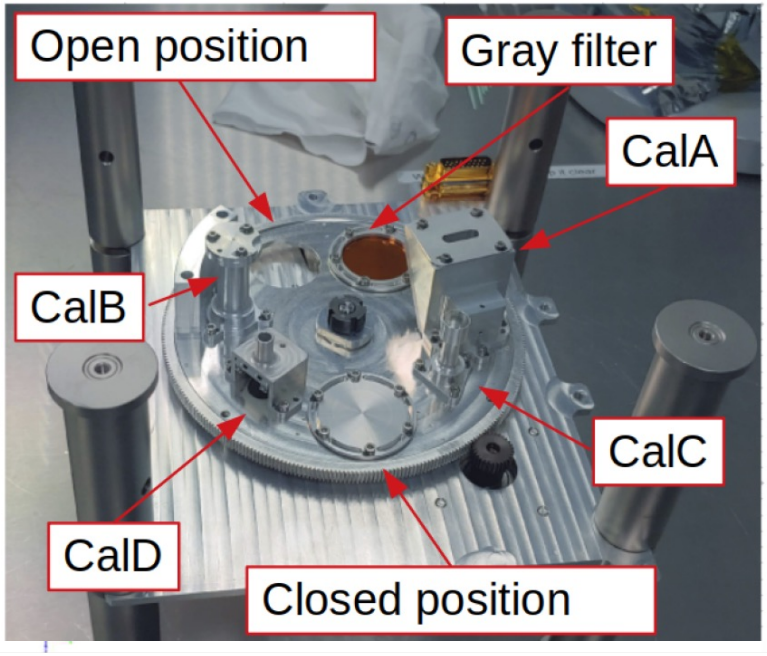
FILTER Calibration Wheel Assembly (In-flight calibration)





Flight Polarized X-ray sources





Ferrazzoli et al., 2020

^{55}Fe-powered calibration sources:

Cal A – Bragg-reflected polarized 2.98-keV (Ag-Lα fluorescence) and 5.89-keV (Mn-Kα)

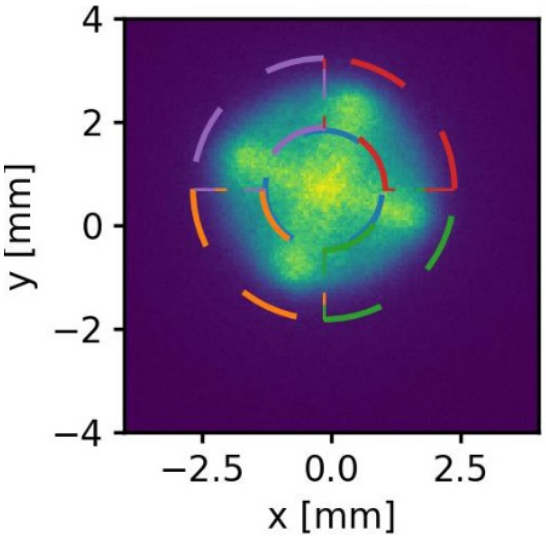
Cal B – unpolarized 5.89-keV spot

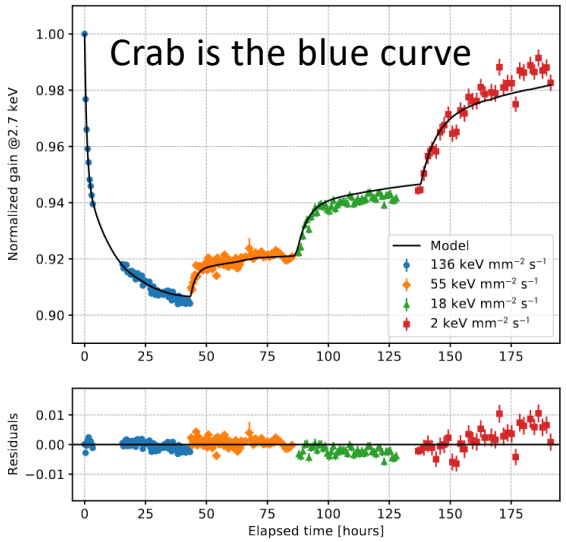
Cal C – unpolarized 5.89-keV flood

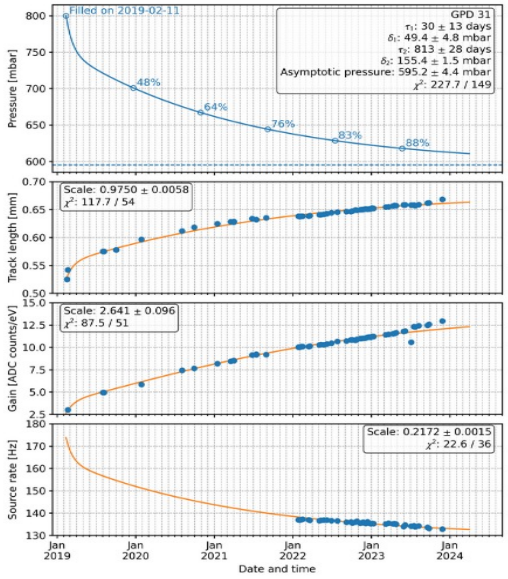
Cal D – unpolarized 1.74-keV (Si-Kα fluorescence) flood

IXPE Imaging X-Ray Polarimetry Explorer

A FEW GPD PATHOLOGIES AND RECOVERY ACTIONS



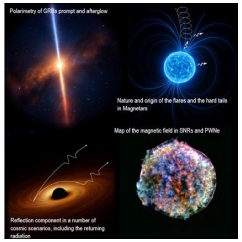




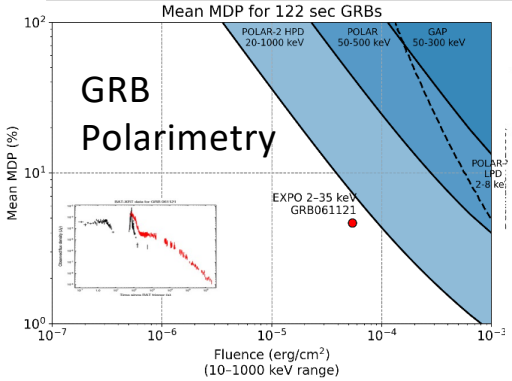
Being un-useful the rotation, a dithering is required to facilitate the ground calibration.

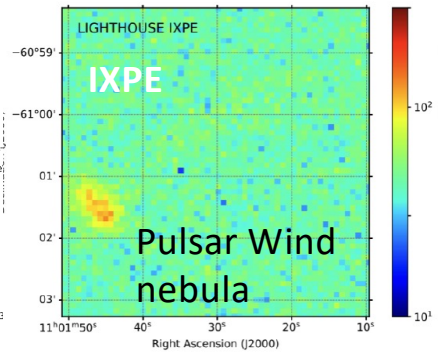
Gain shift due to charging is not yet totally corrected. Charging is responsible for a residual miscalibration of 10-20 eV

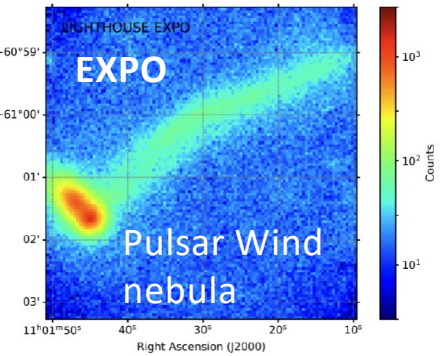
Pressure drop due to absorption of the DME by the glue (model in Baldini L. et al 2021). c.a. 650 mbar current pressure (much more precise value in the CalDB)

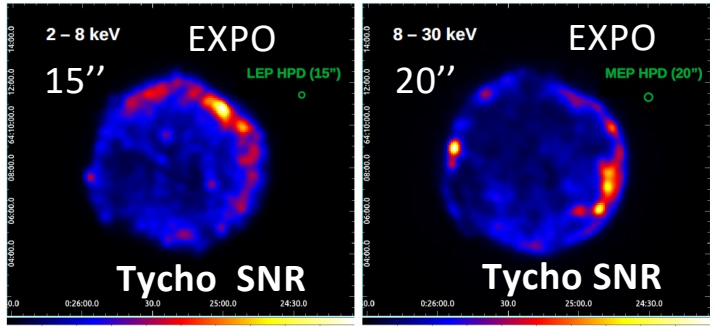


Astrophysical expectations (from EXPO Science team)
Coordinated by G. Matt (chair) and R. Ferrazzoli (deputy)



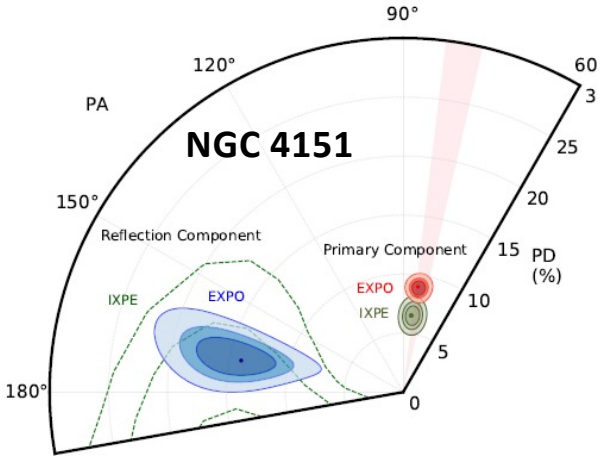


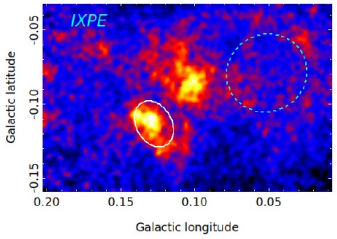


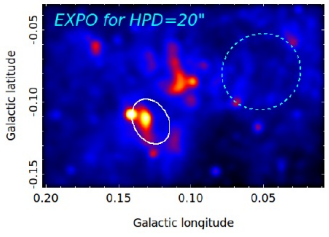


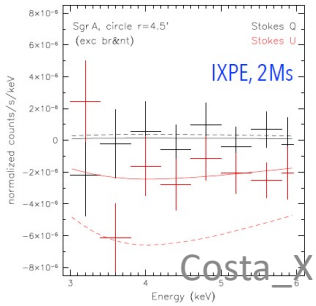
EXPO can prove different morphology in SNR

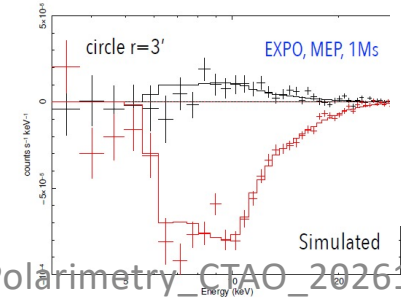
Prompt + early afterglow
(plateau & reflaring)

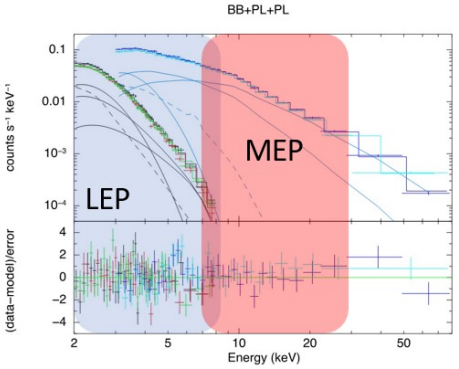






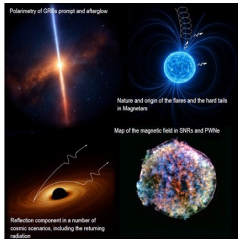






1E 1841-45
(100 ks, Magnetar)

LEP MDP = 5 %
MEP MDP = 6%



So why an ESA M mission of X-ray polarimetry ?

The scientific goals of EXPO complement brand new research areas with the necessary follow-up studies of the most puzzling results of IXPE.

Open problems after IXPE discoveries.

- Current models cannot explain the energy dependence of the X-ray polarization observed in somblack-hole binaries.
- The observed polarization degree of X-ray pulsars is often significantly lower than predicted while Rotating Vector Model works.
- A larger sample of magnetars should be observed, as they exhibit a wide diversity in their polarization properties.

New research area for EXPO.

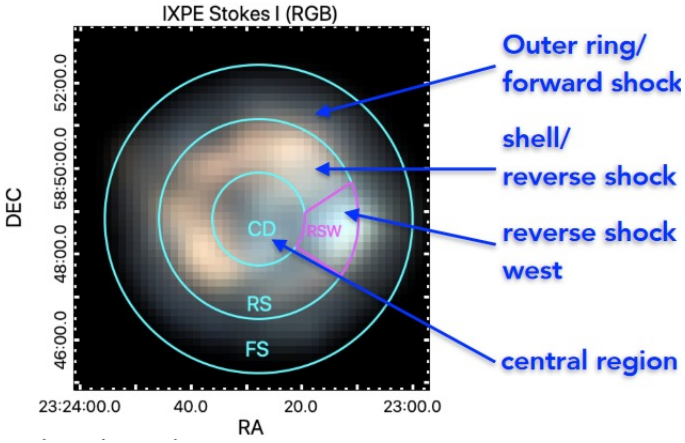
- The role of the magnetic field in the prompt emission and early afterglows of gamma ray bursts.
- The vacuum birefringence search in intermediate flares of magnetars.
- The possible modification of the funnel structure in microquasars at the birth of a jet.
- The hard energy tails of magnetars or of the Low Mass X-ray binaries.
- The polarization of cyclotron lines as a probe of radiation transport in strongly magnetized plasma.
- The synchrotron emission above 8 keV from shocks in Supernova Remnant.
- The Compton reflection bump in AGN and binaries above the energy of iron lines.

The next step after an Explorer mission is indeed an Observatory

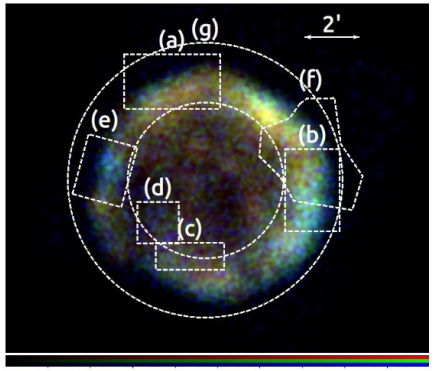
Credit: XPoI simulator, CTAO, ©2261816

IXPE
Imaging
X-Ray
Polarimetry
Explorer

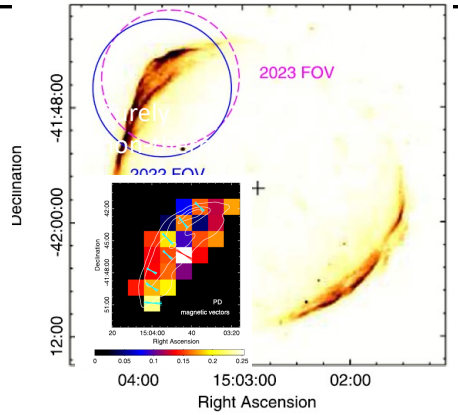
SUPER-NOVA REMNANTS



Core collapse, AD 1667?
Vink et al., 2022



Type Ia, AD 1572
Ferrazzoli et al. ApJ 2023



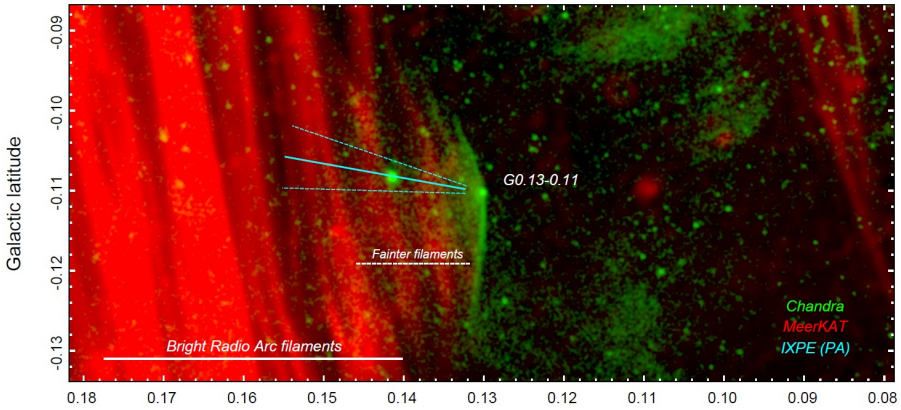
Type Ia
Zhou, P. et al., ApJ 2023

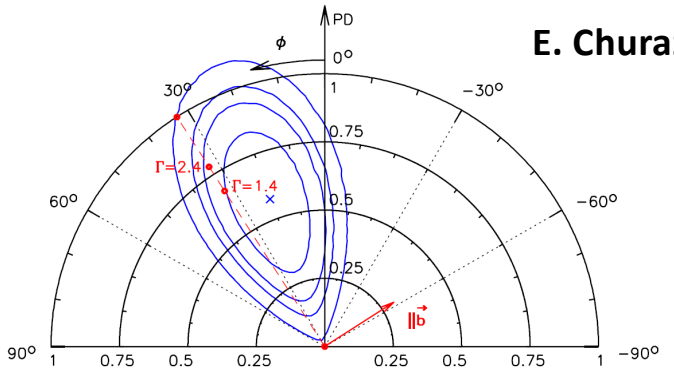
RX J1713.7

Cas A, Tycho and SN1006: both radio and X-rays point to radial magnetic field → Turbulent magnetic field and realignment close to the shock: They show a relative increase of the polarization: decreasing level of turbulence
The ambient density is decreasing: it might be an environment dependence of the turbulence
RX J1713.7 is the oldest of this sample and it shows magnetic field which is tangential to the shock front.

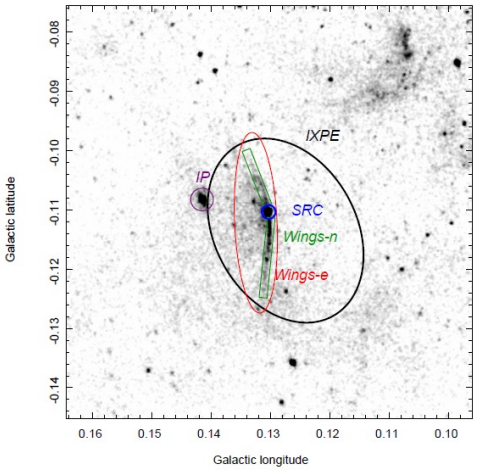
IXPE
Imaging X-Ray Polarimetry Explorer

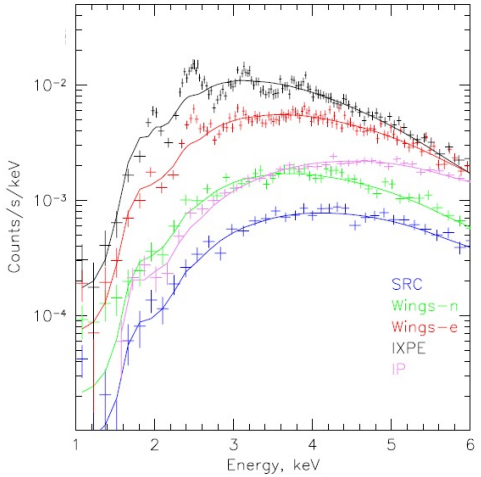
A VERY NICE SERENDIPITOUS DISCOVERY: POLARIZED EMISSION FROM THE X-RAY BRIGHT FILAMENT G0.13-0.11





E. Churazov, A&A 2024 et al.





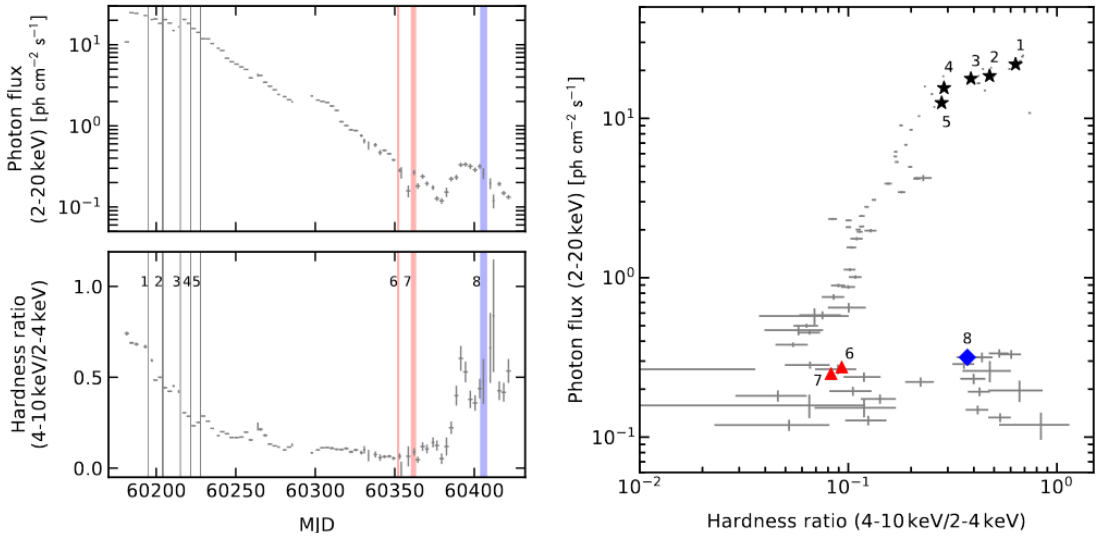
- A tight upper limit would neglect synchrotron emission or the magnetic field is very disordered at variance of other radio filament or G01.13-0.11 is not a PWN
- The polarization angle found is perpendicular to that of the molecular clouds. Tomography of the molecular clouds around the GC would be affected by smaller PD.

The high degree of polarization proves the synchrotron origin of X-rays. The polarization angle shows that the magnetic field (≈ 100 μGauss) is parallel to the radio filaments that may be part of the GC Radio Arc

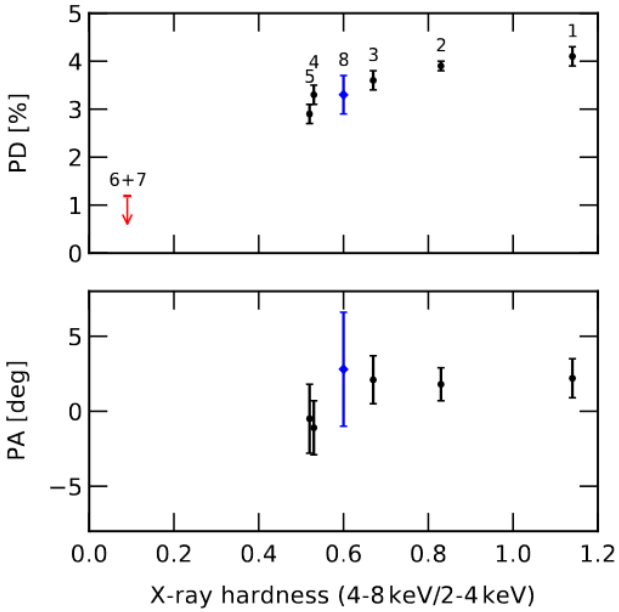
IXPE TRACES A STATE TRANSITION WITH SWIFT J1727.8-1613

Discovered on 24th August 2023 (7 Crab in 2-20 keV band)

Most probably a BH-binary transient: (X-ray spectrum, QPO, flat-spectrum radio emission)



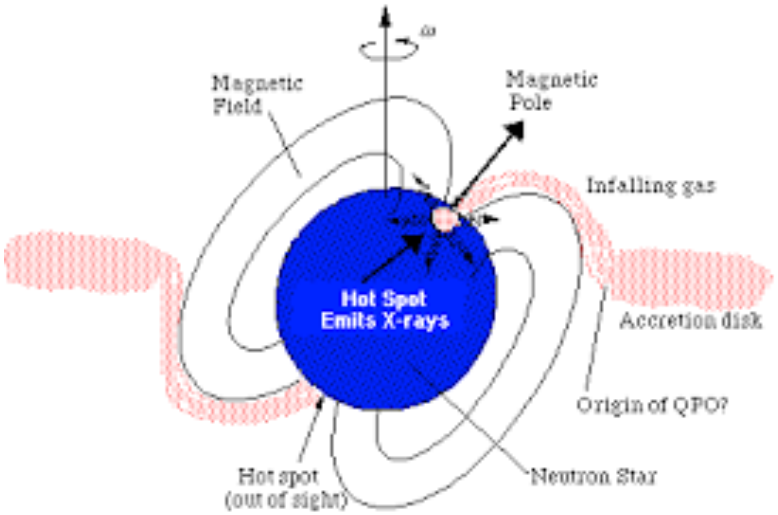
Ingram, A. et al., ApJ 2024, Podgorny A&A 2025



- **IXPE is covering the hard-to-soft-hard transition. X-ray PA is parallel to Radio-PA implying that corona is extended along the disk in all observations.**
- **PD decreases with time implying that disk emission with orthogonal or null polarization is coming into play.**
- **PD increases with energy as in others BH-Binaries.**
- **PD drops in the soft state while recovers in the hard dim state at level of outburst.**

ACCRETING NS – X-RAY PULSARS HER X-1

An X-ray pulsar is a binary system made of a magnetized neutron star (10^{12} G) accreting matter from a normal stellar companion. Gas is accreted from the stellar companion and is channeled by the neutron star's magnetic field on to the magnetic poles producing two or more localized X-ray hot spots. *Doroshenko et al. 2022*



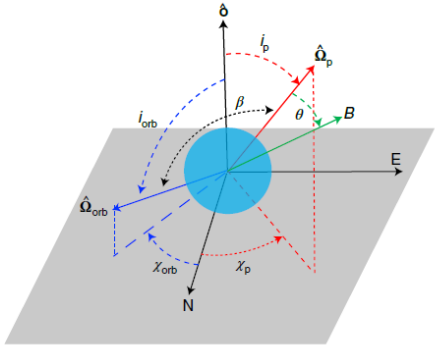


Fig. 4 | Geometry of the system from the observer's perspective. The grey plane is the plane of the sky, labelled with north and east axes, perpendicular to the line of sight towards the observer $\hat{\mathbf{o}}$. The angles between the line of sight and the vectors of the pulsar spin $\hat{\Omega}_p$ and the orbital angular momentum $\hat{\Omega}_{orb}$ are the inclinations i_{orb} and i_p. The corresponding position angles χ_p and χ_{orb} are the azimuthal angles of the spin vectors projected onto the sky, measured from north to east. The misalignment angle β is defined as the angle between $\hat{\Omega}_p$ and $\hat{\Omega}_{orb}$. The magnetic obliquity θ is the angle between magnetic dipole and the rotational axis.

X-ray pulsars are predicted (Meszaros et al., 1988, Caiazzo and Heyl, 2021, to be very highly polarized, because of the two different opacities while the polarization is lower than expected, but detected with very high significance in a number of sources, e.g. Her X-1 (*Doroshenko et al. 2022*), Cen X-3 (*Tsyganov et al. 2022*), Vela X-1 (*Poutanen et al. 2023*), GRO J1008-57 (*Tsyganov et al. 2023*) + ...

IXPE Imaging X-Ray Polarimetry Explorer

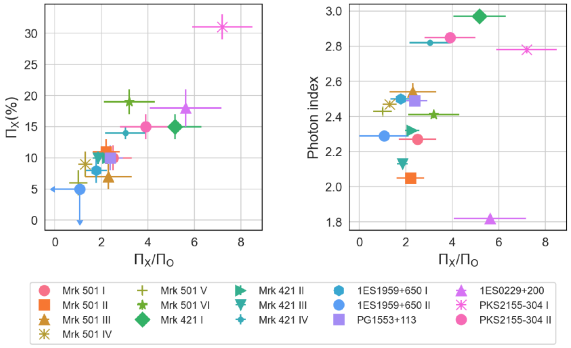
HSP blazars recap:

Marsher, A. et al., 2024

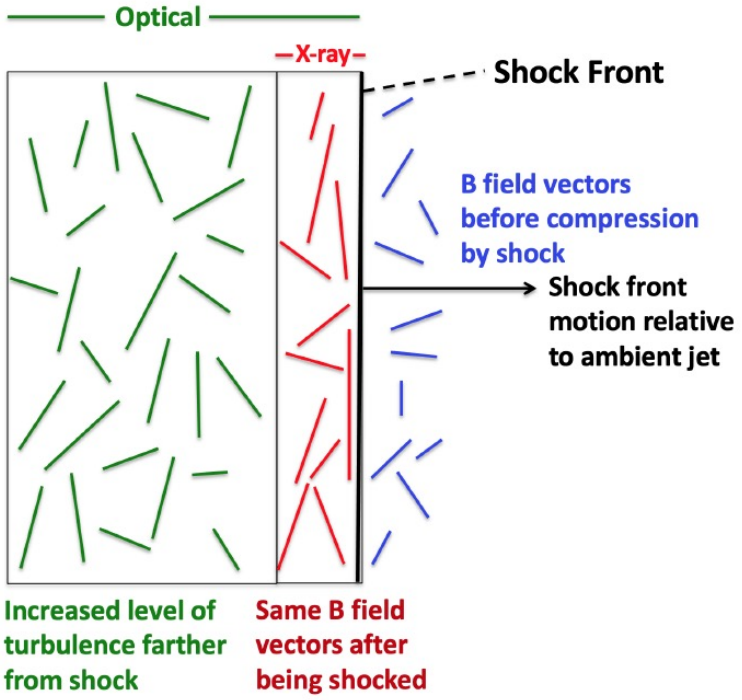
Table 1. Contemporaneous X-ray and optical polarization of HSP blazars.

Object (Date)	X-ray $\Pi_X(\%)$	X-ray $\psi_X(°)$	Optical R-Band [a] $\Pi_O(\%)$	Optical R-Band [a] $\psi_O(°)$	Jet PA(°) at 43 GHz [b]
1ES0229 + 200 [c] (23 January 2023)	18 ± 3	$25 \pm 5°$	$2.4 \pm 0.7\%$	$2 \pm 8°$	163 ± 8
Mrk421 (5 May 2022)	$15 \pm 2\%$	35 ± 4	2.9 ± 0.5	32 ± 5	-29 ± 18
Mrk421 (5 June 2022)	10 ± 1	Rotation	4.4 ± 0.4	-40 ± 6	-29 ± 18
Mrk421 (8 June 2022)	10 ± 1	Rotation	5.4 ± 0.4	-35 ± 1	-29 ± 18
Mrk421 (17 December 2022)	14 ± 1	-73 ± 3	4.6 ± 1.3	26 ± 9	-29 ± 18
PG1553 + 113 (2 February 2023)	10 ± 2	86 ± 8	4.2 ± 0.5	Rotation	50 ± 10
Mrk501 (7 March 2022)	9.8 ± 1.7	136 ± 5	6.6 ± 0.4	110 ± 5	120 ± 12
Mrk501 (27 March 2022)	10.3 ± 1.4	115 ± 4	4.7 ± 0.3	120 ± 3	120 ± 12
Mrk501 (9 July 2022)	6.9 ± 1.8	134 ± 8	2.7 ± 0.5	109 ± 5	120 ± 12
Mrk501 (12 February 2023)	9.0 ± 2.4	110 ± 8	6.6 ± 0.9	150 ± 4	120 ± 12
Mrk501 (19 March 2023)	6.0 ± 2.1	107 ± 11	6.1 ± 0.7	125 ± 3	120 ± 12
Mrk501 (16 April 2023)	18.5 ± 2.2	103 ± 3	5.9 ± 1.5	108 ± 6	120 ± 12
1ES1959 + 650 (3 May 2022)	8.0 ± 2.3	123 ± 8	4.5 ± 0.2	159 ± 1	120–150
1ES1959 + 650 (10 June 2022)	< 5.1 [d]	—	4.7 ± 0.6	151 ± 19	120–150
1ES2155−304 (30 October 2023)	31 ± 2	129 ± 2	4.3 ± 0.7	116 ± 8	135 ± 45
1ES2155−304 (4 November 2023)	15 ± 2	125 ± 4	3.8 ± 0.9	116 ± 8	135 ± 45

Dawoon Kim, 2024



Energy stratified shock acceleration model:
If the pre-shock medium is turbulent the PA can fluctuate around the jet direction.



IXPE Imaging X-Ray Polarimetry Explorer

BH-BINARIES OBSERVED BY IXPE

Table 1.6 IXPE polarimetric measurements of BHXRB: source name, accretion state, band-integrated polarization degree (PD) and polarization angle (PA), and literature reference. Errors are 1σ; upper limits follow the confidence reported in the cited works. Cyg X-1, GX 339-4 and Swift J1727.8–1613 showed a PA in HS parallel to their jet direction (These sources were the only ones in the IXPE sample for which both the PA and jet direction were available).

Source	State	PD [%]	PA [deg]	Reference
Cyg X–1	HS 1 (sum)	3.9 ± 0.2	-23 ± 2	Krawczynski et al. (2022)
Cyg X–1	SS 1 (sum)	2.2 ± 0.1	-21 ± 2	Steiner et al. (2024)
Cyg X–1	HS 2 (sum; weighted)	4.0 ± 0.3	-29 ± 2	Kravtsov et al. (2025)
Cyg X–1	SS 2 (sum; weighted)	2.8 ± 0.2	-22 ± 2	Kravtsov et al. (2025)
Cyg X–3	HS 1	19.5 ± 0.4	89.9 ± 0.5	Veledina et al. (2024a)
Cyg X–3	HS 2	20.0 ± 0.5	91.8 ± 0.7	Veledina et al. (2024a)
Cyg X–3	IMS	9.3 ± 0.3	92 ± 1	Veledina et al. (2024a)
Cyg X–3	SS	11.9 ± 0.5	94 ± 1	Veledina et al. (2024b)
LMC X–1	SS	< 2.5 (99%)	—	Podgorný et al. (2023)
LMC X–3	SS	3.2 ± 0.6	-42 ± 6	Majumder et al. (2024) Svoboda et al. (2024a)
4U 1957+11	SS	1.9 ± 0.6	-41.8 ± 7.9	Marra et al. (2024)
Swift J1727.8–1613	HIMS (sum; weighted)	3.63 ± 0.09	2.2 ± 0.7	Veledina et al. (2023), Ingram et al. (2024)
Swift J1727.8–1613	Soft state (combined)	< 1.2 (99%)	—	Svoboda et al. (2024b)
Swift J1727.8–1613	Dim hard (reverse transition)	3.3 ± 0.4	3 ± 4	Podgorný et al. (2024)
GX 339–4	Soft–intermediate (SIMS)	1.3 ± 0.3 (3–8 keV)	-74 ± 7	Mastroserio et al. (2025)
	SS	≤ 1.2 (3σ)		Mastroserio et al. (2025)
4U 1630–47	High/soft (thermal)	8.32 ± 0.17	17.8 ± 0.6	Ratheesh et al. (2024)
4U 1630–47	Steep power-law (very high)	6.75 ± 0.21	21.3 ± 0.9	Rodriguez Cavero et al. (2023)
IGR J17091-3624	HS	9.1 ± 1.6	83 ± 5	Ewing et al. (2025)
SWIFT J151857.0	HSS	≤ 1.1 (99%)	—	Ling et al. (2024)

In addition:

-***MAXI J1744-294*** aka *Swift J174540.2−290037*, S.S. UL 1.3% (3σ) Marra et al. 2026

-***GS 1354-64****:* DDT 26 February, Intermediate State strong (from 2% to 11%) increasing with energy (Ravi et al. 2026).

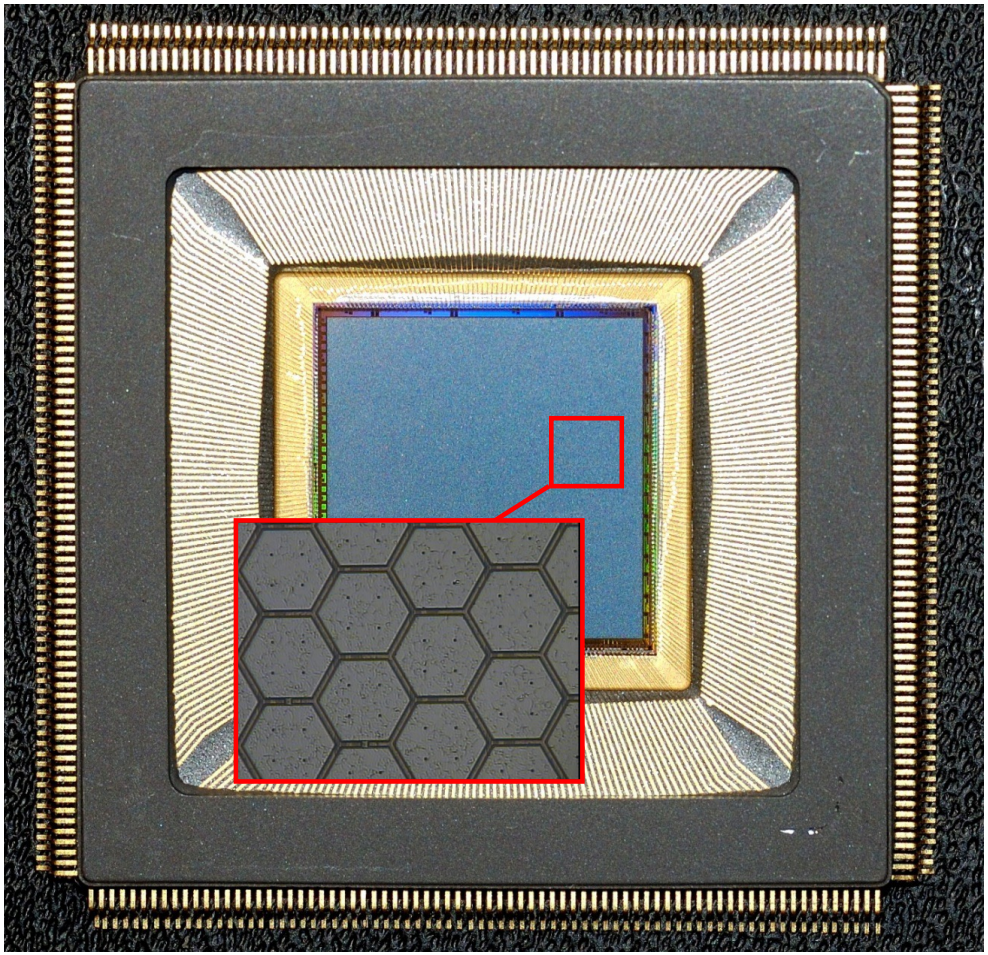
-SS 433

-***4U 1957+115*** New Observation

-***GRS 1915+105*** not detected by IXPE.

IXPE Imaging X-Ray Polarimetry Explorer

ASIC FEATURES 105600 PIXELS 50 MM PITCH



- Peaking time: 3-10 μs, externally adjustable;
- Full-scale linear range: 30000 electrons;
- Pixel noise: 50 electrons ENC;
- Read-out mode: asynchronous or synchronous;
- Trigger mode: internal, external or self-trigger;
- Read-out clock: up to 10MHz;
- Self-trigger threshold: 2200 electrons (10% FS);
- Frame rate: up to 10 kHz in self-trigger mode (event window);
- Parallel analog output buffers: 1, 8 or 16;
- Access to pixel content: direct (single pixel) or serial (8-16 clusters, full matrix, region of interest);
- Fill fraction (ratio of metal area to active area): 92%)

The chip is self-triggered and low noise. The top layer is the collection plane. The bottom 4 layers are a complete analogue chain for each pixel with preamplifier/shaper/sample and hold and serial readout.

It defines the sub-frame that surrounds the track. The dead time, downloading an average of 1000 pixels is 100 time lower, than for 1E5 pixels.

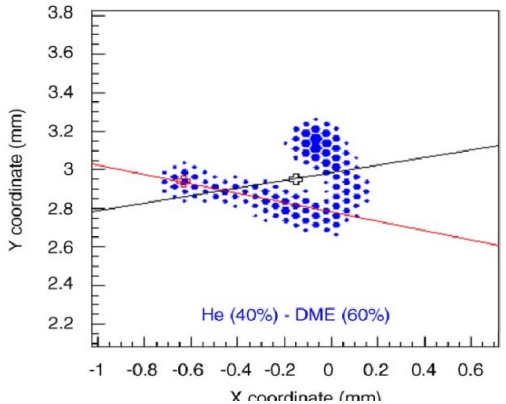
Bellazzini et al., NIM, 2006

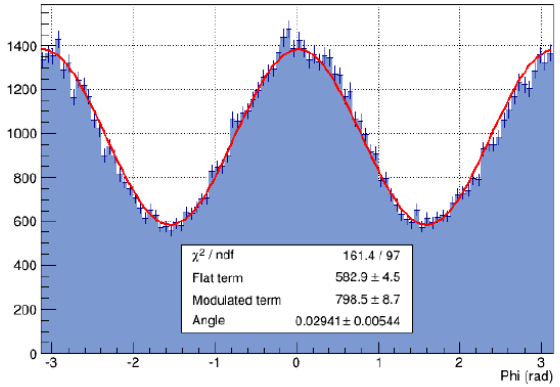
IXPE
Imaging X-Ray Polarimetry Explorer

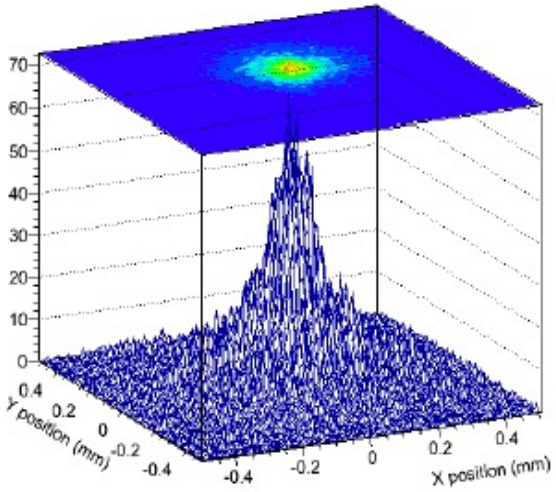
PHOTOELECTRIC EFFECT TO MEASURE POLARIZATION OF X-RAYS

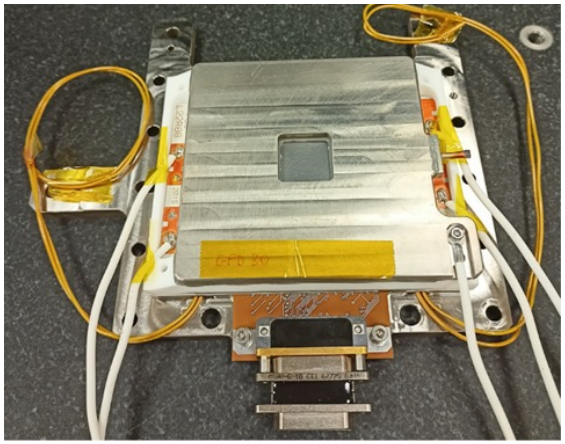
Proposed missions to date

Mission	Date	PI
XMM	Late 80’	G.W. Fraser (UK)
SXRP /SRG	Late 80’ Early 00’	R.Novick (USA)
XEUS/IXO	2007-2012	R. Bellazzini (IT)
POLARIX	2007-2008	E. Costa (IT)
IXPE (OLD)	2007	M. Weisskopf (USA)
HXMT	2007-2009	E. Costa (IT)
NHXM	2011	G. Tagliaferri (IT)
LAMP	2013	H. Feng (China)
XIPE (Small)	2014	E. Costa (IT)
ADAELI+	2014	F. Berrilli (IT)
SEEPE (ESA-CAS)	2014	S.Liu-P. Soffitta
XIPE M4	2014-2017	P. Soffitta (IT)
IXPE	**2017+**	**M. Weisskopf (USA)**









Costa et al., 2001, Bellazzini et al, 2005,2006,

IXPE
Imaging
X-Ray
Polarimetry
Explorer

2014-2017 A tough competition in NASA and ESA

ESA

In 2014 **ESA** issued an AOO for the 4th Scientific Mission of Medium Size (M4) with a budget of 450 M€ (+ national contributions).

3 missions have been selected on 2015 for phase A study:

1) XIPE: and X-ray Imaging Polarimeter based on GPD
2) ARIEL: a mission for the spectroscopy of Exoplanets
3) Thor: a mission to study turbolence on Solar Wind

On May/June 2017 one of these 3 missions is selected for flight

Launch in 2026

NASA

In 2014 **NASA** issued an AOO for a Small Explorer Mission (budget of ~ 175 M$)

On july 30 2015 **NASA selected 3 missions for phase A study**

1) IXPE: a Mission of X-ray Polarimetry based on GPD
2) Praxys: a Mission of X-ray Polarimetry based on TPC
3) SPHEREx: a Mission of All Sky Survey of NearIR spectroscopy

On January 2017 NASA will select one of the 3 missions to flight

Launch in 2021

Three out of 6 missions under study were of X-ray Polarimetry

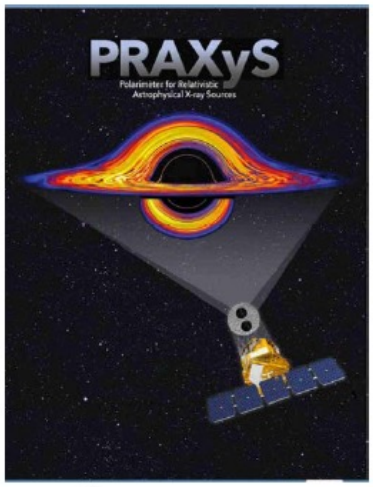
XIPE (ESA-M4 X-ray Imaging Polarimetry Explorer)
IXPE (NASA SMEX Imaging X-ray polarimetry Explorer

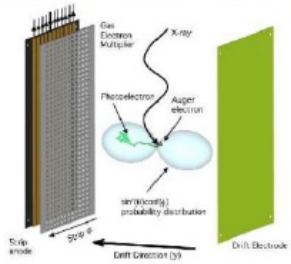




Gas Pixel Detector
Costa et al. 2001
Bellazzini et al. 2006, 2007

- 3 GPDs
- 3 X-ray optics MSFC
- About 350 kg limit (Pegasus)



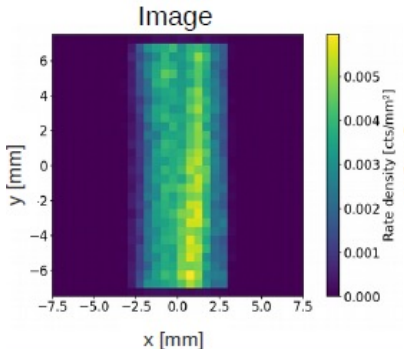


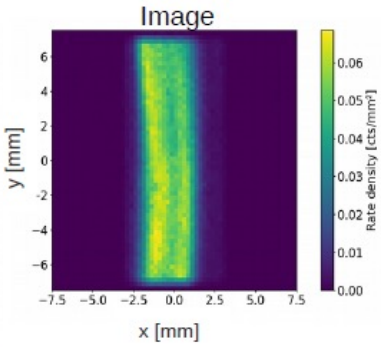
GSFC/NASA

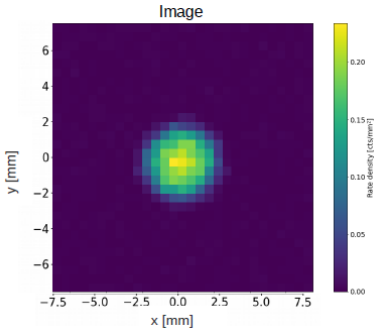
Time Projection Chamber
Black et al. 2007

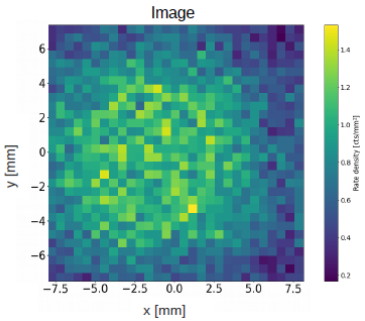
2 TPCs, 2 Optics
About 350 kg limit (Pegasus)

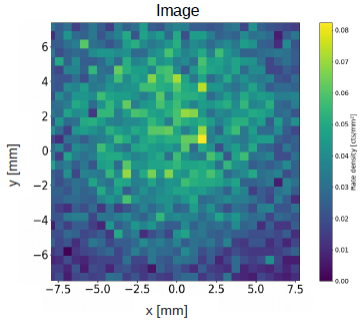
Images and modulation factors of the calibration sources

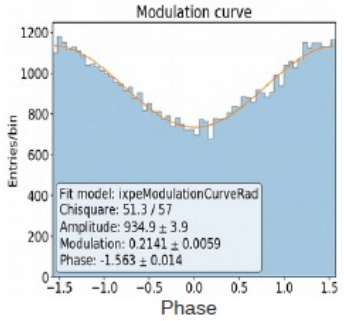


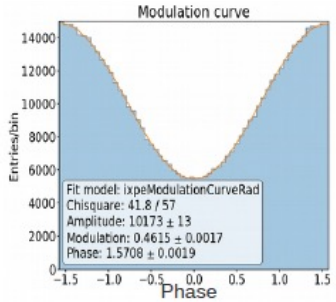


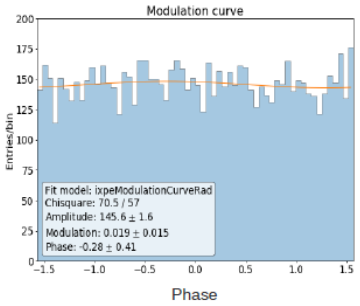


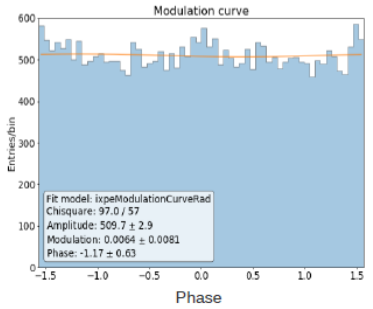


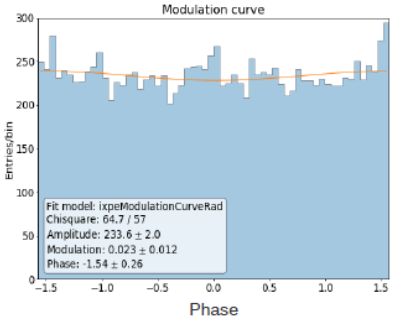










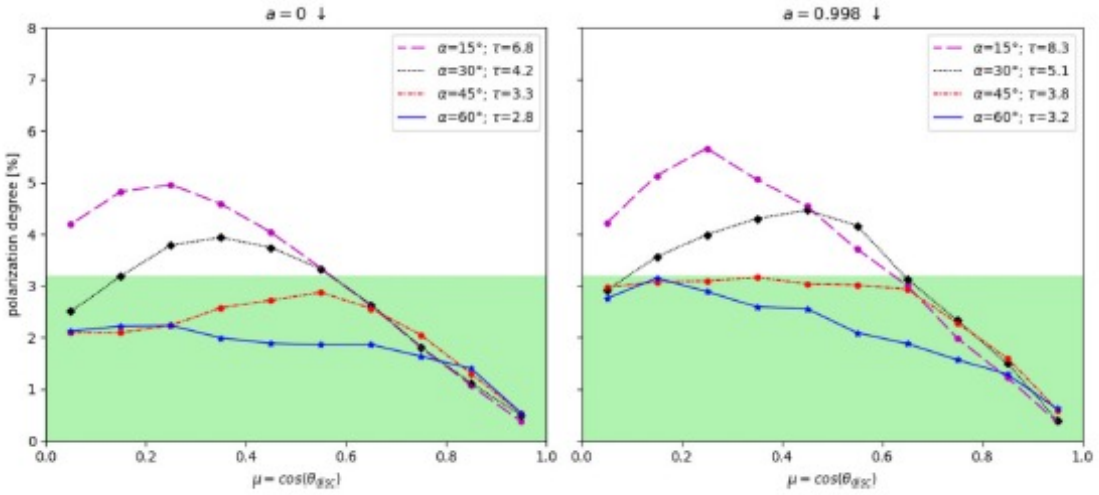


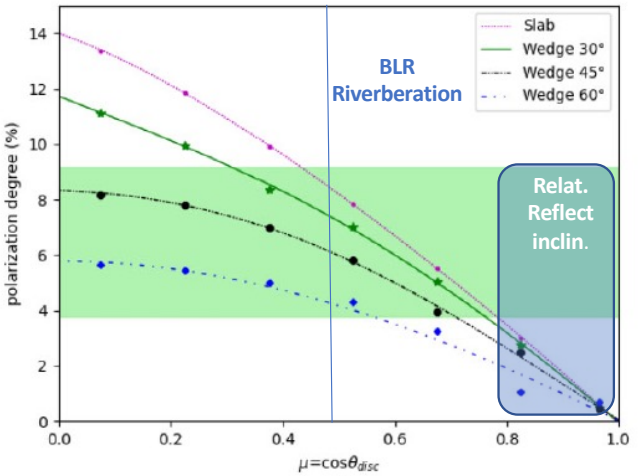
IXPE helps to constrain the geometry of the corona.

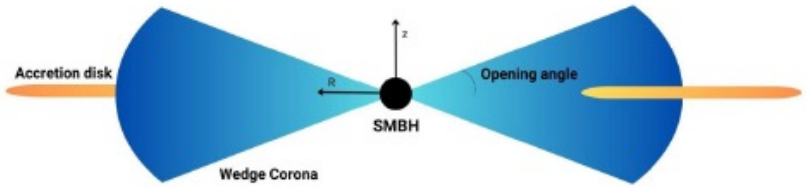
MCG 05-23-16 (Tagliacozzo et al. 2023)

Simulations with MONK

NCG 4151 (Gianolli et al 2023)







For both MCG 05-23-16 and NGC 4151 Slab o Wedge geometry of he corona are consistent with the IXPE data. NCG4151 favors disk inclinations obtained by reverberation and disfavor inclination obtained by spectra

IXPE Imaging X-Ray Polarimetry Explorer

HER-X1 FREE PRECESSION AS THE CAUSE OF THE 35-D SUPER ORBITAL PERIOD

PD

PA

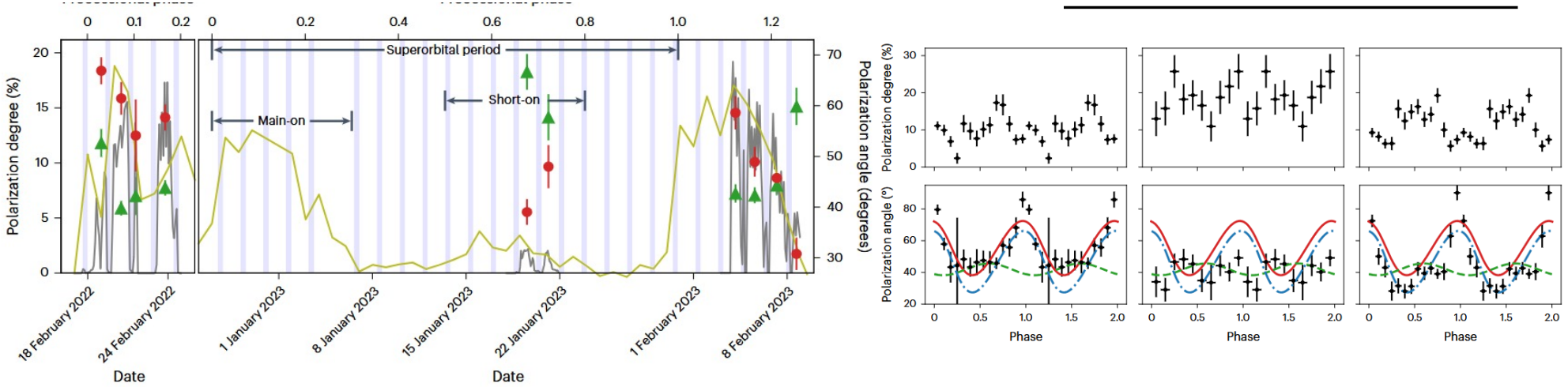
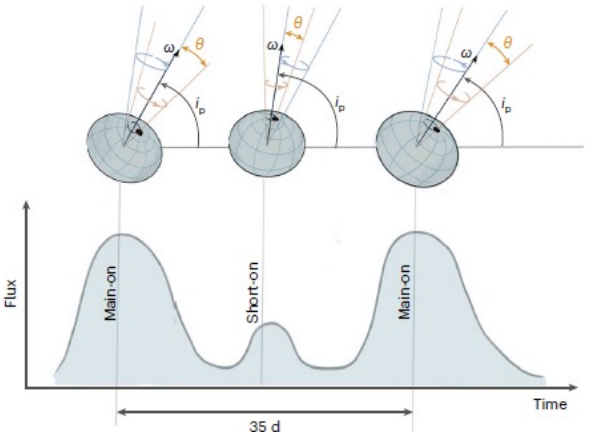
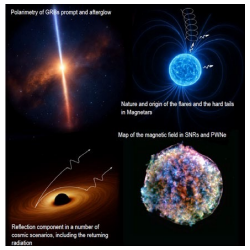


Fig. 1 | Evolution of the observed flux, PA and PD from Her X-1. Flux from IXPE is depicted by a grey curve and from Swift by olive. PD is depicted by green triangles (left *y* axis), and PA by red circles (right *y* axis). Time and phase of the 35 d superorbital precession cycle are given by the two *x* axes. The turn-on time on 18 February 2022 was estimated from IXPE data. Those of 26 December 2022 and 30 January 2023 were estimated from Swift data. The main-on lasts from precessional phase 0 to 0.3 (26 December 2022 to 8 January 2023), and the short-on lasts from 0.5 to 0.8 (15–25 January 2023). These phases repeat every 34.84 d (the superorbital period). The reported values and the uncertainties correspond to the mean values and 1σ (68%) confidence intervals and agree with previously reported results[2,6]. The shaded regions depict the intervals when the companion star and its accretion stream eclipse the neutron star. We define the superorbital phase of zero to coincide with the beginning of the main-on[2,7].



Heyl et al. 2024

The 35-d super-orbital period is explained by using IXPE data as due to free precession of the accreting neutron star as the neutron star is asymmetric for few parts per ten million.



The consortium

EXPO is proposed by:

Paolo Soffitta (Lead Proposer)	**INAF-IAPS**	**Italy**
Sébastien Guillot (WFI PI)	IRAP	France
Ian Hutchinson (SIC PI)	Univ. Leicester	UK
Fabio Muleri (XRP PI)	INAF-IAPS	Italy
Mark Pearce (XRP Co-I)	KTH	Sweden
Andrea Santangelo (ICU PI, SIC Co-PI)	Univ. Tuebingen	Germany
Daniele Spiga (MUs Co-I)	INAF-OAB	Italy

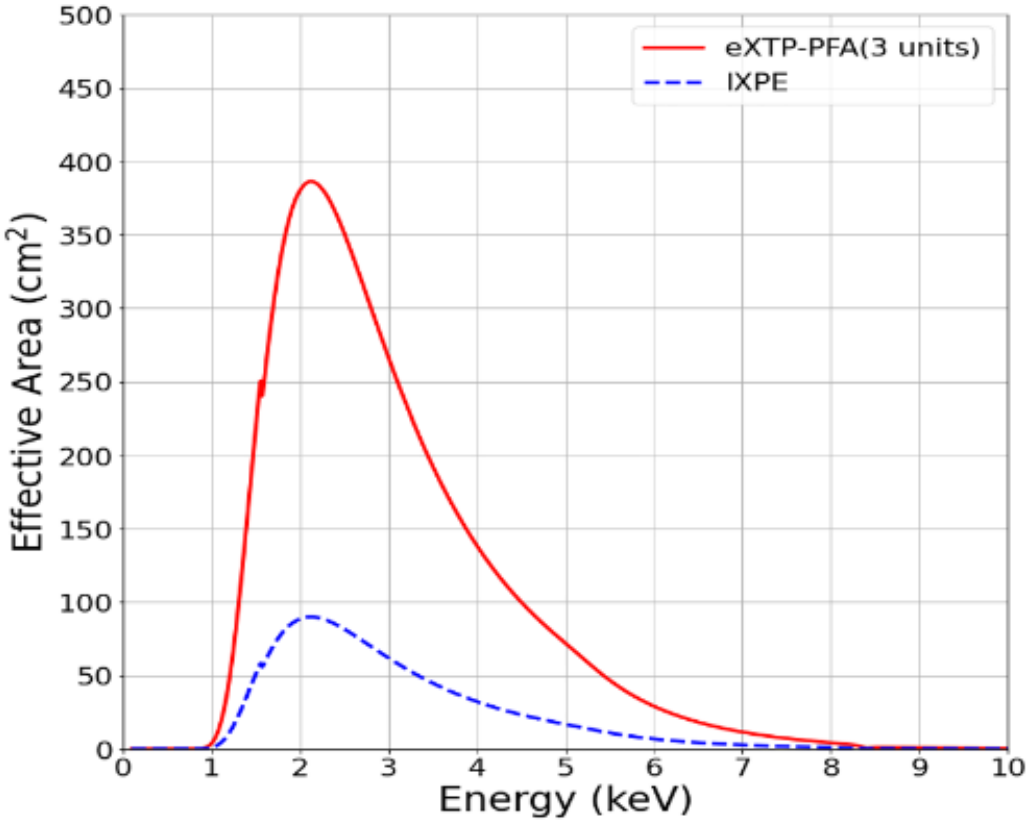
Science Team: Ivan Agudo, Lorenzo Amati, Alessio Anitra, Maria Cristina Baglio, Elisabetta Baracchini, Thibault Barnouin, tefano Bianchi, Fabrizio Bocchino, Markus Boettcher, Niccolò Bucciantini, Sara Capecchiacci, Fiamma Capitanio, Martina Cardillo, Eugene Churazov, Enrico Costa, Stefano Covino, Filippo D'ammando, Nicolas De Angelis, Laura Di Gesu, Alessandro Di Marco, Tiziana Di Salvo, Michal Dovciak, Lorenzo Ducci, Hua Feng, Riccardo Ferrazzoli, Davide Fiorina, Giorgio Galanti, Szymon Gburek, Giancarlo Ghirlanda, Vittoria Elvezia Gianolli, Andrea Gnarini, Emanuele Greco, Sebastien Guillot, Jeremy Heyl, Adam Ingram, Svetlana Jorstad, Philip Kaaret, Ildar Khabibullin, Fabian Kislat, Henric Krawczynski, Josefin Larsson, Yannis Liodakis, Frédéric Marin, Andrea Marinucci, Lorenzo Marra, Alan Marscher, Herman Marshall, Giorgio Matt, Marco Miceli, Riccardo Middei, Romana Mikusincova, Fabio Muleri, Alexander Mushtukov, Kirpal Nandra, Lara Nava, Paul O'Brien, Giuseppe Maria Oppedisano, Salvatore Orlando, Simone Pagliarella, Alessandro Papitto, Pierre-Olivier Petrucci, Oleh Petruk, Stefano Piacentini, Mark Pearce, Jakub Podgorny, Juri Poutanen, Arne Rau, Agata Roszanska, Felix Ryde, Vincenzo Sapienza, Patrick Slane, Paolo Soffitta, James Steiner, Valery Suleimanov, Jiri Svoboda, Daniele Tagliacozzo, Gianpiero Tagliaferri, Antonella Tarana, Fabrizio Tavecchio, Roberto Taverna, Francesco Tombesi, Sergey Tsygankov, Youli Tuo, Roberto Turolla, Francesco Ursini, Alexandra Veledina, Jacco Vink, Martin C. Weisskopf, Fei Xie, Silvia Zane, Haocheng Zhang, Menglei Zhou.

Instrument Team: Ivan Agudo, Gino Bruno Amata, Jarosław Bakala, Elisabetta Baracchini, Stefano Basso, Jörg Bayer, Benedikt Bergmann, Jaroslaw Borek, Enrico Bozzo, Søren Krinstian Brandt, Carl Budtz-Jørgensen, Vadim Burwitz, Stefano Cesare, Jerome Chenevez, Enrico Costa, Elisa Costantini, Vincenzo Cotroneo, Walter Cugno, Riccardo Ferrazzoli, Nicolas De Angelis, Desiree Della Monica Ferreira, Klaus Desch, Giorgio Dho, Giuseppe Di Persio, Sergio Fabiani, Davide Fiorina, Szymon Gburek, Markus Gruber, Sebastien Guillot, Allan Hornstrup, Ian Hutchinson, Jennifer Jones, Jochen Kaminski, Mózsi Kiss, Irfan Kuvvetli, Alessandro Lacerenza, Carlo Lefevre, Hannah Lerman, Hooghui Liu, Pasqualino Loffredo, Niels Lund, Hemanth Manikantan, Melissa McHugh, Fabio Muleri, Paul O'Brien, Stephane Paltani, Giovanni Pareschi, Mark Pearce, Stefano Piacentini, Vladislavs Plesanovs, John Rankin, Ajay Ratheesh, Selina Ringsborg Howalt Owe, Alda Rubini, Miguel Andrés Sánchez, Andrea Santangelo, Emanuele Scalise, Konrad R. Skup, Paolo Soffitta, Daniele Spiga, Gianpiero Tagliaferri, Chris Tenzer, Berend Winter, Silvia Zane.

eXTP (new ASIC with a dead time 8 times lower than IXPE)

Table 5 PFA specifications (3 telescopes with GPD at focal plane)

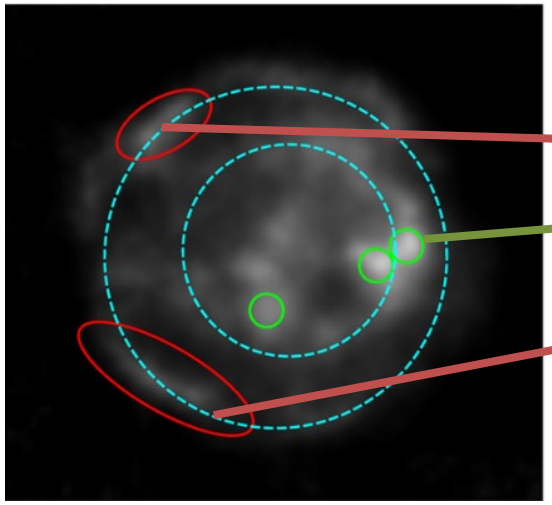
Indicator	Requirement
Total effective area	$\geqslant$ 180 cm^2@3 keV
Energy range	2-8 keV
Energy resolution (FWHM)	$\leqslant$ 1.8 keV@6 keV
Field of view	9.8′ × 9.8′
Angular resolution	HPD $\leqslant$ 30″@3 keV
Time resolution	$\leqslant$10 μs
Dead time	$\leqslant$ 10%@1 Crab
Polarization modulation factor	$\geqslant$ 50%@6 keV
Minimum detectable polarization	$\leqslant$ 3% (1 mCrab, 10^6 s)



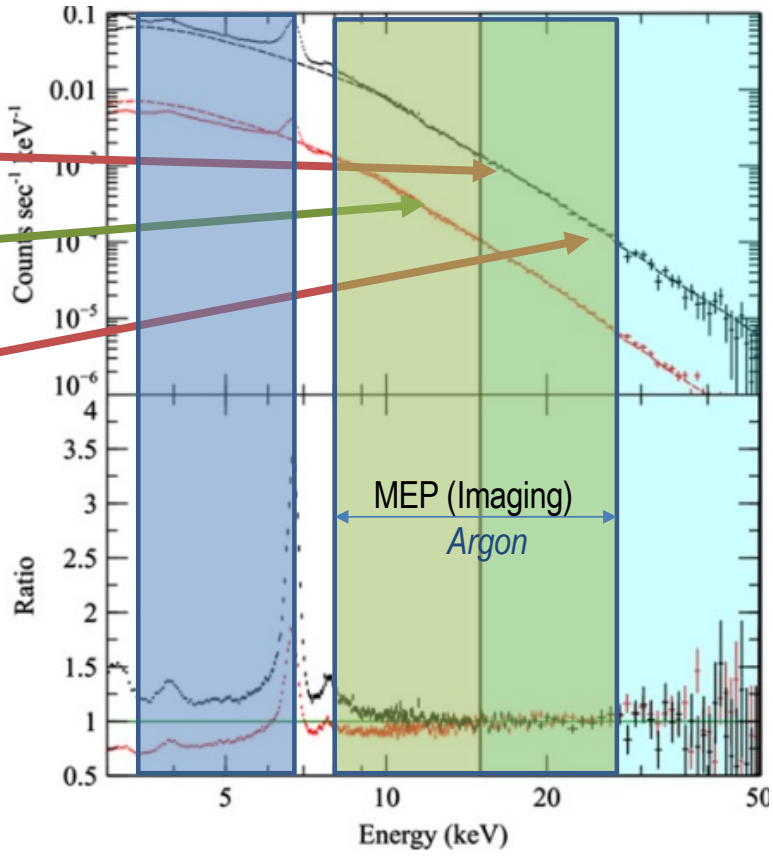
3.8 times less time to get the same results of IXPE: A factor 5 increase on the number of sources for each class, better study of variability.

Zhang et al., SPIE 2022

Photoelectric Imaging Polarimetry above 6 keV: SNR



15–20 keV NuSTAR image of CasA

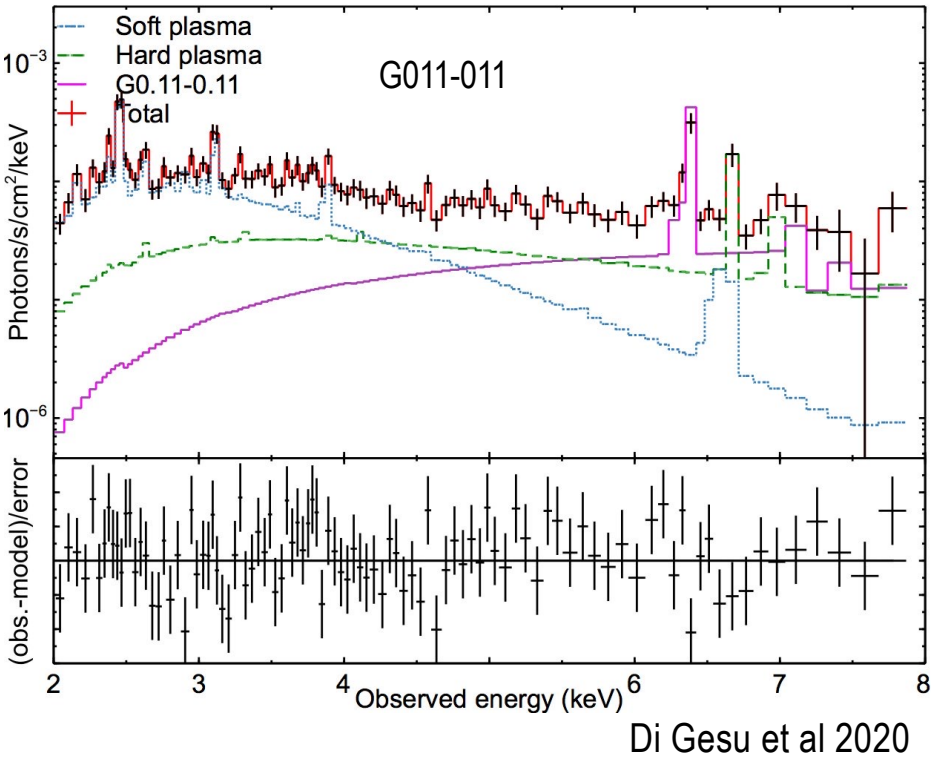


Grefenstette, 2015

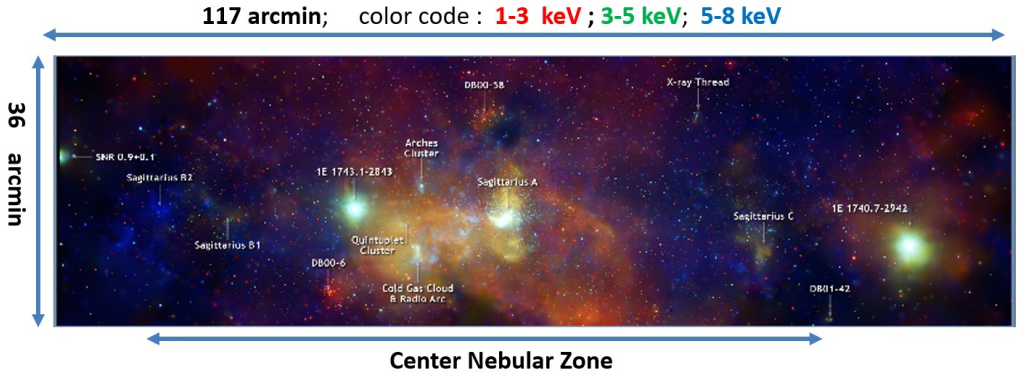
The origin of E >15 keV is a mistery.
It is not dominated by forward or reverse shock but by filaments and knots.
Is the bright knots emission synchrotron (10-100 TeV electrons) or non-thermal bremsstrahlung (10-100 keV electrons) ?

IXPE probes the non thermal emission diluted with thermal bremsstrahlung (blue)
Imaging Hard X-ray polarimetry of genuine non thermal emission (Green 9-30 keV)

Photoelectric Imaging Polarimetry above 6 keV: Molecular Clouds



Di Gesu et al 2020

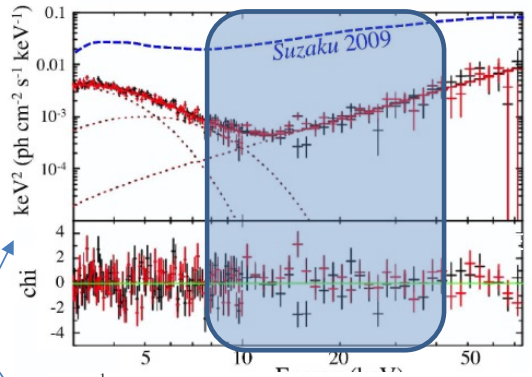


Cold molecular clouds are reflecting X-rays emitted 200 year ago from SgrA* (Marin et al., 2023).

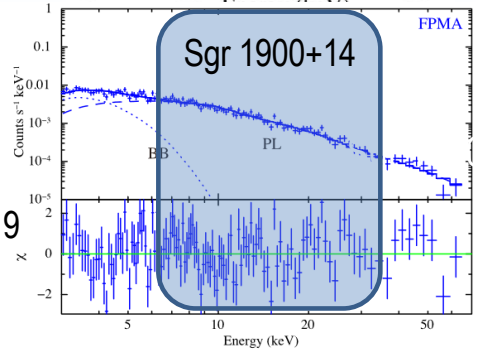
Molecular clouds in the galactic center region are embedded in a two temperatures thermal plasma
The contribution of the thermal plasma can be made negligible above 7 keV

Photoelectric Imaging Polarimetry above 6 keV: hard tails of Magnetars

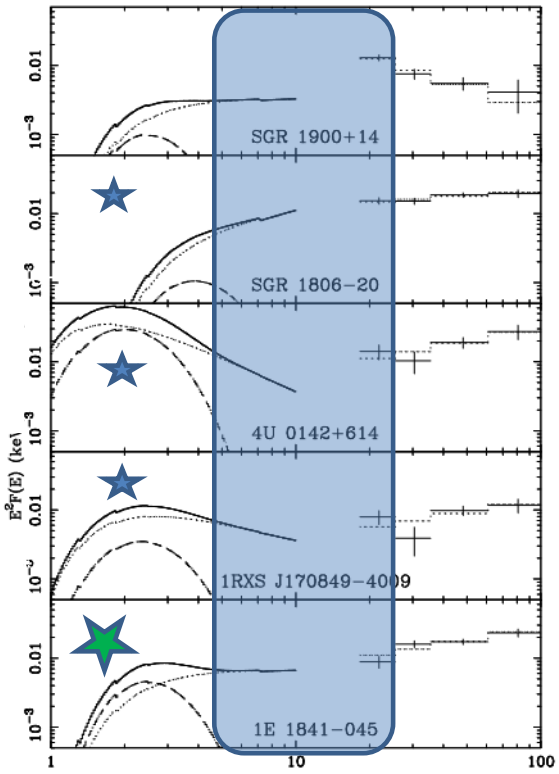
1E 1547.0−5408
Makishima et al., 2021



NuSTAR



Tamba et al. 2019



Götz et al., 2006

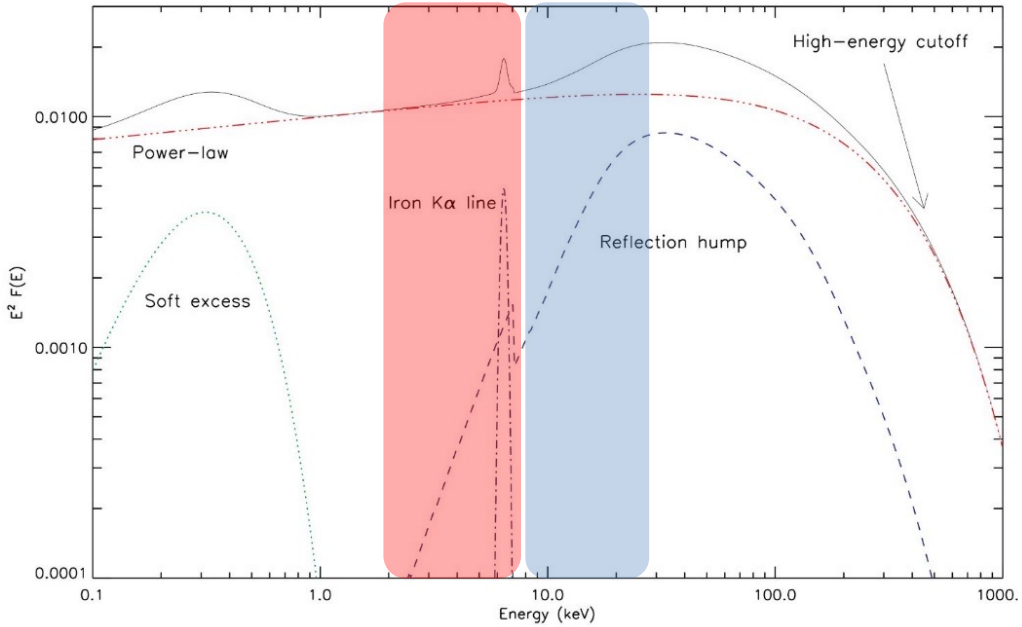
- Hard tails detected by IBIS-Integral and Nustar
- Fluxes in the mCrab range
- Resonant Compton upscattering of soft thermal photons from the neutron star surface

★ Observed by IXPE

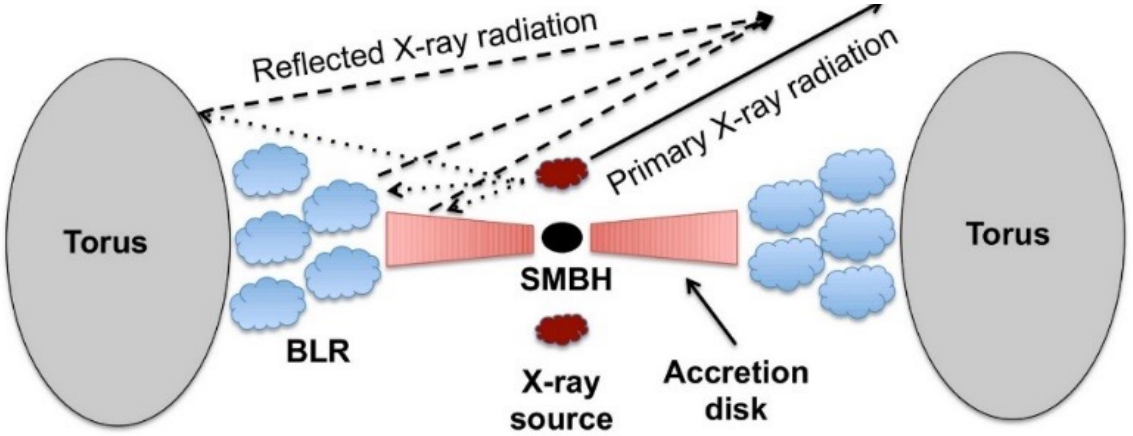
★ Next IXPE ToO start 2024/09/23

With hard X-ray imaging polarimetry we can probe the transition between power-law and hard tail emission

Photoelectric Imaging Polarimetry above 6 keV: reflection phenomena in AGNs



Wider energy band & imaging for AGNs



Credit Ricci, C.

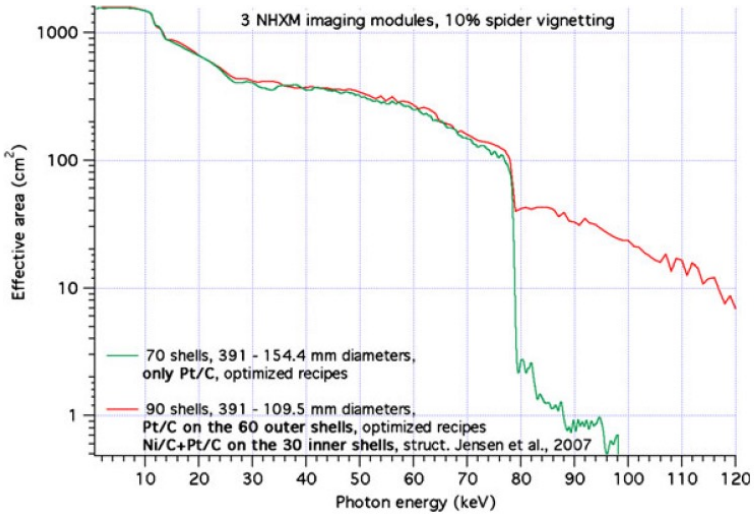
IXPE energy band

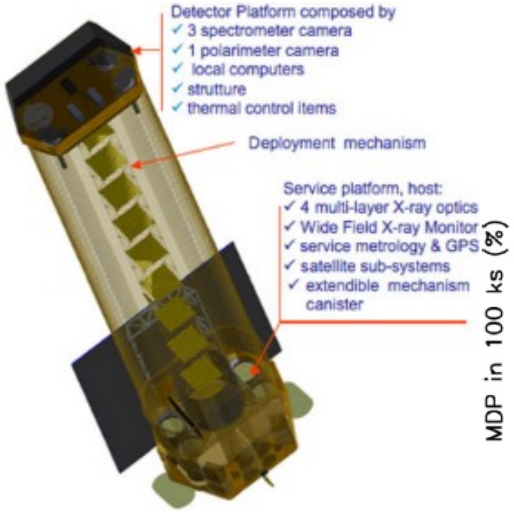
Future hard X-ray imaging polarimetry

IXPE polarimetry to study reflection phenomena suffers of small effective area. Hard-X ray imaging (low background polarimetry) is highly desirable.

X-ray polarimetry in a wide energy band

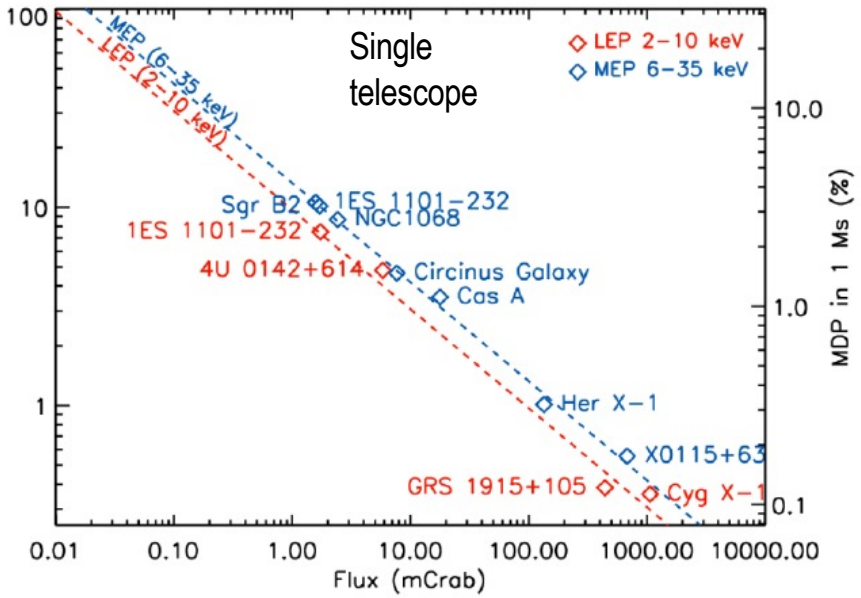
Tagliaferri et al., 2010





550 cm^2 2-10 keV.
one NHXM optics = whole IXPE.

Tagliaferri et al., 2010

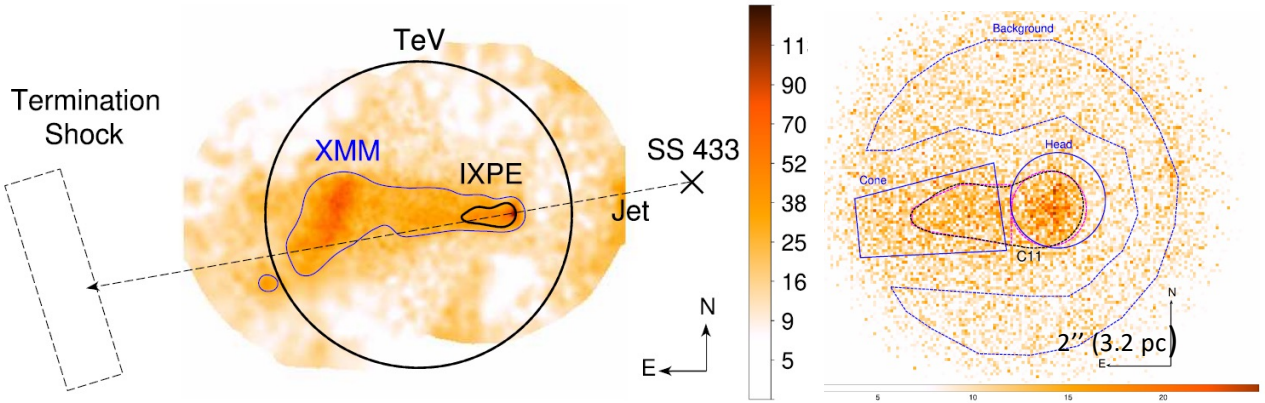


New Hard X-ray Mission (NHXM) was proposed in 2010 as an M-3 ESA mission.
Four multilayer optics 3 optics for spectroscopy/Imaging and 1 optics for polarimetry.

We could revert the NHXM design assigning three optics to polarimetry and one optics to a detector for imaging/spectroscopy. One NHXM mirror is efficient as the three IXPE ones.

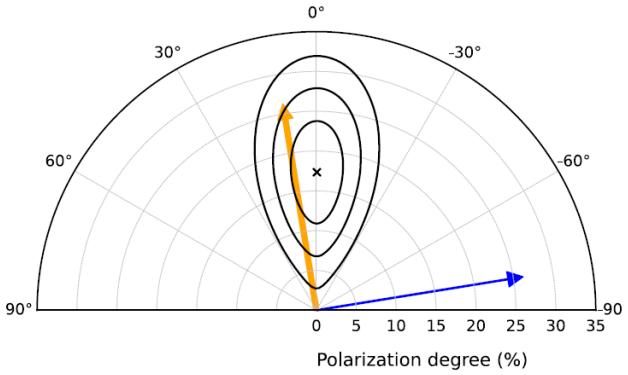
IXPE
Imaging X-Ray Polarimetry Explorer

X-RAY POLARIZATION OF THE EASTERN LOBE OF S433



- The jet X-rays are thermal.
- East and West lobes (from 30 pc) are non-thermal (synchrotron).
- Termination shock is thermal.
- Lobes show TeV emission (HAWC, LHAASO. HESS)
- Head: non-thermal hard X-ray emission Γ≈1.6
  Head site of acceleration ?

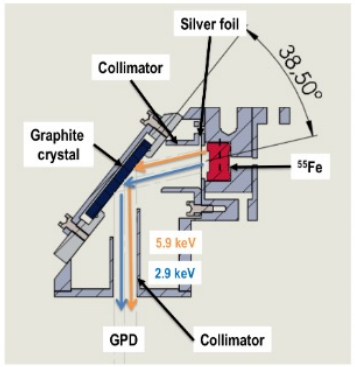
The same electrons which produces X-rays produce TeV photons via Inverse Compton scattering on CMB. ùTherefore IXPE probes probes the magnetic field configuration in the same region producing VHE



The key result of IXPE observations is that the magneti field near the acceleration region contains a significant component that is well ordered and parallel to the flow direction (shear ? Loclized ordered magnetic field ?. Acceleration: Stochastic by shock, stochastic by turbulence, reconnection ?

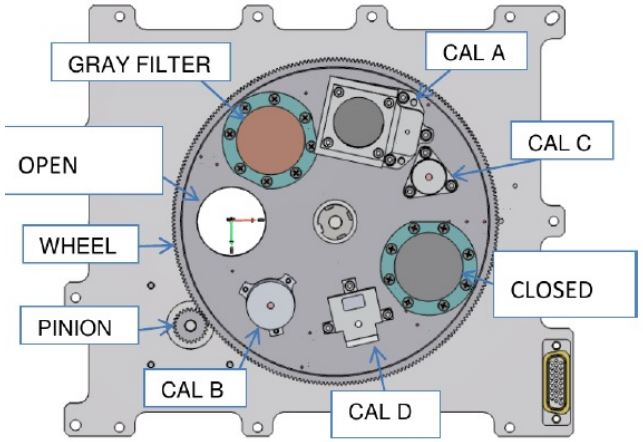
Alternative scenario is scattering from SS433 being a ULX. But large optical depth requested

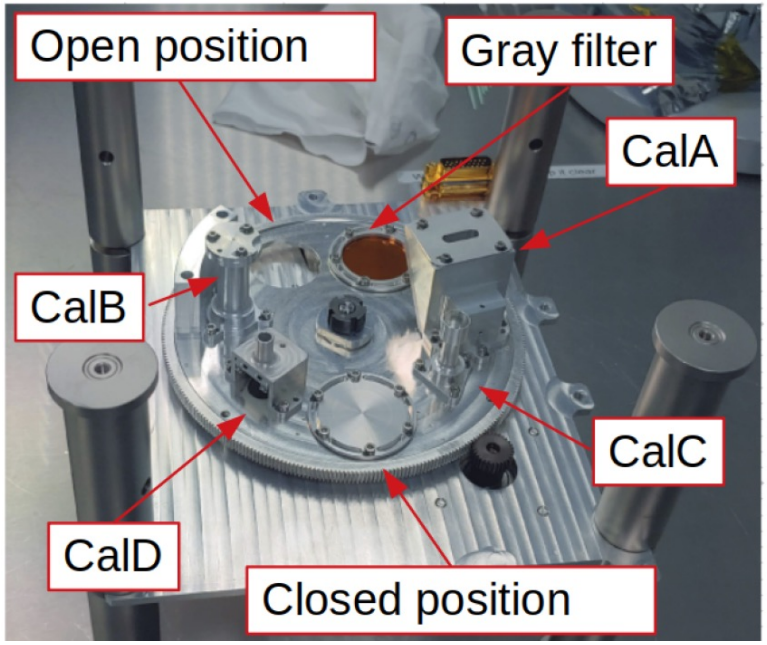
FILTER Calibration Wheel Assembly (In-flight calibration)





Flight Polarized X-ray sources





Ferrazzoli et al., 2020

^{55}Fe-powered calibration sources:

Cal A – Bragg-reflected polarized 2.98-keV (Ag-Lα fluorescence) and 5.89-keV (Mn-Kα)

Cal B – unpolarized 5.89-keV spot

Cal C – unpolarized 5.89-keV flood

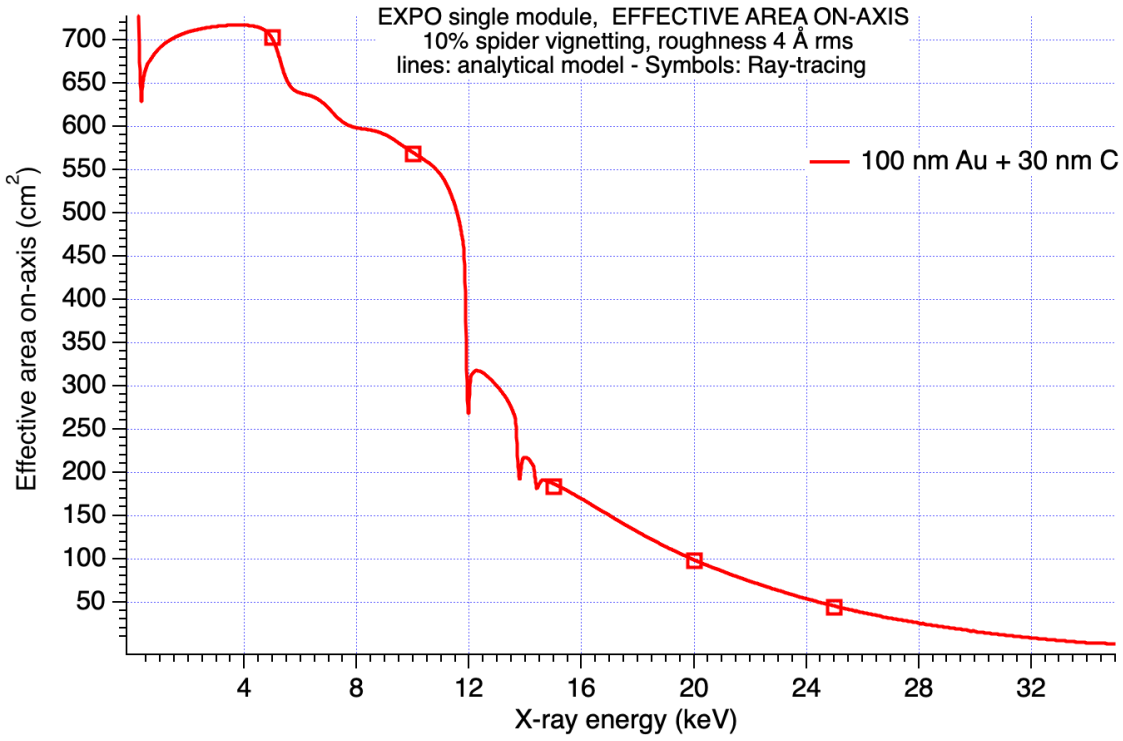
Cal D – unpolarized 1.74-keV (Si-Kα fluorescence) flood

WHAT IN THE PRESENT OR IN THE NEAR FUTURE IN X-RAYS IN CONTIGOUS BANDS?

goSOX (MIT Kavli) a Pioneer Mission to be launched on 2030

Polarimetry in soft X-Ray range not covered by IXPE (0.2-0.4 keV).
Wolter I optics. Critical Angle Transmission Gratings, Multilayer Mirrors, CCD Detectors. Diffraction on artificial components.
Main targets pulsars and blazars
2026arXiv260802891M

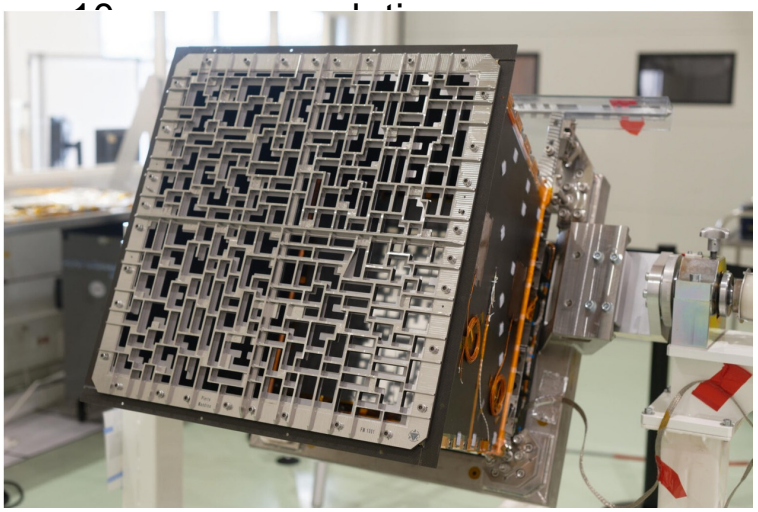
Wider band – Better Resolution – Very fast re-pointing



Optics: 6 telescopes

7.5m focal

Extended band gold coating)

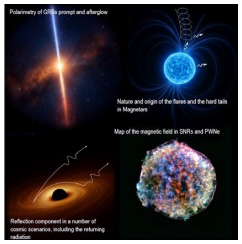


A clone of SVOM as **Wide Field Monitor**

Field of view: 2 sr

Source localization: 12 arcsec

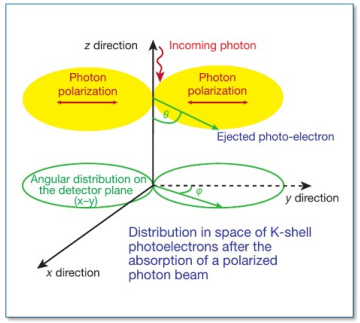
Band: 40 – 150 keV

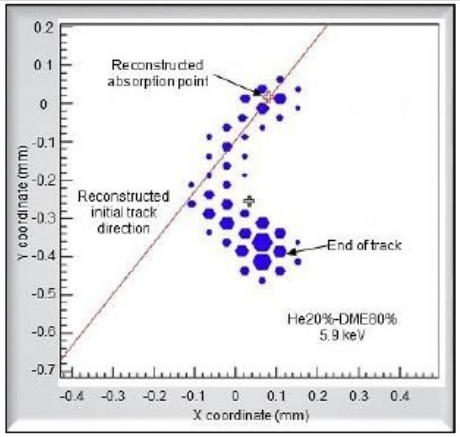


IMPROVING THE PHOTOELECTRIC TECHNIQUE

The photoelectric effect

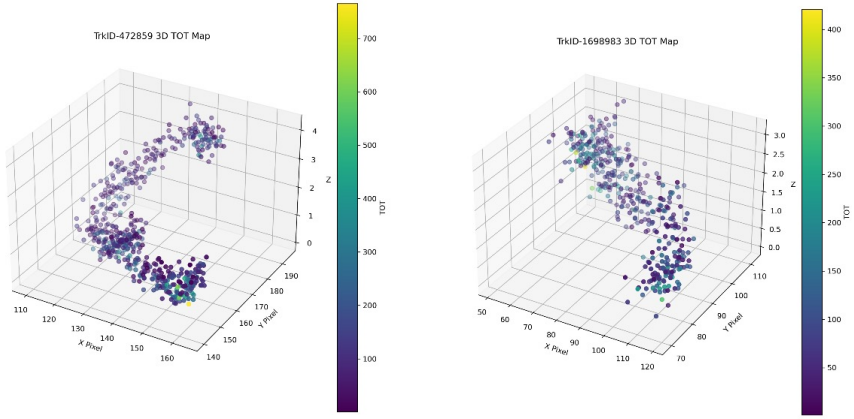
$$\frac{\partial\sigma}{\partial\Omega} = r_0^2 \frac{Z^5}{137^4}\left(\frac{mc^2}{h\nu}\right)^{7/2} \frac{4\sqrt{2}\sin^2(\theta)\cos^2(\varphi)}{(1-\beta\cos(\theta))^4}$$





Costa et al., 2001

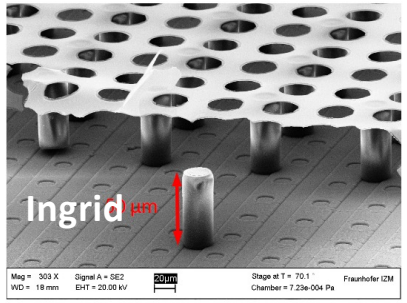
2D → 3D



Real 3D tracks (17.4 keV) Ar-DME 80-20 1.2 atm

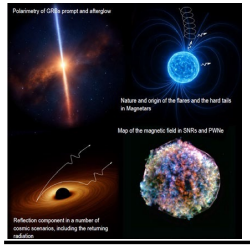
Parameter	GPD	GridPix
Pixel matrix	300x352=105600 pixels	256 x 256 = 65536 pixels (2x4 superpixels)
Pixel size	50 µm (hex. pattern)	55 x 55 µm^2
Technology	CMOS 180 µm	CMOS 120 nm
Measurement type	1. Analogue ROI base 2. Analogue Full Frame	1. Simultaneous per pixel 10 bit TOT, 14 + 4 bit ToA 2. 14 + 4 bit ToA only 3. 14 bit integral ToT
Readout type	1. Data-Driven (no zero-suppress.) 2. Frame based no-zero suppr.	1. Data Driven (zero-suppression) sparse readout 2. Frame based (zero-suppression)
Dead time	1.2 ms (150 µs) per ROI	ToT + 457 ns (pulse processing + data transfer) per pxel
Maximum Counting rate (10 % dead-time fraction)	100 (700)	10^6
Time resolution	1 µs	1.56ns
Front End noise, Minimum threshold	50 e_{rms} (30 e_{rms}) 2300 e^- (200 e^-)	60 e_{rms} , 500 e^-



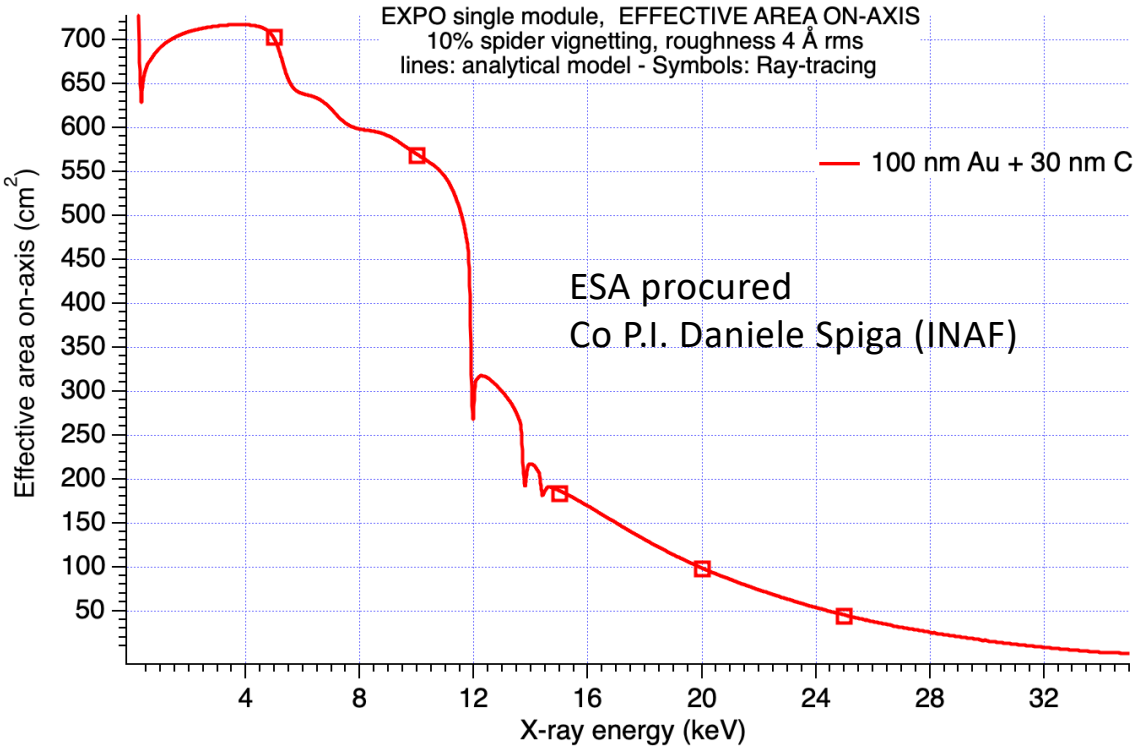


Timepix3 + InGrid = Gridpix

Timepix3 allows for 3D track imaging and negligible deadtime



SUPER-POLISHED

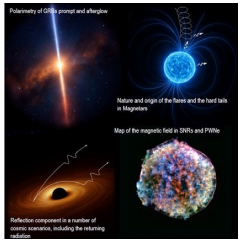


Property	Value
Number of modules	6
Mirror shells per module	80
Inner, outer shell diameter	138.5, 400 mm
Total shell length	600 mm
Inner, outer shell thickness	200, 300 um
Shell material	Nickel, Au + C coated
Effective area per module	705 cm^2 (2 keV) 570 cm^2 (10 keV) 95 cm^2 (20 keV)
Angular resolution	10'' HPD (1 keV)
Detector limited FOV	6.4 arcmin
Focal length	7.5 m (XMM-like)
Mass (1 module)	121.8 kg

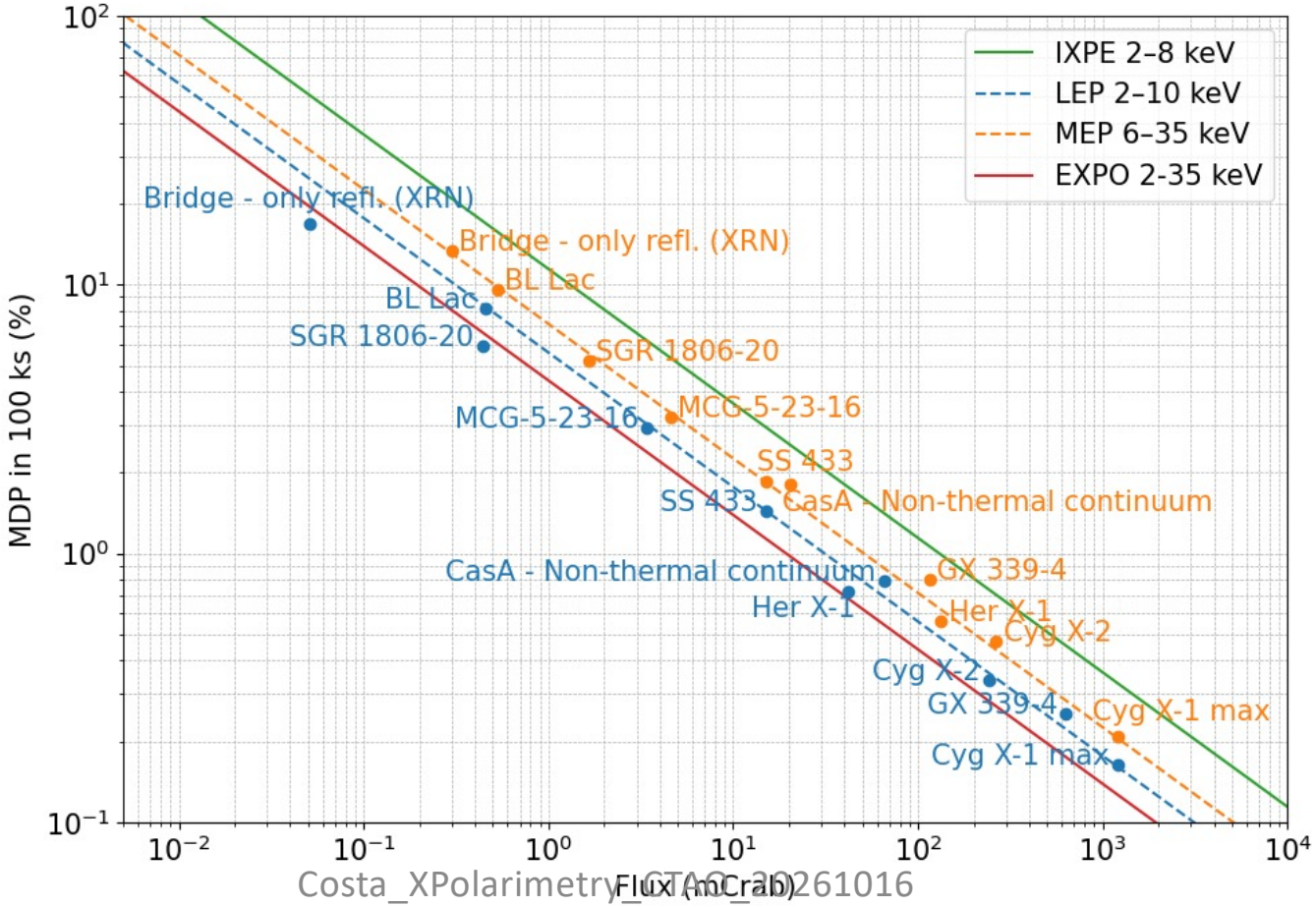
Well established standard fabrication technology.
eRosita shell assembling technique.

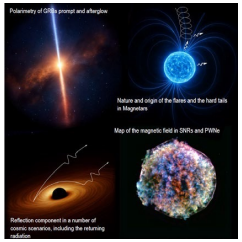
X-Ray Polarimetry now and tomorrow: the limits of IXPE

1. Limitation to data at level of memory and telemetry. Continous monitoring of BH transient not possible
2. Poor coverage with other satellites due to LEO and fixed panels
3. The limited replanning capability. Very few TOOs in >3 days. Fast transients (GRB, SGR, ..) totally missed. Very few follow-up.
4. The band too narrow 2 – 8 keV.
5. The energy resolution i that of proportional counters (18% @ 6 keV). Wherever thermal and not thermal are *mixed* they can be separated by skipping lines (not bremmstrahlung). With a poor resolution it is less effective.
6. Angula resolution of 30 arcsec
7. The dead time is high. A source > 2 Crab needs an absorber.



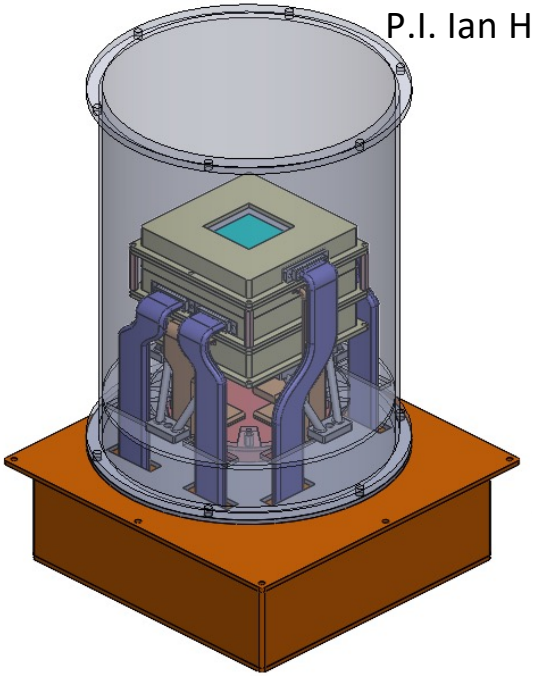
The EXPO Polarimetric sensitivity

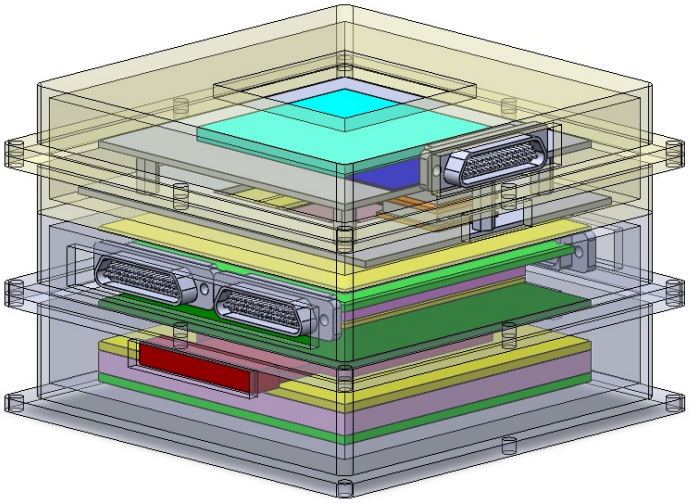




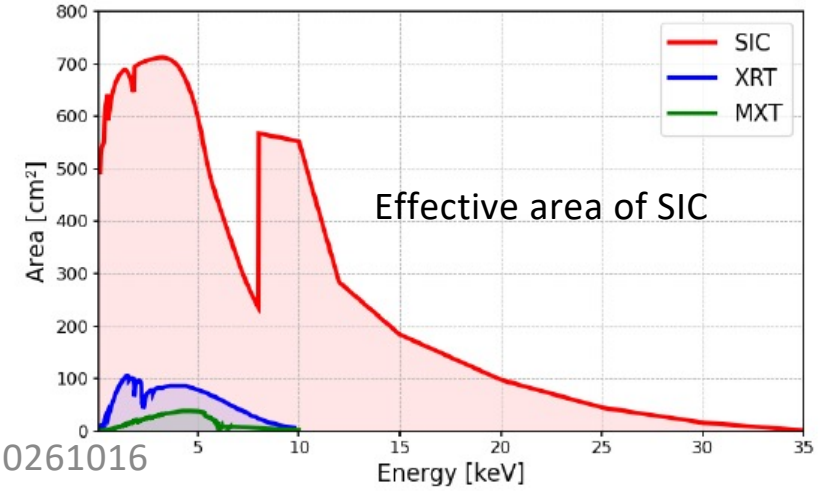
The Spectral Imaging Camera (SIC)

P.I. Ian Hutchinson (Leicester University, UK)

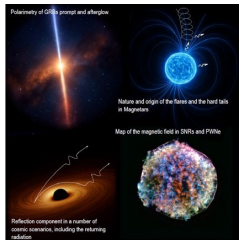




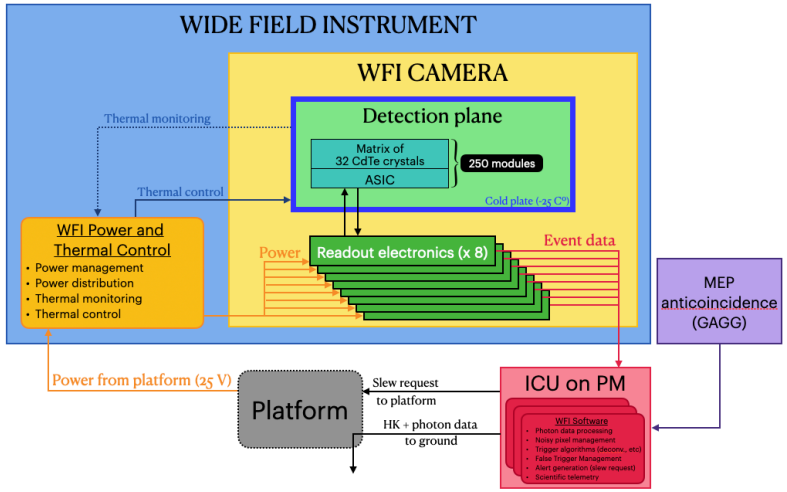
Parameter	SIC Characteristic
Energy range	0.5–35 keV
HEW	10” ($<$ 10 keV) 15” ($>$ 10 keV)
Mirror resolution	10-15”
Mirror area	700 cm^2 (@ 5 keV)
Field of view	$\sim$ 16’
Energy resolution (FWHM)	LED: $\sim$ 180 eV (@ 5.9 keV) HED: $\sim$1 keV (@ 17.5 keV)
Time resolution	LED (window mode): $< 5ms$ HED: $< 5\mu s$
Detection plane area	$\sim$ 4x4 cm^2

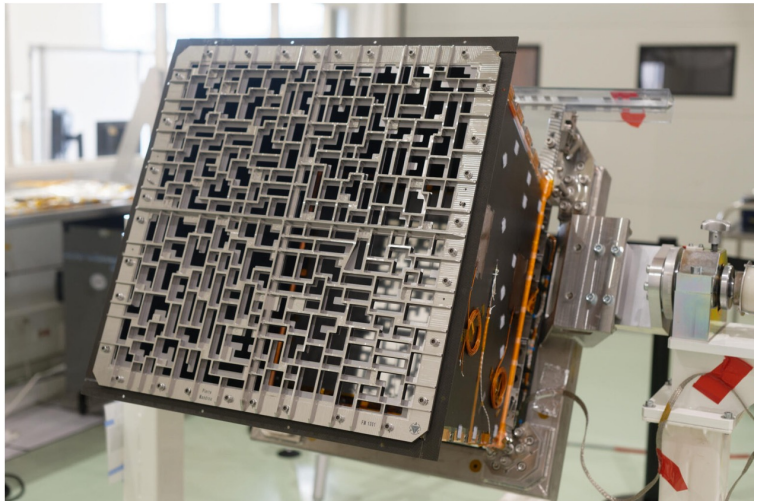


Support MEP&LEP for precise spectroscopy and imaging
High Quantum Efficiency & Large Field of View (16 arcmin)
Wide Energy covering 0.3-40 keV
Ancillary Science (high time resolution)



THE WIDE FIELD INSTRUMENT: A CLONE OF SVOM/ECLAIRS



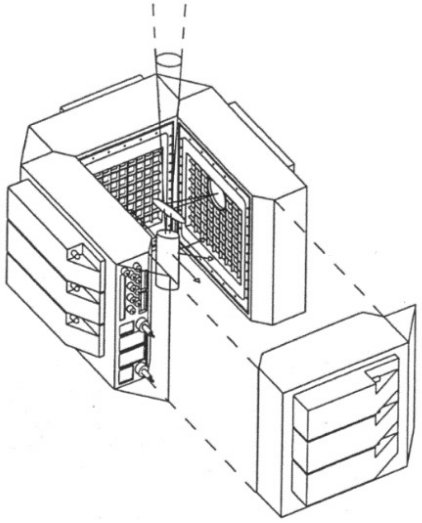


Parameter	WFI Characteristic
Energy range	4.0–150 keV
Angular resolution	1.5°
Source localization	$< 12''$
Field of view	$89° \times 89°$ (2.05 sr)
Energy resolution (FWHM)	$\sim$ 1.2 keV (@ 60 keV)
Sensitivity (over 1 s in 5–50 keV)	2.5×10^{-8} erg cm^{-2}s^{-1}
Number of GRB per year	~65
Detection plane area	$\sim$ 950 cm^2
Dead time	<10% for 10^5 c/s

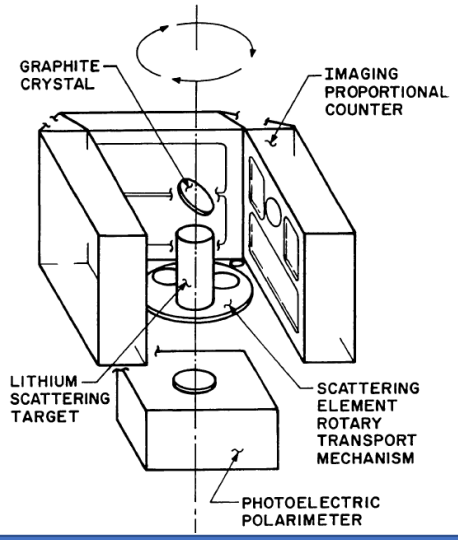
P.I. Sebastien Guillot, IRAP (France)

The EXPO Wide Field Imager is ia clone of SVOM/ECLAIRs and it is included in the Service Module on a side with respect to the 6 mirrors.

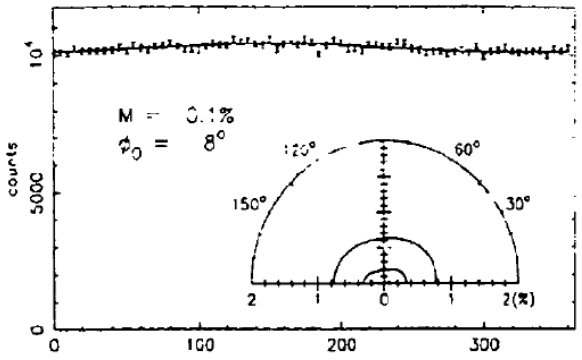
FROM A MISTAKE TO A TRUE PHOTOELECTRIC X-RAY POLARIMETRY



The Stellar X-ray Polarimeter on board Spectrum-X-Gamma SRG
(USA, Italy, Russia)



Hanany, S. et al., 1995



Kaaret et al., OptEng 1990, SPIE 1994 Tomsick et al., SPIE 1997, Soffitta et al., NIM A, 1998

The photoelectric polarimeter, as configured, did not worked for a experimental mistake but the expected sensitivity was great in the soft-X-rays albeit with low modulation factor.

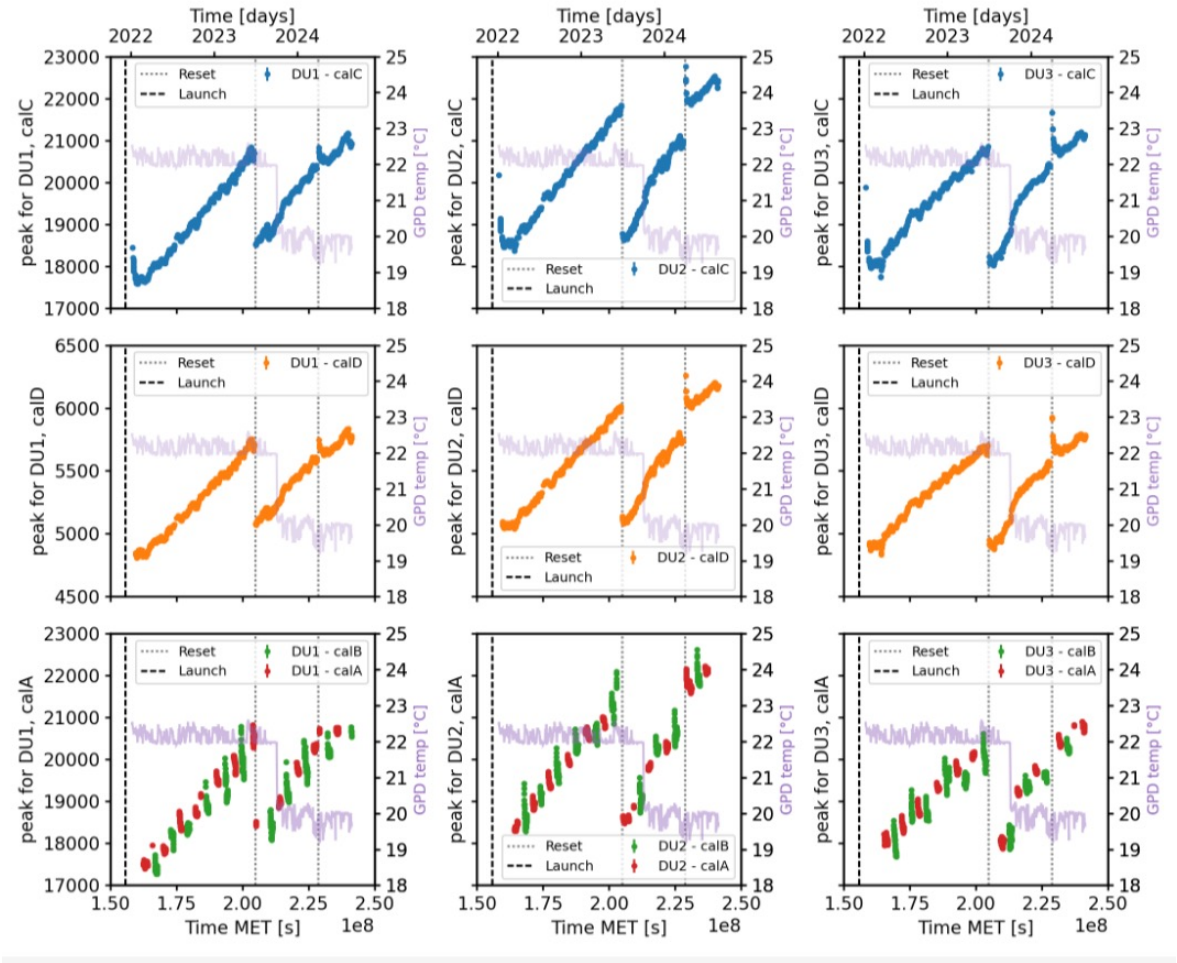
So Enrico Costa and Paolo Soffitta had the idea to replace CsI photocatode and vacuum with a suitable gas mixture (with low atomic number!) to make the charge image of the track of the photoelectron! and went to visit Ronaldo Bellazzini.

TABLE I. Sample observing plan for the SXRP mission.

Source	Observing Time (10^5sec)	Min. Det. Pol. (%) Graphite	Lithium	Observing Time (10^5sec)	MDP (%) CsI
Energy (keV)		2.6	5 – 10		0.1 – 5
Radio Pulsars					
Crab Primary Pulse (Avg.)	2	6.0	6.2	1	0.8
Leading Edge	2	8.0	7.6	1	1.1
Trailing Edge	2	9.4	7.6	1	1.2
Supernova Remnants					
Crab Nebula	2	0.5	0.4	1	< 0.1
PSR 1055-52				2	10
Binary Pulsars*					
Her X-1**	7	2.8	1.6	1.5	0.8
4U0900-4	1	2.8	0.9	0.5	0.5
GX1+4	1	4.3	1.2	0.5	0.8
4U1223-62	2	3.8	0.9	1	0.7
4U1626-67	2	3.4	1.8	1	0.6
Cen X-3	1	1.8	0.6	0.2	0.5
Black Hole Candidates					
Cyg X-1	6			1	
Low State		1.0	0.8		0.2
High State		0.3	0.2		< 0.1
LMC X-1				4	1.0
QPOs					
Cyg X-3	1	1.5	0.6	0.2	0.4
Sco X-1	1	0.7	0.1	0.01	0.2
4U1822-37				2	3.6
AGN's					
Cen A	1	7.6	1.9	1	1.0
Mkn 421	6	4.6	18.6	1	1.9
3C273	6	3.8	6.1	1	1.6
PKS2155-304				1	1.5
ESO 141-G55				1	2.6
NGC 7469				1	1.9
Mkn 509				1	1.7
Mkn 501				1	2.1
2A1218+304				1	1.8

IXPE
Imaging X-Ray Polarimetry Explorer

SECOND WE USE TO CORRECT FOR THE SECULAR GAIN INCREASE



The gain increase is well understood in terms of absorption of the gas from the glue which is used to build the detector.

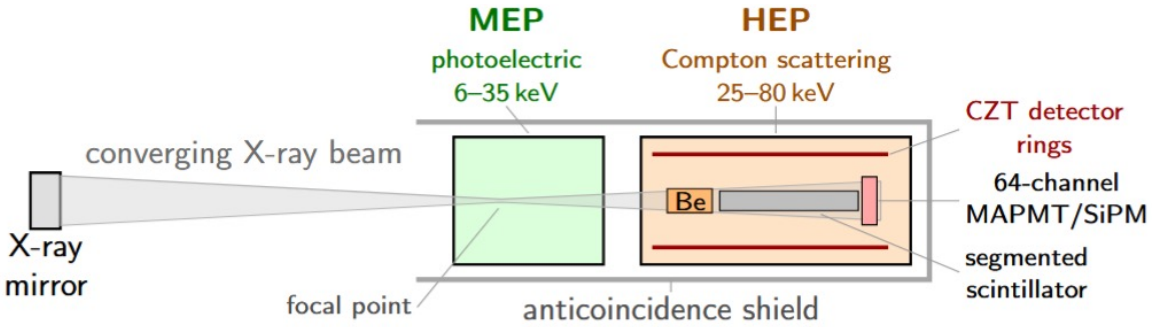
It is accompanied by a decrease of the pressure at level of 1.2 %/year

The modulation factor increases with time making the loss of sensitivity very small

It requires:
(1) Adjustment of the HV once/year
(2) New response matrices each 6 months

A further increase of band. Ballon-borne scattering polarimetry

WUSTL, INAF-IAPS, KTH, OsakaU, KyiotoU, HiroshimaU



H. Krawczinsky PI

Goal 1. The design of different polarimeter stacks focusing on a LEP, MEP, and HEP stack (for a satellite) and a MEP, and HEP stack (Ballon).

Goal 2. The fabrication and testing of an flight ready MEP and HEP stack

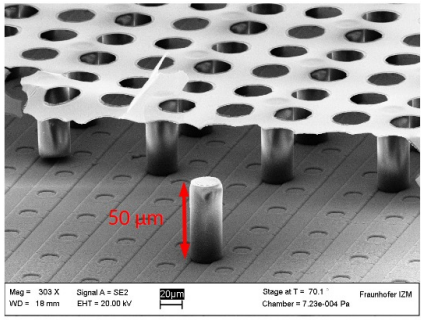
Goal 3. the fabrication and testing of an flight ready MEP and HEP stack;

APRA funds request duration 3 years starting from feb. 2027 if funded.
Followed by a request of funds for a ballon-borne experiment.

TimePIX3: from MEDIPIX CERN collaboration

Timepix3: a 65K channel hybrid pixel readout chip with simultaneous ToA/ToT and sparse readout





Kaminski, 2017, Lupberger 2015

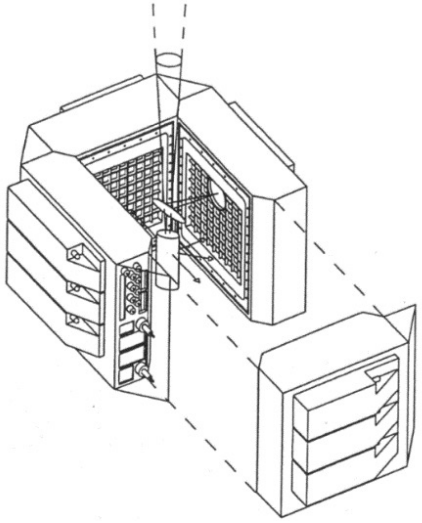
Parameter	Value
Pixel matrix	256 x 256 = 65536 pixels (2x4 superpixels)
Pixel size	55 x 55 µm^2
Technology	CMOS 120 nm
Measurement type	1. Simultaneous 10 bit TOT, 14 + 4 bit ToA 2. 14 + 4 bit ToA only 3. 14 bit integral ToT
Readout type	1. Data Driven (zero-suppression) 2. Frame based (zero-suppression)
Dead time per pixel	ToT + 457 ns (pulse processing + data transfer)
Output bandwidth	Up to 5.12 Gbs (parallel 8 channels x 640 Mbps)
Maximum Counting rate	Data Driven up to 40Mhits/cm^2/s with duty cycle of 100 %
TOA precision (resolution)	1.56ns
Front End noise, minimum threshold	60 e_{rms} , 500 e^-

3-D imaging of the track is possible.

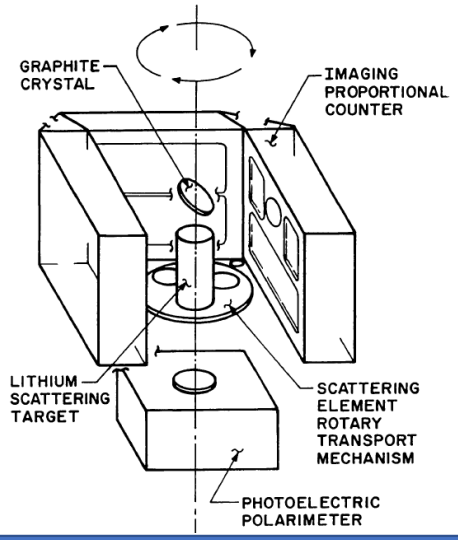
High rate for large optics is possible

Ongoing collaboration with University of Bonn

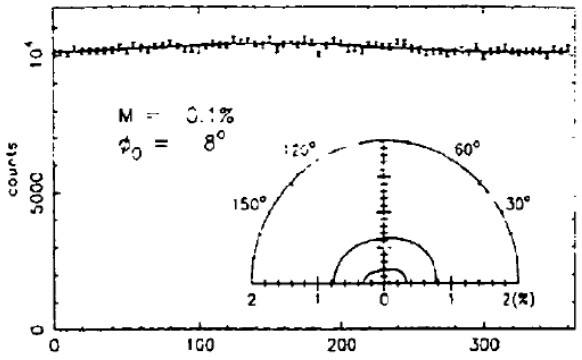
FROM A MISTAKE TO A TRUE PHOTOELECTRIC X-RAY POLARIMETRY



The Stellar X-ray Polarimeter on board Spectrum-X-Gamma SRG
(USA, Italy, Russia)



Hanany, S. et al., 1995



Kaaret et al., OptEng 1990, SPIE 1994 Tomsick et al., SPIE 1997, Soffitta et al., NIM A, 1998

The photoelectric polarimeter, as configured, did not worked for a experimental mistake but the expected sensitivity was great in the soft-X-rays albeit with low modulation factor.

So Enrico Costa and Paolo Soffitta had the idea to replace CsI photocatode and vacuum with a suitable gas mixture (with low atomic number!) to make the charge image of the track of the photoelectron! and went to visit Ronaldo Bellazzini.

TABLE I. Sample observing plan for the SXRP mission.

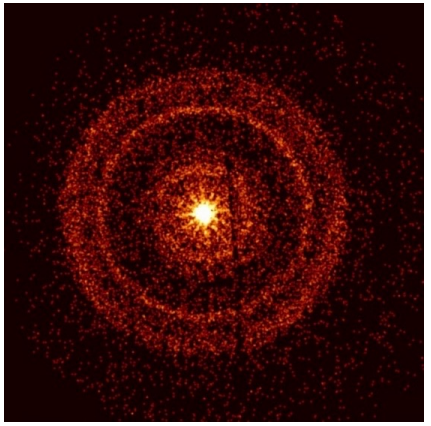
Source	Observing Time (10^5sec)	Min. Det. Pol. (%) Graphite	Lithium	Observing Time (10^5sec)	MDP (%) CsI
Energy (keV)		2.6	5 – 10		0.1 – 5
Radio Pulsars					
Crab Primary Pulse (Avg.)	2	6.0	6.2	1	0.8
Leading Edge	2	8.0	7.6	1	1.1
Trailing Edge	2	9.4	7.6	1	1.2
Supernova Remnants					
Crab Nebula	2	0.5	0.4	1	< 0.1
PSR 1055-52				2	10
Binary Pulsars*					
Her X-1**	7	2.8	1.6	1.5	0.8
4U0900-4	1	2.8	0.9	0.5	0.5
GX1+4	1	4.3	1.2	0.5	0.8
4U1223-62	2	3.8	0.9	1	0.7
4U1626-67	2	3.4	1.8	1	0.6
Cen X-3	1	1.8	0.6	0.2	0.5
Black Hole Candidates					
Cyg X-1	6			1	
Low State		1.0	0.8		0.2
High State		0.3	0.2		< 0.1
LMC X-1				4	1.0
QPOs					
Cyg X-3	1	1.5	0.6	0.2	0.4
Sco X-1	1	0.7	0.1	0.01	0.2
4U1822-37				2	3.6
AGN's					
Cen A	1	7.6	1.9	1	1.0
Mkn 421	6	4.6	18.6	1	1.9
3C273	6	3.8	6.1	1	1.6
PKS2155-304				1	1.5
ESO 141-G55				1	2.6
NGC 7469				1	1.9
Mkn 509				1	1.7
Mkn 501				1	2.1
2A1218+304				1	1.8

IXPE
Imaging X-Ray Polarimetry Explorer

GRB 221009A

We did not plan to follow-up on GRBs, because of the relatively slow reaction time (2-3 days).

However, GRB 221009A (the 'BOAT' GRB) was so exceptional in terms of brightness, that we decided to observe it.



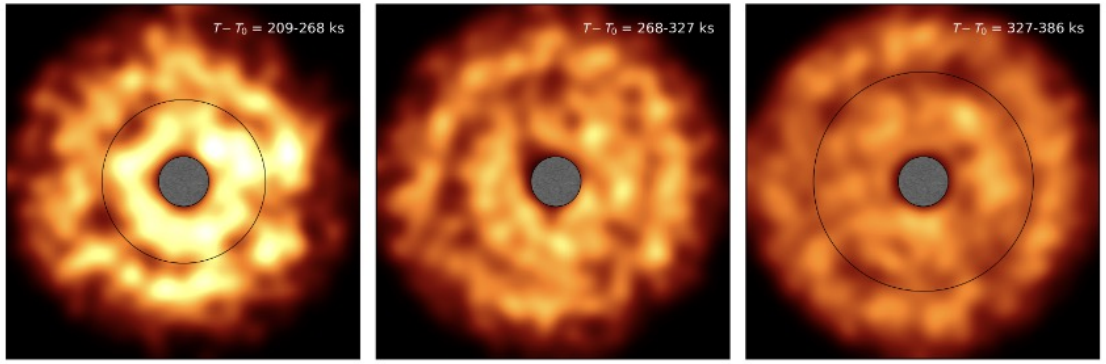
Swift/XRT image

P<13.8% (99% c.l.)

(Negro et al. 2023)

Dust rings also observed →

polarization of the prompt emission (<55%)



Time evolution of dust rings as seen by IXPE

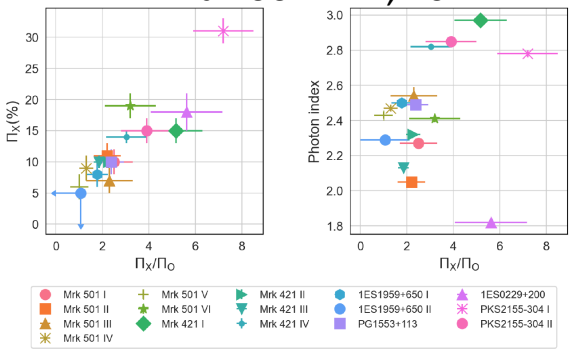
HSP blazars recap:

Marsher, A. et al., 2024

Table 1. Contemporaneous X-ray and optical polarization of HSP blazars.

Object (Date)	X-ray $\Pi_X(\%)$	X-ray $\psi_X(^\circ)$	Optical R-Band [a] $\Pi_O(\%)$	Optical R-Band [a] $\psi_O(^\circ)$	Jet PA(°) at 43 GHz [b]
1ES0229 + 200 [c] (23 January 2023)	18 ± 3	$25 \pm 5^\circ$	$2.4 \pm 0.7\%$	$2 \pm 8^\circ$	163 ± 8
Mrk421 (5 May 2022)	$15 \pm 2\%$	35 ± 4	2.9 ± 0.5	32 ± 5	-29 ± 18
Mrk421 (5 June 2022)	10 ± 1	Rotation	4.4 ± 0.4	-40 ± 6	-29 ± 18
Mrk421 (8 June 2022)	10 ± 1	Rotation	5.4 ± 0.4	-35 ± 1	-29 ± 18
Mrk421 (17 December 2022)	14 ± 1	-73 ± 3	4.6 ± 1.3	26 ± 9	-29 ± 18
PG1553 + 113 (2 February 2023)	10 ± 2	86 ± 8	4.2 ± 0.5	Rotation	50 ± 10
Mrk501 (7 March 2022)	9.8 ± 1.7	136 ± 5	6.6 ± 0.4	110 ± 5	120 ± 12
Mrk501 (27 March 2022)	10.3 ± 1.4	115 ± 4	4.7 ± 0.3	120 ± 3	120 ± 12
Mrk501 (9 July 2022)	6.9 ± 1.8	134 ± 8	2.7 ± 0.5	109 ± 5	120 ± 12
Mrk501 (12 February 2023)	9.0 ± 2.4	110 ± 8	6.6 ± 0.9	150 ± 4	120 ± 12
Mrk501 (19 March 2023)	6.0 ± 2.1	107 ± 11	6.1 ± 0.7	125 ± 3	120 ± 12
Mrk501 (16 April 2023)	18.5 ± 2.2	103 ± 3	5.9 ± 1.5	108 ± 6	120 ± 12
1ES1959 + 650 (3 May 2022)	8.0 ± 2.3	123 ± 8	4.5 ± 0.2	159 ± 1	120–150
1ES1959 + 650 (10 June 2022)	< 5.1 [d]	—	4.7 ± 0.6	151 ± 19	120–150
1ES2155−304 (30 October 2023)	31 ± 2	129 ± 2	4.3 ± 0.7	116 ± 8	135 ± 45
1ES2155−304 (4 November 2023)	15 ± 2	125 ± 4	3.8 ± 0.9	116 ± 8	135 ± 45

Dawoon Kim, 2024

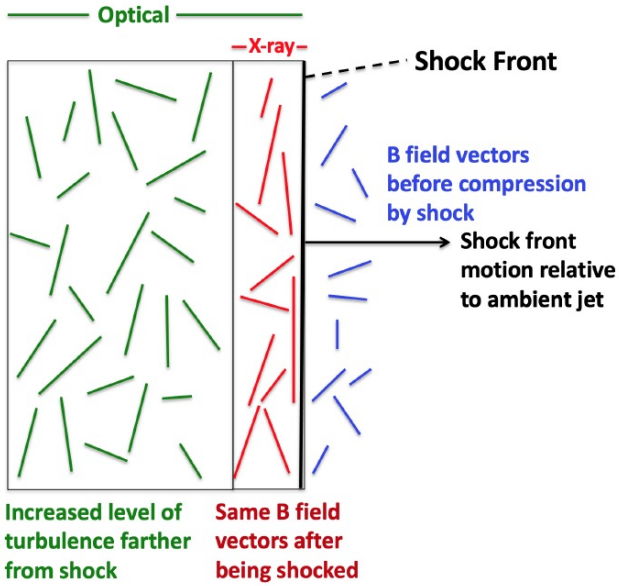


PD & PA shows variability for most of the IXPE observed HSP.

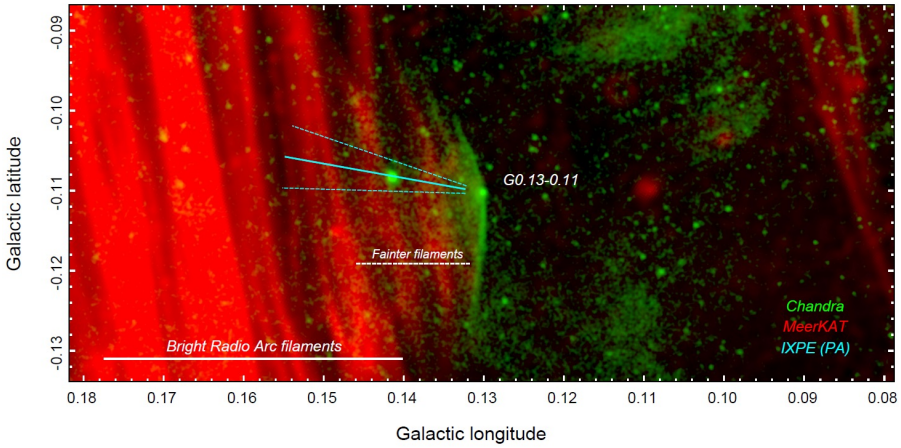
Magnetic reconnection can provide (1) stratification if acceleration start on a single small size (2) polarization angle parallel to the jet and (3) variability in turbulent region.

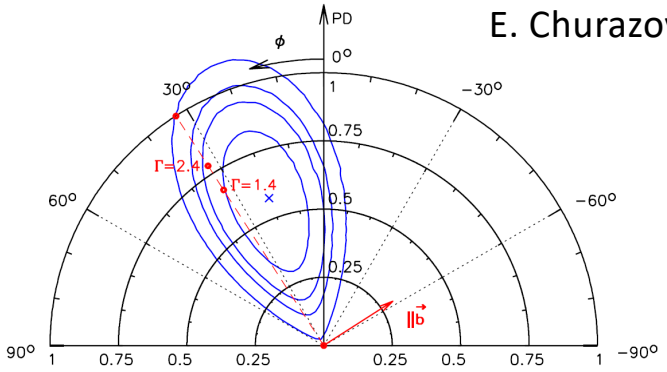
Costa_XPolarimetry_CTAO_20261016

Energy stratified shock acceleration model: If the pre-shock medium is turbulent the PA can fluctuate around the jet direction.

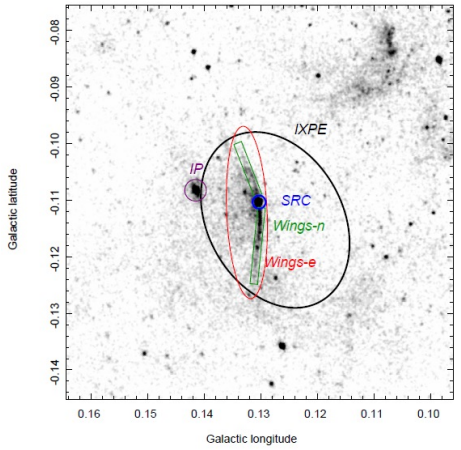


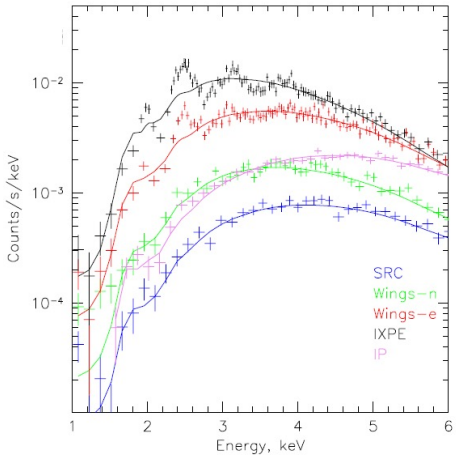
A VERY NICE SERENDIPITOUS DISCOVERY: POLARIZED EMISSION FROM THE X-RAY BRIGHT FILAMENT G0.13-0.11





E. Churazov, A&A 2024 et al.



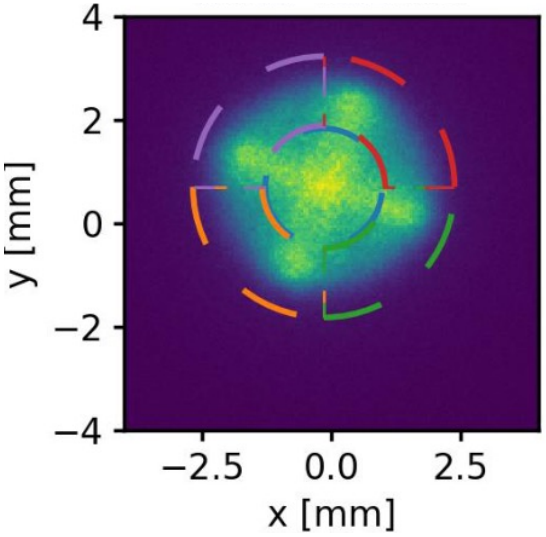


- A tight upper limit would neglect synchrotron emission or the magnetic field is very disordered at variance of other radio filament or G01.13-0.11 is not a PWN
- The polarization angle found is perpendicular to that of the molecular clouds. Tomography of the molecular clouds around the GC would be affected by smaller PD.

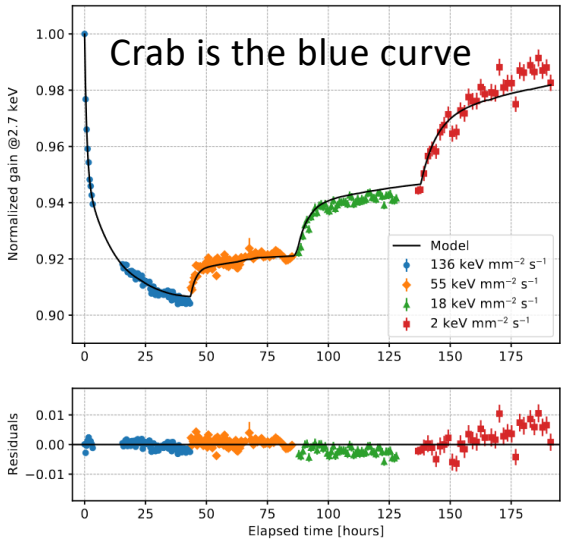
The high degree of polarization proves the synchrotron origin of X-rays. The polarization angle shows that the magnetic field (≈ 100 μGauss) is parallel to the radio filaments that may be part of the GC Radio Arc

IXPE
Imaging X-Ray Polarimetry Explorer

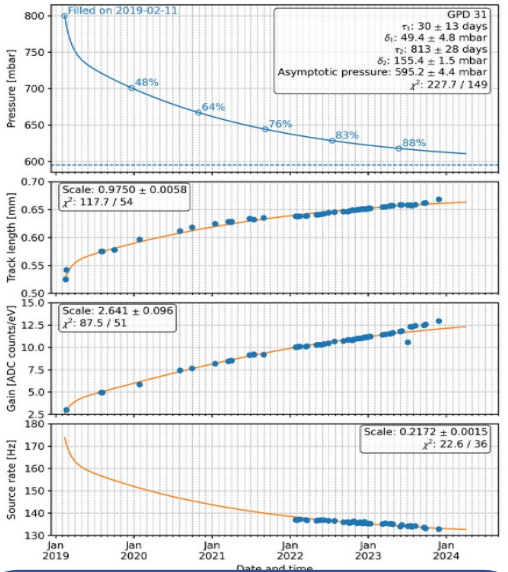
Peculiarity of the current GPD design



Being un-useful the rotation, a dithering is required to facilitate the ground calibration.



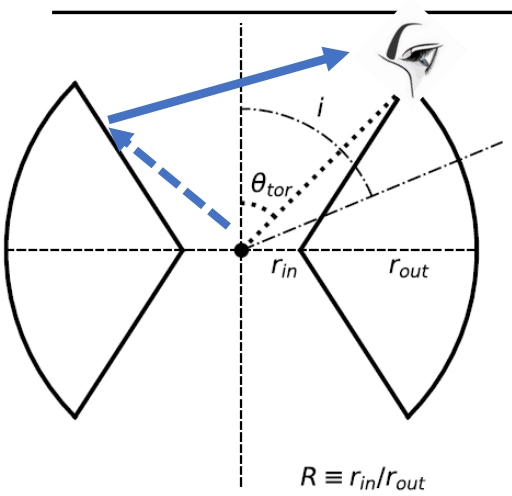
Gain shift due to charging is not yet totally corrected.
Charging is responsible for a residual mis-calibration of 10-20 eV

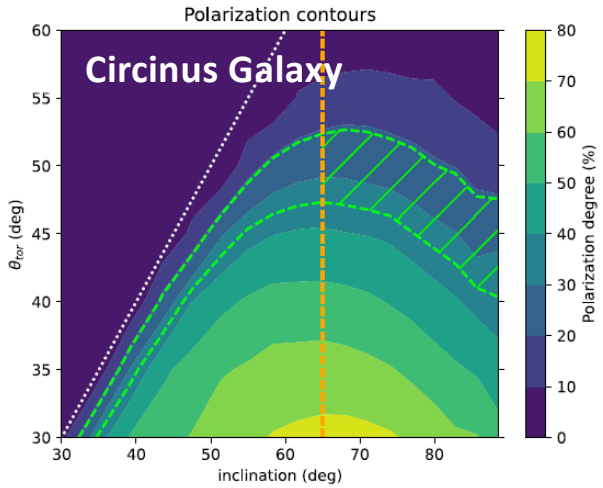


Pressure drop due to absorption of the DME by the glue.
650 mbar current pressure

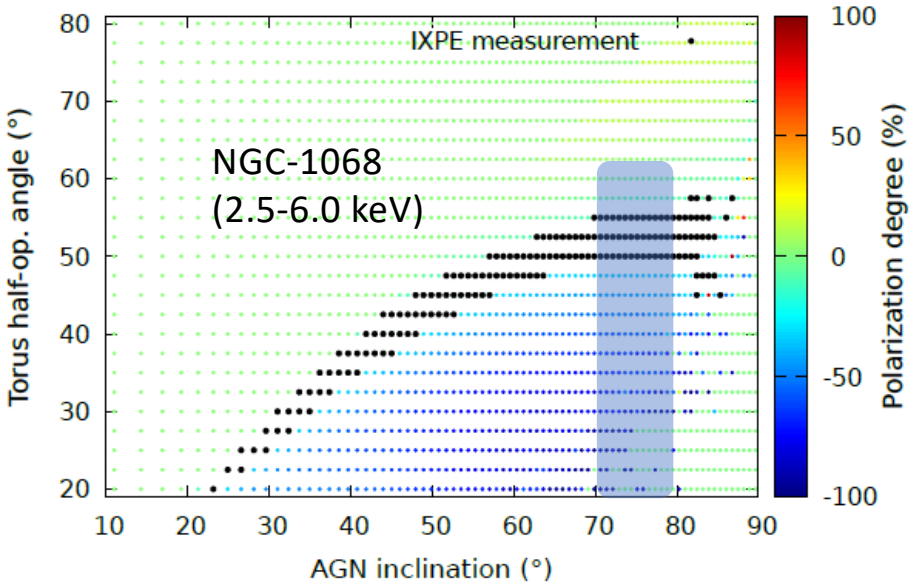
IXPE Imaging X-Ray Polarimetry Explorer

IXPE HELPS TO CONSTRAIN THE TORUS OPENING ANGLE





The orange vertical line set the lower limit to the inclination as provided by the inclination of the galaxy. The dashed lines mark the 68% confidence level region consistent with the measured polarization of the cold reflector. The hashed region mark the constraints on inclination and torus aperture.

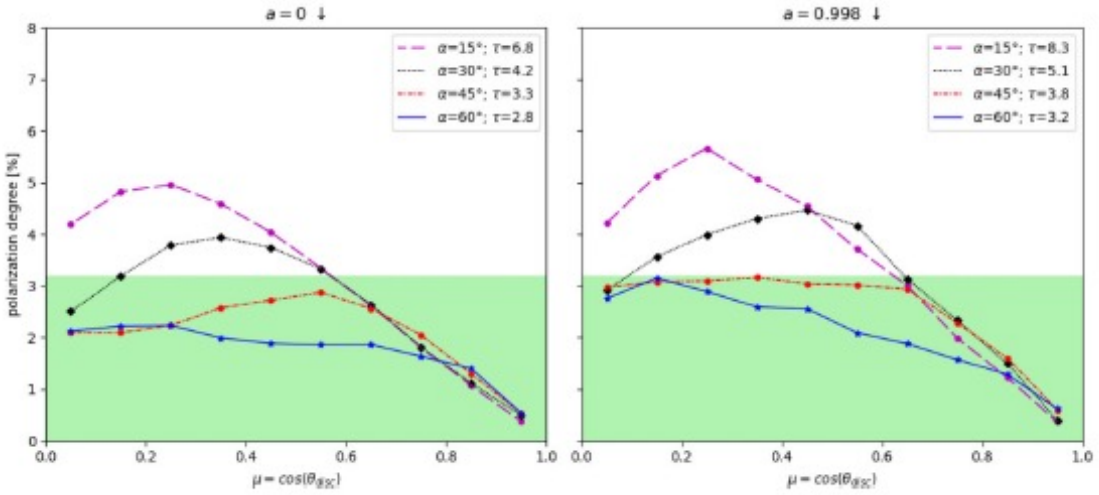


The positive polarization is parallel to the jet, the negative polarization is perpendicular to the jet. Each colored dot represent a simulation. Black dots are consistent with IXPE polarimetry. Shaded region is the constraint from the literature on the torus inclination.

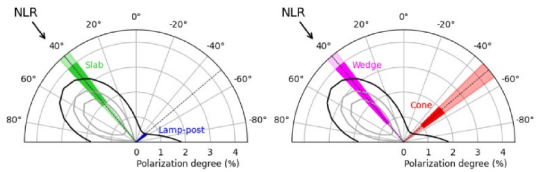
For both Circinus galaxy and NGC-1068 X-ray polarimetry constraints on the torus aperture are similar 50°-55°

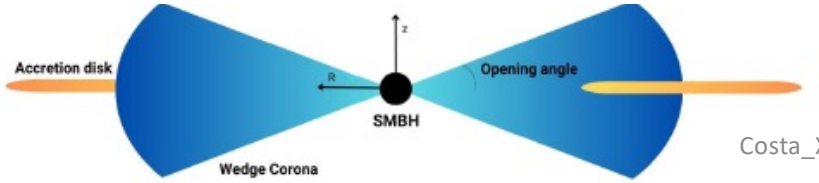
IXPE helps to constrain the geometry of the corona.

MCG 05-23-16 (Tagliacozzo et al. 2023)

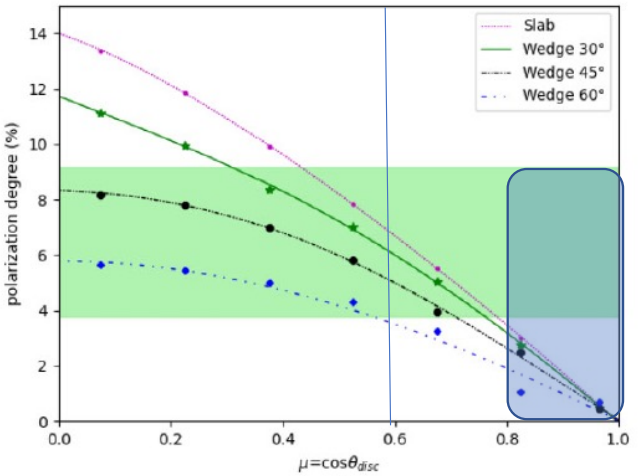


Simulations with MONK





NCG 4151 (Gianolli et al 2023)



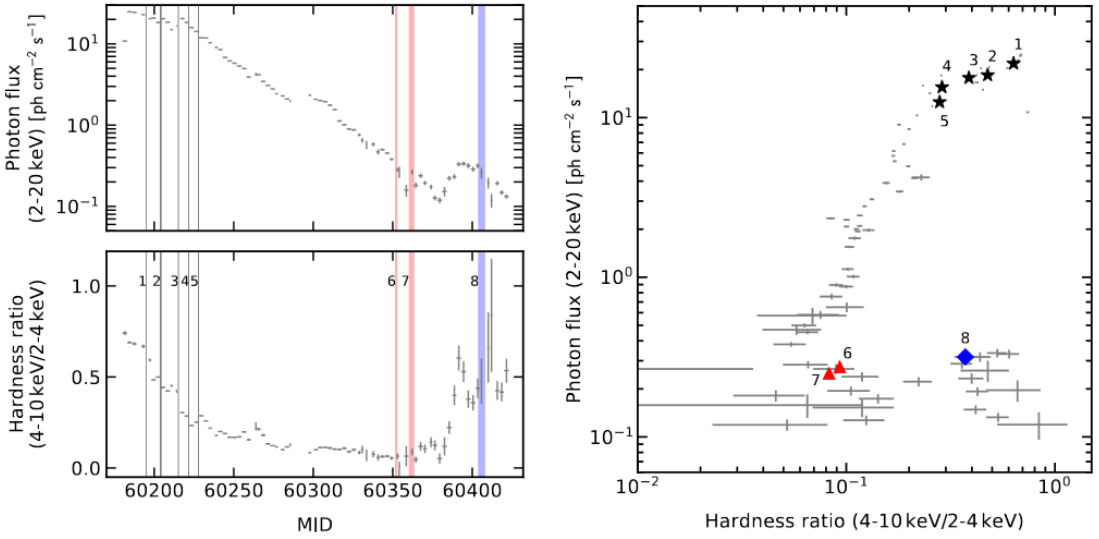
For both MCG 05-23-16 and NGC 4151 Slab o Wedge geometry of he corona are consistent with the IXPE data. NCG4151 favors disk inclinations obtained by reverberation and disfavor inclination obtained by spectra

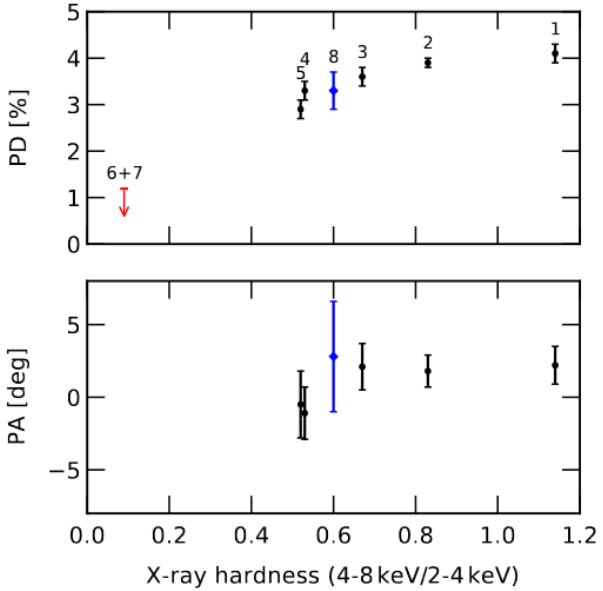
IXPE TRACES A STATE TRANSITION WITH SWIFT J1727.8-1613

Discovered on 24th August 2023 (7 Crab in 2-20 keV band)

Most probably a BH-binary transient: (X-ray spectrum, QPO, flat-spectrum radio emission)

Ingram, A. et al., ApJ 2024, Podgorny A&A 2025





IXPE is covering the hard-to-soft-hard transition. X-ray PA is parallel to Radio-PA implying that corona is extended along the disk in all observations.

PD decreases with time implying that disk emission with orthogonal or null polarization is coming into play.

PD increases with energy as in others BH-Binaries

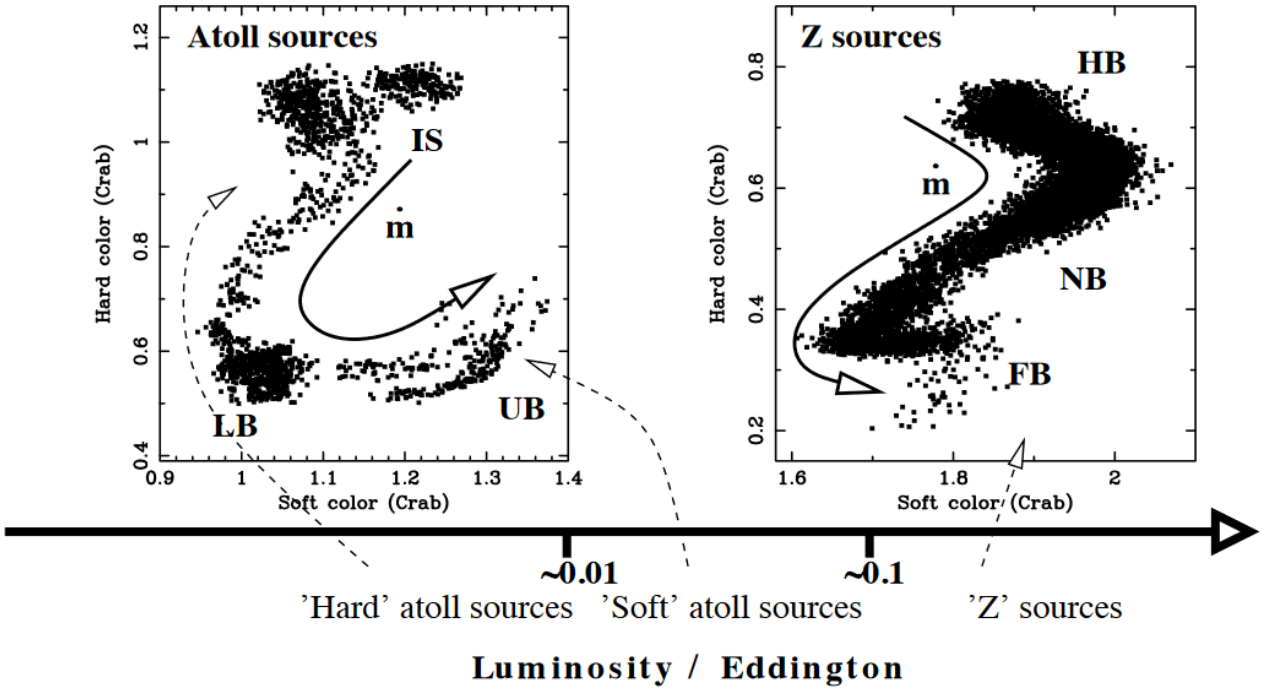
PD drops in the soft state while recovers in the hard dim state at level of outburst

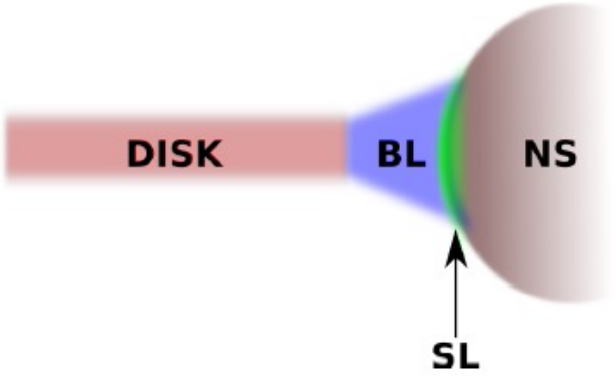
LOW MAGNETIZED NEUTRON STARS

IS = Iland State, LB= Lower Banana, UB = Upper Banana

HB = Horizontal Branch, NB = Normal Branch, FB = Flaring Branch

BL = Boundary Layer; SL = Spreading Layer





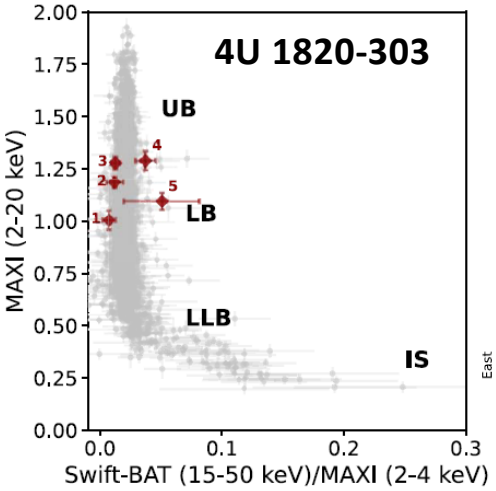
NS: $B < 10^{10}$ G,
$M_{com} \approx M_{\odot}$
Accreting matter via Roche-lobe overflow

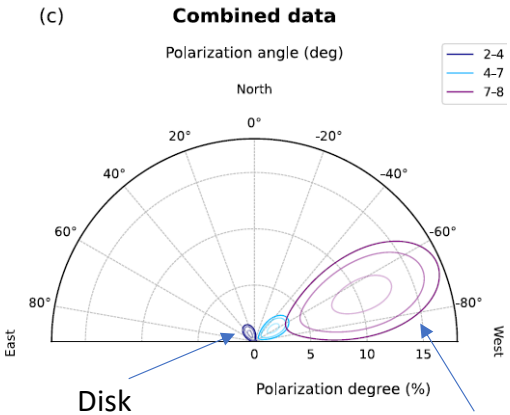
Di Salvo et al., 2023

IXPE Imaging X-Ray Polarimetry Explorer

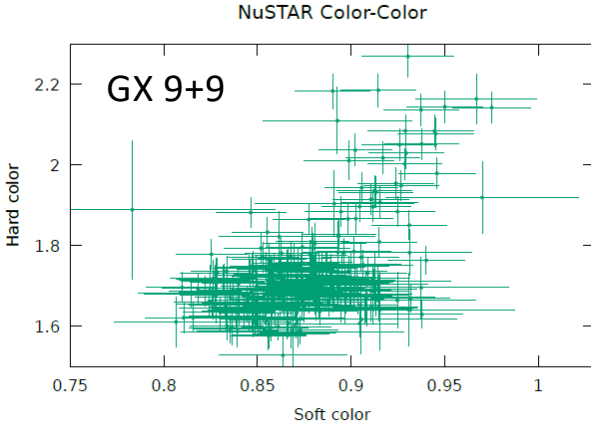
ATOLL SOURCES, 4U 1820-303, GX9+9

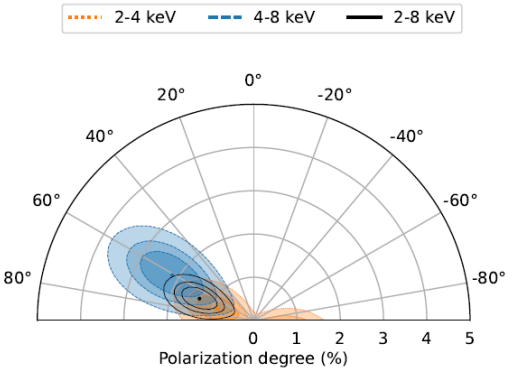
Di Marco et al., 2023





Ursini et al. 2023





Spreading (boundary layer)

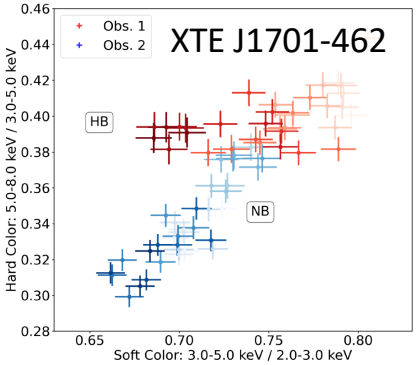
In 4U 1820 a rotation of the polarization angle of 90° with energy may indicate that the disk (low energy) is polarized orthogonal to the spreading/boundary layer. The reflection fraction is negligible < 5%.

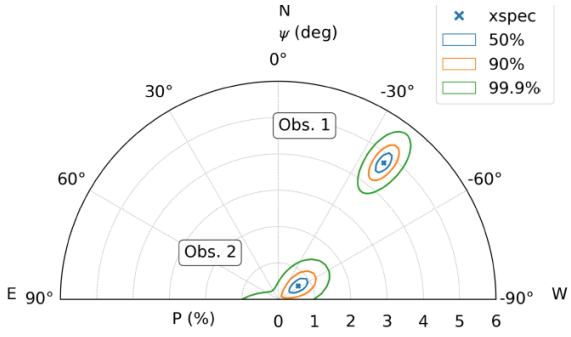
In GX 9+9 the 4-8 keV polarization is significant and may be a combination of reflection from the disk and a of Comptonization (boundary/spreading layer) and reflection from the disk.

In GS1826-238 (Capitanio et al., 2023) only upper limit albeit significant were measured.

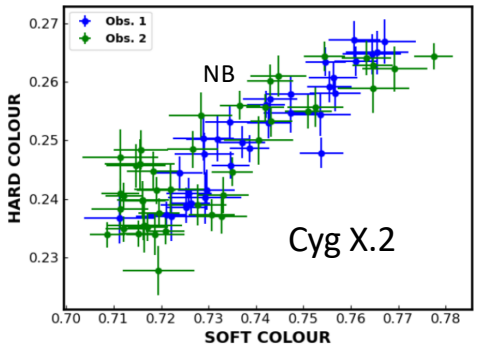
Z-SOURCE SOURCES: XTE J1701-462, CYG X-2 AND SCO X-1

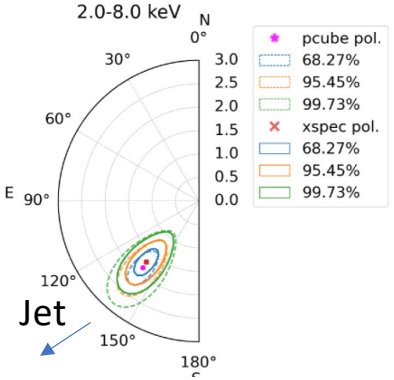
Cocchi et al., 2023



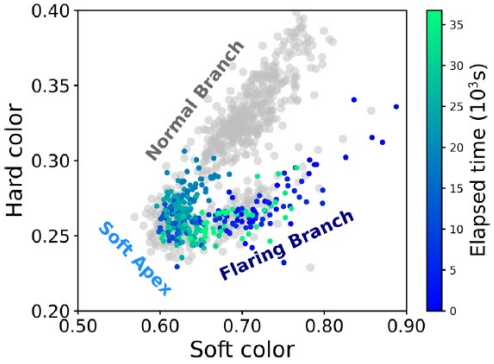


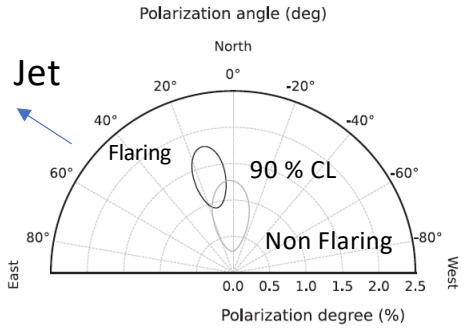
Farinelli et al. 2023

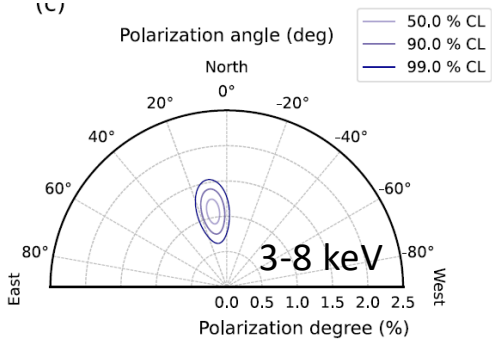




La Monaca et al 2024







The polarization on the Horizontal Branch seems larger with respect to the polarization of the Normal Branch (See also GX 5.1, Fabiani et al., 2023). In Sco X-1 flaring and non Flaring seems to have comparable PD and PA not aligned with the jet. I

Data shows a larger polarization with energy may be connected to a larger contribution of scattering.

IXPE Imaging X-Ray Polarimetry Explorer

BLACK HOLES X-RAY BINARIES:

- High Mass X-ray binaries:

Source (no. obs)	Goal of the study
Cyg X-1 Hard State (2)	Corona
Cyg X-1 Soft State (5)	Corona + Disk
Cyg X-3 hard & Intermediate (2)	Reflection from cone
LMC X-1 High Soft State (1)	Disk
LMC X-3 High Soft State (1)	Disk

- Low Mass X-ray binaries:

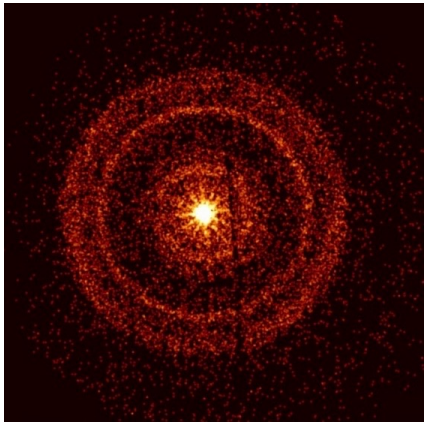
Source (no. obs)	Goal of the study
4U 1630-47 High-Soft State (1)	Disk
4U 1630-47 Steep PL/Interm (1)	Disk + Corona
SWIFT J1727 Low Hard/Inter (5)	Disk + Corona
SS 433 Eastern Lobe (1)	Synchrotron emission

IXPE
Imaging X-Ray Polarimetry Explorer

GRB 221009A

We did not plan to follow-up on GRBs, because of the relatively slow reaction time (2-3 days).

However, GRB 221009A (the 'BOAT' GRB) was so exceptional in terms of brightness, that we decided to observe it.



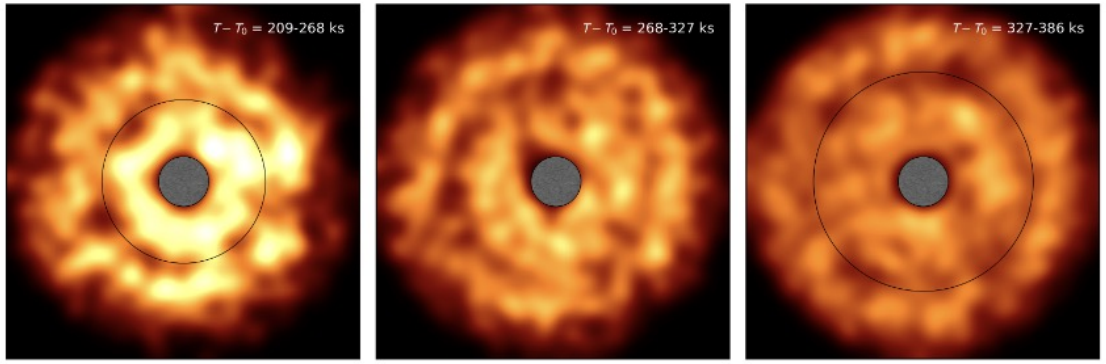
Swift/XRT image

P<13.8% (99% c.l.)

(Negro et al. 2023)

Dust rings also observed →

polarization of the prompt emission (<55%)



Time evolution of dust rings as seen by IXPE

IXPE Imaging X-Ray Polarimetry Explorer

SUMMARY OF HBL MULTI-WAVELENGTH POLARIMETRY

Table 1. Contemporaneous multiwavelength polarization properties of HSPs.

Source	X-ray		Optical & IR [a]		Radio [a]	
	$\Pi(\%)$	$\psi(^\circ)$	$\Pi(\%)$	$\psi(^\circ)$	$\Pi(\%)$	$\psi(^\circ)$
Mrk 501 I [1]	10 ± 2	134 ± 5	4 ± 1	119 ± 9	1.5 ± 0.5	152 ± 10
Mrk 501 II [1]	11 ± 2	115 ± 4	5 ± 1	117 ± 3	–	–
Mrk 421 I [2]	15 ± 2	35 ± 4	2.9 ± 0.5	32 ± 5	3.4 ± 0.4	55 ± 2
Mrk 421 II [3]	10 ± 1	Rotation	4.4 ± 0.4	140 ± 6	2.4 ± 0.1	139 ± 8
Mrk 421 III [3]	10 ± 1	Rotation	5.4 ± 0.4	145 ± 1	–	–
Mrk 421 IV [4]	14 ± 1	107 ± 3	4.6 ± 1.3	206 ± 9	1.8 ± 0.1	167 ± 4
1ES1959+650 I [5]	8 ± 2	123 ± 8	4.5 ± 0.2	159 ± 1	–	–
1ES1959+650 II [5]	<5	–	4.7 ± 0.6	151 ± 19	<1.6	–
PG1553+113 [6]	10 ± 2	86 ± 8	4.2 ± 0.5	Rotation	2.6 ± 0.7	133 ± 7
1ES0229+200 [7]	18 ± 3	25 ± 5	3.2 ± 0.7	-5 ± 9	<7	–

[1–8] Results compiled from the following references: [57–63]; [a] median polarization properties during the IXPE observation. Especially for optical and IR polarization, only corrected polarization values, accounting for the dilution of polarization by unpolarized starlight from the host galaxy, were considered for calculation; [b] at the lowest radio frequency (4.85 GHz).

Kim et al., 2024

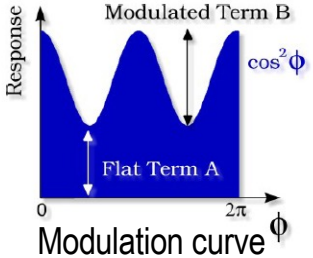
X-ray polarization of HBL are comparable higher than at longer wavelength

Notably Mrk 421 was found rotating in X-rays and not in longer wavelength while PG1553 was rotating in longer wavelength but not in X-rays

THE FORMALISM

Fit function: $\mathcal{M}(\phi) = A + B\cos^2(\phi - \phi_0)$

Modulation: $\frac{\mathcal{M}_{max} - \mathcal{M}_{min}}{\mathcal{M}_{max} + \mathcal{M}_{min}} = \frac{B}{B + 2A}$



Polarization: $\frac{1}{\mu}\frac{B}{B + 2A}$ μ is the modulation factor, i.e. the modulation for 100% polarized radiation

Or by using Stokes Parameters

$$S(\varphi) = I + U\sin(2\varphi) + Q\cos(2\varphi)$$

$$I = (A + \frac{B}{2}) \qquad U = \left(\frac{B}{2}\right) * \sin(2\varphi_0) \qquad Q = \left(\frac{B}{2}\right) * \cos(2\varphi_0)$$

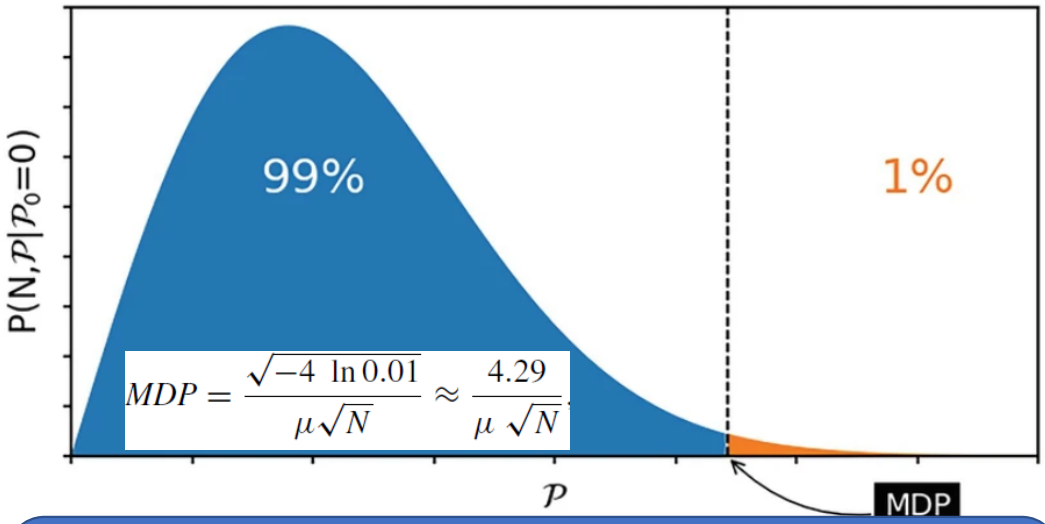
$$P = \frac{\sqrt{Q2+U2}}{I} \qquad \varphi = \frac{1}{2}atan\frac{U}{Q}$$

No V → no circular polarization with present techniques

Kislat et al. (2015) introduced the Stokes parameters from the direction of the single carrier of polarimetric observation

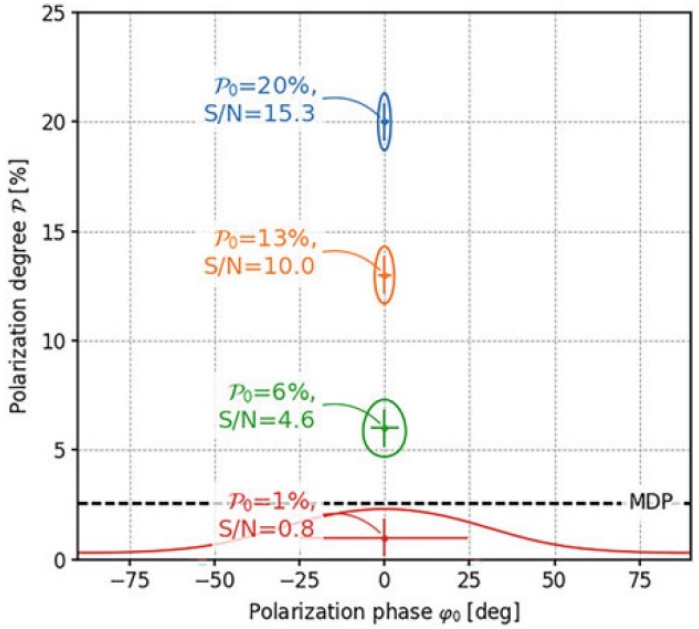
IXPE Imaging X-Ray Polarimetry Explorer

POLARIZATION ANALYSIS: MDP AND CONTOURS



The probability to measure a polarization P from an un-polarized source. The value of P for which this probability is 1 % or smaller is the Minimum Detectable Polarization (MDP).

Muleri F., 2023



Contours representing the joint probability for P.D. and P.A. at 68 % confidence level. P.D. and P.A. are covariant.

For P < MDP the angle is unconstrained albeit not all the angle are equiprobable.

IXPE Imaging X-Ray Polarimetry Explorer

THE FIRST LIMIT: IN POLARIMETRY THE SENSITIVITY IS A MATTER OF PHOTONS

$$MDP = \frac{4.29}{\mu R_S}\sqrt{\frac{R_S + R_B}{T}}$$

Minimum Detectable Polarization (MDP)

R_S is the Source rate, R_B is the Background rate, T is the observing time
μ is the modulation factor: the response of the polarimeter to a 100% polarized beam (spanning from 0 or no sensitivity, to 1 or maximum sensitivity)

If background is negligible: $$\mathrm{MDP} = \frac{4.29}{\mu\sqrt{N_{ph}}}$$

To reach MDP=1% with μ=0.5: $$N_{ph} = \left(\frac{4.29}{\mu\ \mathrm{MDP}}\right)^2 = 736\ 10^3\ \mathrm{ph}$$

Source detection > 10 counts
Source spectral slope > 100 counts
Source polarization > 100.000 counts

Caution: the MDP describes the capability of rejecting the null hypothesis (no polarization) at 99% confidence.

IXPE Imaging X-Ray Polarimetry Explorer

Some IXPE results

TWG 1: (Pulsar Wind Nebulae): The magnetic field is very ordered even at a large distance from the pulsar.

TWG 2: (Supernova Remnants): The magnetic field can be radially directed even in vicinity of the shock.

TWG 3: (Accreting Black Holes): The corona in hard X-ray is along the disk plane the accretion disk and the lamp-post is excluded.

TWG 4: (Accreting Neutron Stars): The rotating vector model works in X-rays. The degree of polarization is 5-6 times smaller with respect to models predictions.

TWG 5: (Magnetars): Different magnetars showed unexpectedly very different behavior on the polarization degree and angle.

TWG 6: (Radio-Quiet AGN & SgrA clouds): Corona is sandwiching the disk. Lamp-post is excluded. Reflection confirms obscuring torus in Compton-thick AGNs. Molecular clouds points to Sgr A* as origin of their reflected emission.

TWG 7: (Blazars and Radio Galaxies): Energy stratified shock acceleration is confirmed. In X-ray fast rotation of the polarization vector with time is present in Synchrotron dominated blazars. Inverse Compton dominated blazars

IXPE Imaging X-Ray Polarimetry Explorer

BLACK HOLES X-RAY BINARIES SOME PUBLICATIONS:

- High Mass X-ray binaries:

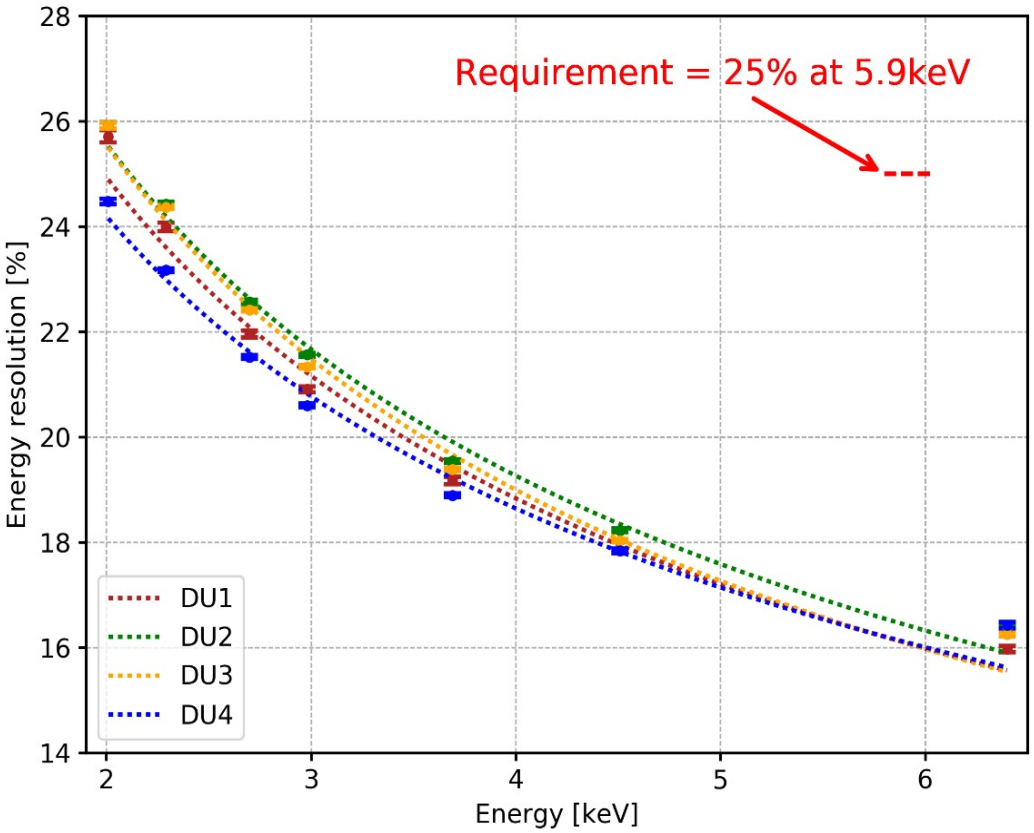
Source	Main result	Reference
LMC X-1 High Soft State	MDP_{99}=1.1% Standard thin disk compatible	Podgorny et al., MNRAS, 2023
LMC X-3 High Soft State	PD=(3.2+/-0.6)% PA=-42°+/-6° Low-spin (a= 0.2, a<0.7 from pol. analysis only)	Svoboda et al., ApJ, 2024

- Low Mass X-ray binaries:

Source	Goal of the study	
4U 1630-47 Steep PL/Interm.	PD = (6.8+/-0.2)% PA = 21°.3+/-0°.9 PL emitting region like the disk ?	Rodriguez Cavero, N., ApJ, 2023
4U 1957+11 High Soft State	PD: (1.9+/-0.4)%; PA:-41° +/-5°.7 High spin (a> 0.96)	Marra et al., Sub A&A, 2023
SWIFT J1727 Low Hard/Inter	Disk + Corona (confirming sandwich corona)	Veledina, A. et al ApJ, 2023 Ingram, A. et al. ApJ 2024
SS 433 Eastern Lobe (1)	Synchrotron emission	Kaaret, P. et al, ApJ, 2023

IXPE
Imaging
X-Ray
Polarimetry
Explorer

ENERGY RESOLUTION



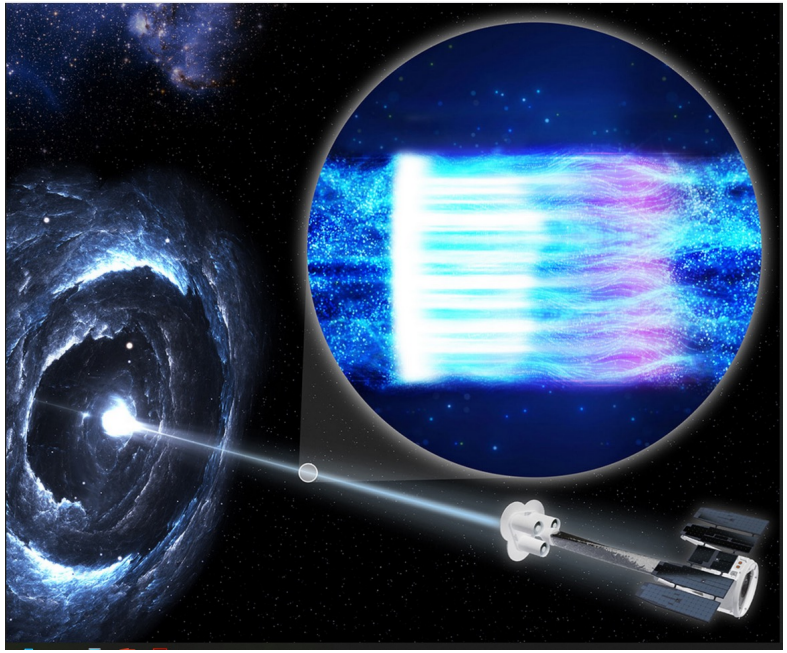
Energy calibration is much better of a typical proportional counter after gain equalization.

The gain equalization (Rankin J., et al. AJ 2023) is performed by comparing the average charge in one pixel with the one of the other pixel in the ROI.

Gain spatial maps are applied to the event energy reconstruction by the flight pipeline

IXPE Imaging X-Ray Polarimetry Explorer

BLAZARS



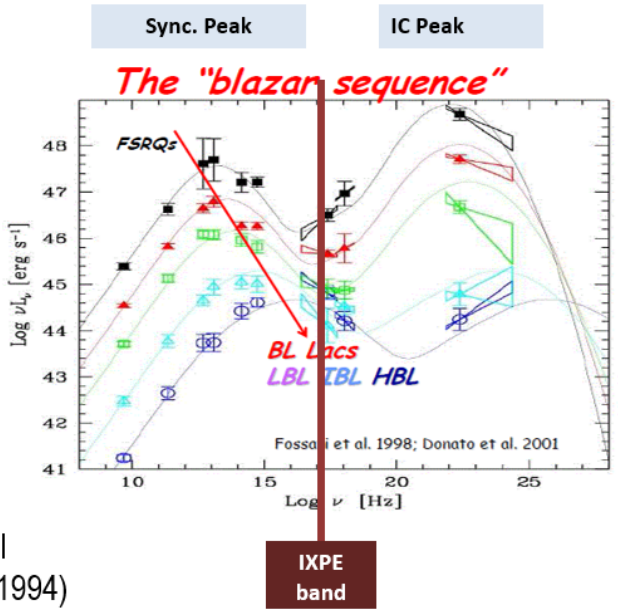
Synchrotron-dominated (with X-ray)

Blazars, multi-λ polarimetry probes **the structure** of the jet and of its **magnetic field**

Inverse Compton dominated (with X-ray)

Blazars, multi-λ polarimetry observations can determine:

- **the composition of the jet** (hadronic vs. leptonic, Zhang & Bottcher, 2013)
- **the origin of the seed photons** Synchrotron-Self Compton (SSC) or External Compton (EC) (Celotti & Matt, 1994; Poutanen 1994)



A blazar is an active galactic nucleus (AGN) with a relativistic jet directed closely towards the observer. Relativistic beaming from the jet makes blazars appear much brighter than they would be if the jet were pointed in a direction away from Earth.

IXPE Imaging X-Ray Polarimetry Explorer

TARGET OF OPPORTUNITIES (TOOS)

IXPE is not a Swift like mission

- Time for a TOO is not earlier than about 3 working days after the proposal
- GRB 221009A was indeed a special case TOO was requested on 10-10-2022 at 16:48 UTC and started on 10-11-2023 at 23:34:28 UTC
- We expect to trigger about one TOO per months.
- After a ToO started, the object that was in the long term planning is somewhat 'lost' and there is some discretion if it will be recovered later in the schedule

TOO (98 requested between new and pre selected more than 16 sources observed)

- Cyg X-1 (TWG 3)
- 4U 1630-472 (TWG 3)
- XTE 1701-46 (TWG 4)
- GRB 221009A No TWG
- EXO 2030 + 375 (TWG 4)
- Cyg X-3 (TWG 3)
- LS V + 44 17 (TWG 4)
- 4U 1630-47 (TWG 3)
- Swift J0243.6+6124 (TWG 4)
- 1ES 1959+650 (TWG 7)
- Swift J1727.8-1613 x 2 (TWG 3) multiple times
- GX 339-4 (BH, pre assigned)
- SRGA J144459.2-604207 (AMS, pre assigned)
- Swift J151857.0-572147 (BH)
- Cyg X-3 & Cyg X-1 (XL-Calibur simultaneous)
- 1E 1841-045

Mission	Allowed Sun Angle (deg)
HST	60-180 (+/-30 deg)
IXPE	65-115 (+/-25deg)
NICER	45-180
NuSTAR	43-180
SWIFT	47-180
XMM	70-110 (+/-20deg)

From HEASARC tools website

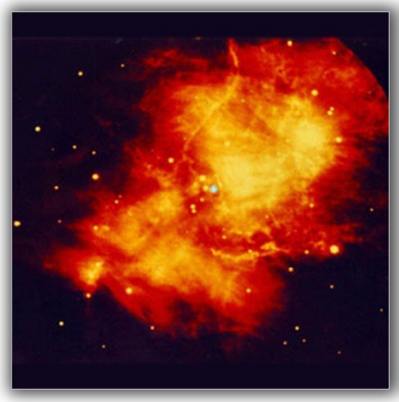
IXPE Allowed Sun Angle now increased up to +/- 34 deg

IXPE
Imaging X-Ray Polarimetry Explorer

THE CRAB NEBULA (BEFORE IXPE)



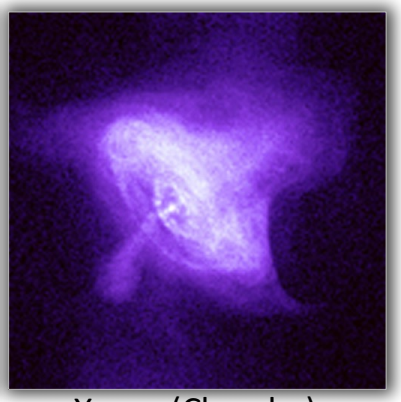
Radio (VLA)



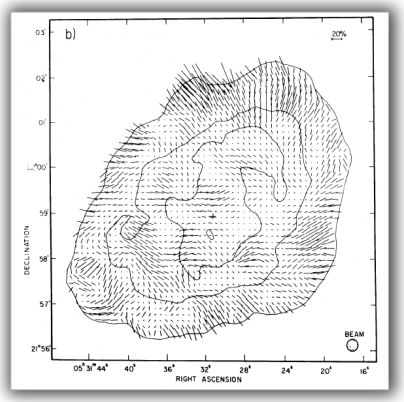
Infrared (Keck)



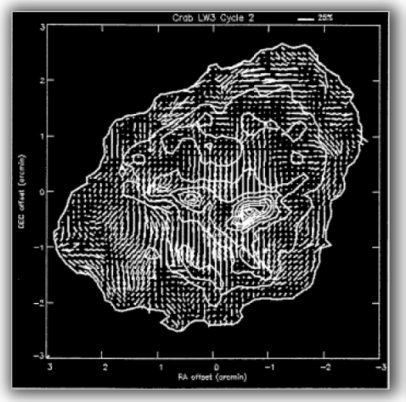
Optical (Palomar)



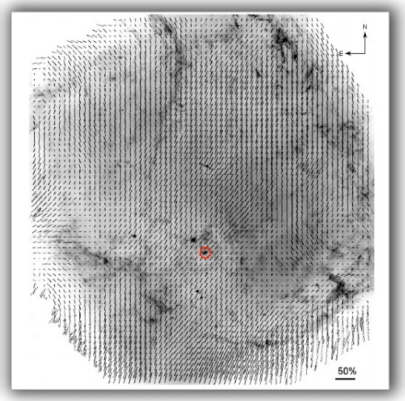
X-rays (Chandra)



Radio polarisation



IR polarisation



Optical polarisation

P=19% **integrated over the entire nebula** (Weisskopf et al. 1978)

X-ray polarisation

X-rays probe **freshly accelerated** electrons and their acceleration site

TOPICAL WORKING GROUPS ACTING IN THE FIRST TWO YEARS

Science Advisory Team (chaired by Giorgio Matt and Roger Romani)

Coordinates science activities required for planning, analyzing, interpreting, and reporting IXPE observations

Organized into seven Topical Working Groups

- *TWG1 Pulsar Wind Nebulae, led by Niccolò Bucciantini (INAF-Arcetri)*

Obtain polarimetric imaging to constrain the magnetic-field geometry of the nebula and the phase-dependent polarization of the pulsar

- *TWG2 Supernova Remnants, led by Pat Slane (CfA)*

Obtain spectral polarimetric imaging of Supernova Remnants (SNR) to constrain the magnetic-field structure of the X-ray emitting regions

- *TWG3 Accreting Black Holes, led by Michal Dovčiak (CAS-ASU) (Juri Poutanen. Next talk)*

Obtain spectral polarimetry of microquasars to constrain the value of the black-hole spin parameter (if in soft state), or constrain the geometry of the corona (if in hard state)

- *TWG4 Accreting Neutron Stars, led by Juri Poutanen (Turku) (Juri Poutanen Next talk)*

Obtain phase-dependent polarimetry of accreting X-ray pulsars (high-magnetic-field binaries) to constrain models and geometries for the pulsing emission. Obtain polarimetry of non pulsating accreting NS to constrain the geometry of the system

- *TWG5 Mag*netars, led *by Roberto Turolla (Uni Padua)*

Obtain phase-dependent polarimetry of magnetars to constrain the effects of vacuum polarization (birefringence in a strong magnetic field)

- *TWG6 Radio-Quiet AGN & Sgr A, led by Frédéric Marin (Strasbourg)*

Obtain polarimetry of RQ AGN to constrain the geometry of the emitting regions

- *TWG7 Blazars & Radio Galaxies, led by Alan Marscher (Boston U)*

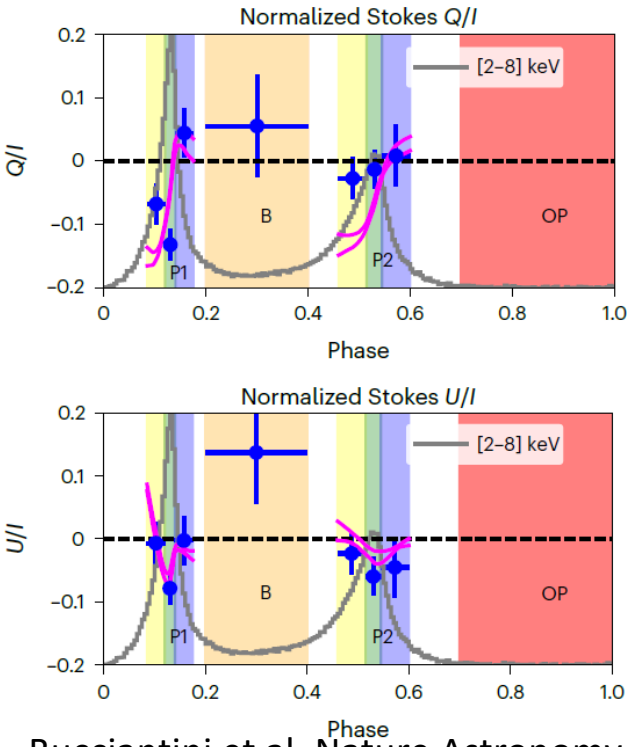
Obtain polarimetry of Blazars and RG to study jet emission

IXPE Imaging X-Ray Polarimetry Explorer

WHAT ABOUT THE PULSAR ?

- Vela pulsar is too weak in the IXPE energy band

PSR B0531+21 (Crab PSR)



Bucciantini et al. Nature Astronomy 2023

Comparison with optical polarization data

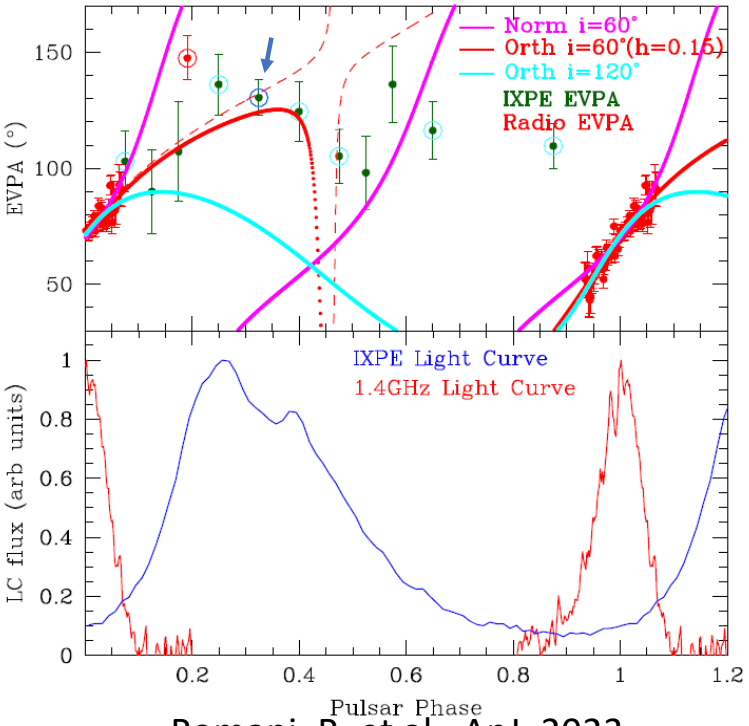
Crab PSR: (70 ks observation)

- **Polarization is > 3-sigma significant in the central bin of P1 (Main Pulse)**
- **Total pulse signal is negligible**
- **Consistency with optical data is marginal. It sweep faster in X-ray than in optical.**

MSH 15-52 PSR:

- **Only the central bin of the peak has been detected with > 3-sigma (17.5 %)**
- **Other bins low PD 10-20 % 2-3-sigma**

PSR B1509-58 (MSH 15-52 PSR)

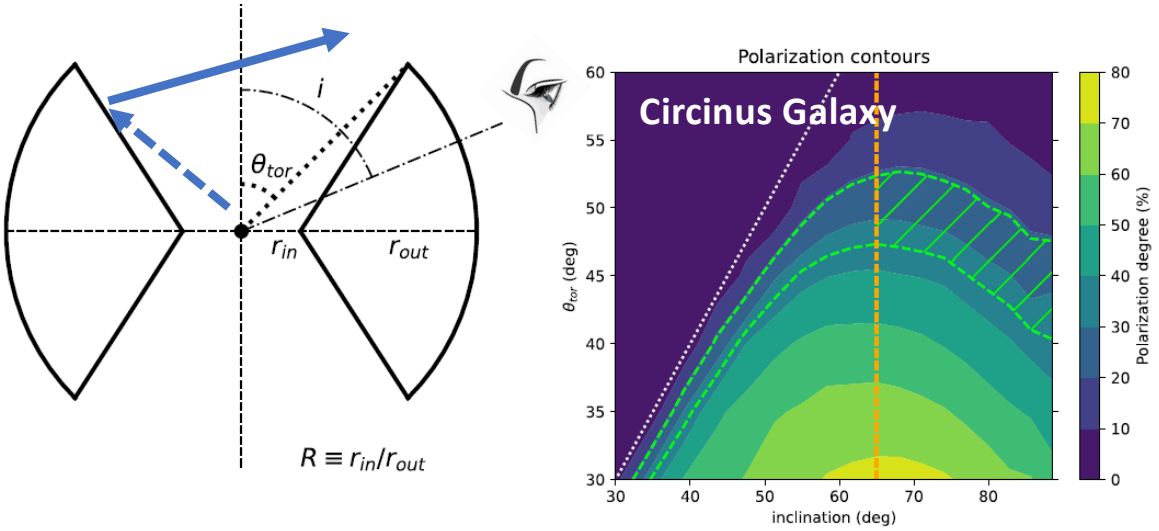


Romani, R. et al., ApJ, 2023

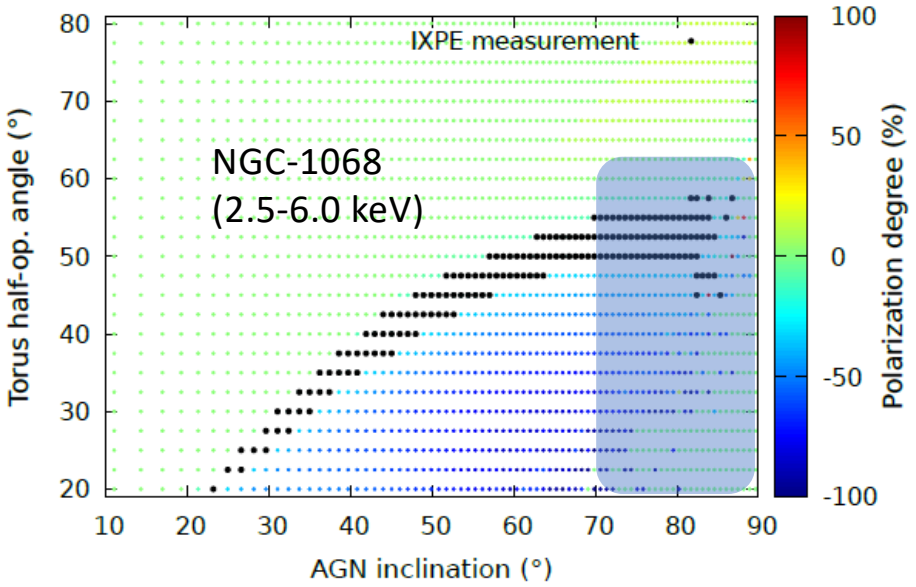
Comparison with radio polarization data

IXPE Imaging X-Ray Polarimetry Explorer

IXPE HELPS TO CONSTRAIN THE TORUS OPENING ANGLE



The orange vertical line set the lower limit to the inclination as provided by the inclination of the galaxy. The dashed lines mark the 68% confidence level region consistent with the measured polarization of the cold reflector. The hashed region mark the constraints on inclination and torus aperture.



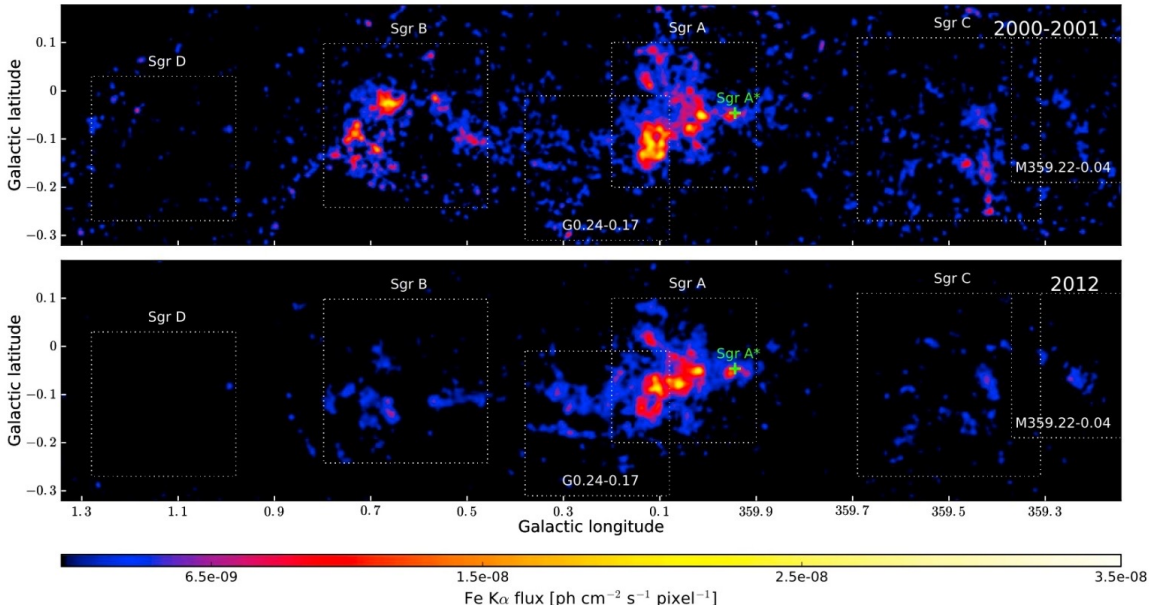
The positive polarization is parallel to the jet, the negative polarization is perpendicular to the jet. Each colored dot represent a simulation. Black dots are consistent with IXPE polarimetry. Shaded region is the constraint from the literature on the torus inclination.

For both Circinus galaxy and NGC-1068 X-ray polarimetry constraints on the torus aperture are similar 50°-55°

FIRST PROBLEM: SGRB2 VANISHES !

In Astronomy usually extended sources vary on a time scale longer than the time needed to select and build a satellite. But this was not our case.

The flux varies with a rapidity unusual for extended sources as from an external cause. There is evidence that the reflection components moves as for radiation coming from the side of the center (already in Koyama+ 2001; see e.g. Ponti+ 2010, Clavel+2013, Churazov+2017, Terrier+ 2018)



The concept that clouds are reflecting past activity of a source not far from SgrA* is favored. But, waiting for a Polarimetry mission, SgrB2 brightness decreases significantly and makes it no more attractive as a target. Study for alternative targets is performed. It becomes more deep in the proximity of IXPE launch. (Marin 2015, Churazov+ 2017, DiGesu 2019, Ferrazzoli+ 2021).

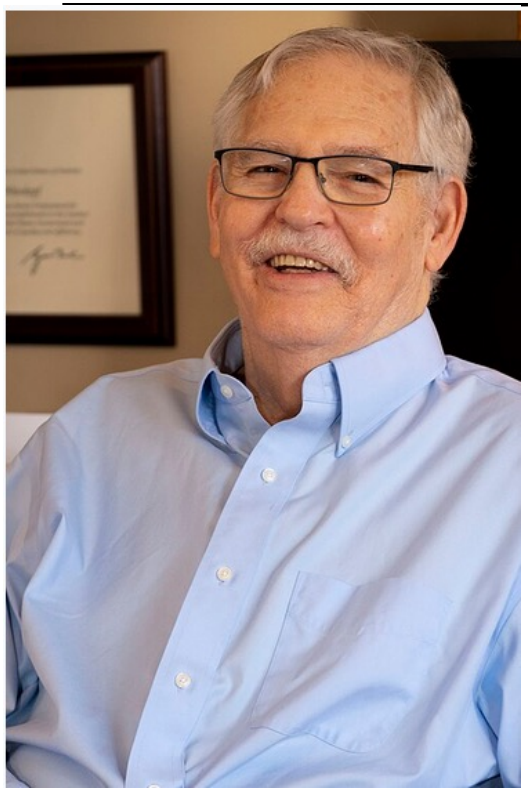
From talk E. Costa @ MG17

IXPE
Imaging
X-Ray
Polarimetry
Explorer

Marshall Space Flight Center

agenzia spaziale italiana

MARTIN C. WEISSKOPF (2042-2026)



Martin



Site Visit (End of IXPE Phase A)

USA and Italian Team at MSFC



Martin's preferred picture in talks.